SP4 Theoretical Neuroscience models - 1st part (D4.7.1 – SGA2)

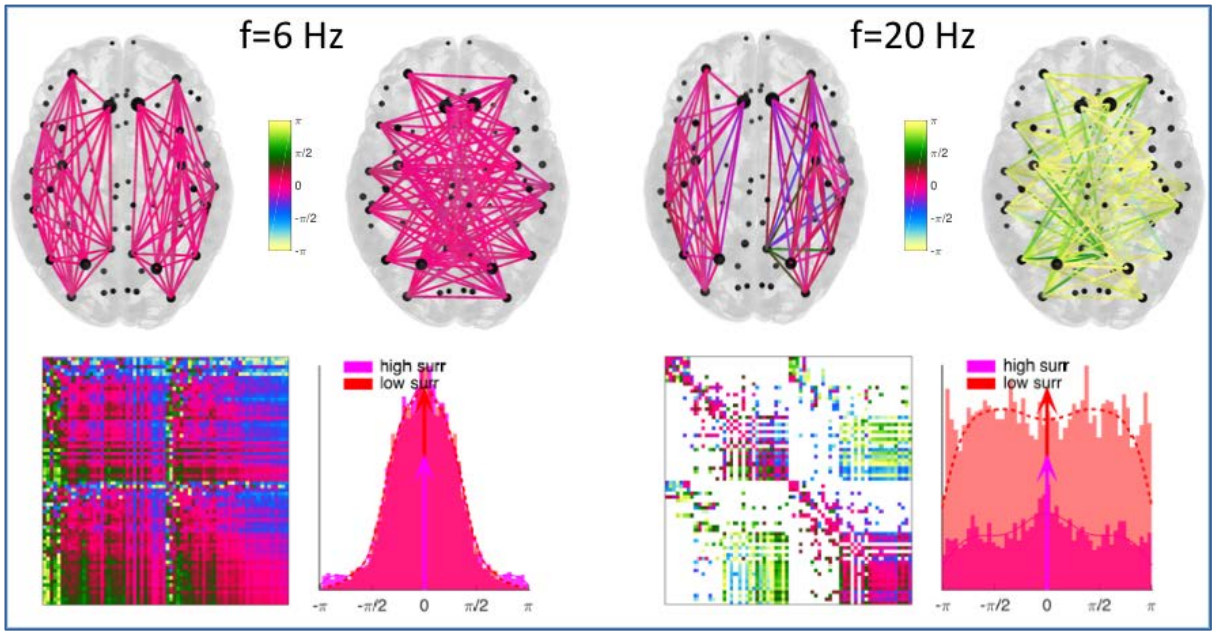

Figure 1: (Left) In- and (Right) anti- phase synchronization between brain hemispheres (KR4.6)

Project Number:	785907	Project Title:	Human Brain Project SGA2
Document Title:	SP4 Theoretical Neuroscience models – 1st part		
Document Filename:	D4.7.1 (D27.1 D18) SGA2 M12 ACCEPTED 201005.docx		
Deliverable Number:	SGA2 D4.7.1 (D27.1, D18)		
Deliverable Type:	Report		
Work Package(s):	WP4.1, WP4.2, WP4.3, WP4.4, WP4.5, WP4.6		
Dissemination Level:	PU = Public		
Planned Delivery Date:	SGA2 M12 / 31 Mar 2019, Request for revision: 22 Jul 2019		
Actual Delivery Date:	Submitted: SGA2 M12 / 24 Apr 2019, resubmitted: 16 Oct 2019 and 28 Sep 2020, accepted 5 Oct 2020		
Authors:	Leonarda Di Candia (CNRS), Alain Destexhe (CNRS), revised by Tom Messier (CNRS)		
Compiling Editors:	Leonarda Di Candia, revised by Tom Messier (CNRS)		
Contributors:	Alain Destexhe (CNRS), Marc deKamps (ULeeds), Gustavo Deco (UPF), Neil Burgess (UCL), Markus Diesmann (Jülich), Gaute Einevoll (NMBU), Olivier Faugeras (INRIA), Wulfram Gerstner (EPFL), Michele Giugliano (UA), Sonja Grün (Jülich), André Grüning (Surrey), Jeanette Kotaleski (KTH), Viktor Jirsa (AMU), Marja-Leena Linne (TUT), Olivier Marre (UPMC), Giovanni Pezzulo (ISTC), Idan Segev (HUJI), Walter Senn (UBERN), Misha Tsodyks (Weizmann), Shimon Ullman (Weizmann), Sacha van Albada (Jülich)		
SciTechCoord Review:			
Editorial Review:			
Description in GA:	SP4 theoretical neuroscience overview of work achieved during SGA2 M1-M12		
Abstract:	This report contains a description of the present status of the different models developed in SP4, as well as the associated publications and outputs.		
Keywords:	Theoretical models, computational models		
Target Users/Readers:	Neuroscientific community, Platform users, Clinicians		

Table of contents

List of Tables

List of Figures

History of Changes made to this Deliverable (post Submission)

Date	Change Requested / Change Made / Other Action
24 Apr 2019	Deliverable submitted to EC
22 Jul 2019	Resubmission with specified changes requested in Review Report Main changes requested: • Change 1 => Which Milestones [out of MS170-MS175 (WP21), MS184 & MS457-MS458 (WP22), MS187-MS188 & MS 196 (WP23), MS193-MS195 (WP24), MS206-MS207 (WP25) expected to be passed by Month 12] have really been achieved and which are clearly still outstanding at this point? • Change 2 => What datasets have been used (e.g. from SPs 1, 2 and 3 or externally) in the development of theoretical models and detail the HBP platforms activities (and related WP or task numbers) to which this SP has direct and tangible links ? • Change 3 => Updating on the publications that have been published in journals
30 Sep 2019	Revised draft sent by SP/CDP to PCO. Main changes made, with indication where each change was made: • Change 1 => Adding the Appendix II: Milestones Status • Change 2 => Adding the Appendix III: Contributions, Data used and Platforms • Change 3 => Adding the Appendix IV: List of Publications in SGA2; publications updated are 8, 42 and 50.
16 Oct 2019	Revised version resubmitted to EC by PCO via SyGMa
28 Sep 2020	Main changes made, with indication where each change was made: Change 1: Figure 1 Change 2: Figure 26 Change 3: Figure 37
28 Sep 2020	Revised version resubmitted to EC by PCO via SyGMa

DESCRIPTION OF CHANGES:

Here are the changes detailed, and comments regarding those.

(1) As requested, we now provide a table summarizing **the status of all milestones** in SP4 (Appendix II: Milestones Status). Note that the milestones (4.1.3/4.3.1/4.4.3, *in red and italics*) which have been achieved after the first submission of the deliverable will be reported in the Month 18 report.

(2) As suggested we have identified the **key tasks in HBP and platform activities where SP4 models contribute**. We also have identified the **datasets in SP1, SP2, SP3** which were (or will be) used to constrain the models developed in SP4. This information was compiled in a table, which is now given in Appendix III: Contributions, Data used and Platform. We plan to complete this table by the end of SGA2, so that each task is fully connected with the rest of HBP.

(3) As suggested, an **updated publication list** which contains the most recent publications (some of them were in arXiv or bioRxiv in the report) – see Appendix IV: List of Publications in SGA2. Note that the publications of SGA2 Year 2 (*in red and italics*) will be reported in the Month 18 report.

We think that no redistribution of resources is needed at this point. All milestones are on track, with slight delay for a couple of them (see Appendix II), so we can say that **all activities of SP4 are globally on track with no major concern**.

Also note that nearly all research themes of SP4 will be continued in SGA3, with more emphasis on large scale models and models based on human data. The activities in SGA2 Year 2 will emphasize these themes to ensure a **smooth transition to SGA3**.

1. Overview

The first work-package of SP4, **WP4.1**, has progressed towards the exploration of the computational role of dendrites as well as towards integrating dendritic models in neuromorphic hardware. The design of mean-field models has also progressed very well, with several papers published including the MIIND simulator. Finally, models of brain signals have made essential steps with the modelling of calcium imaging signals (using neuroscience experiments from the project), and the development of tools such as LFPy.

WP4.2 made further steps towards the construction of a multi-layered model covering 4mm x 4mm cortical surface. This is documented in two arXiv pre-prints (Senk et al. 2018a,c), and van Albada et al. 2018 reports on the successful transfer of the microcircuit building block to the SpiNNaker system. In addition, a model of astrocyte-glia interaction was submitted to PLoS CB (Manninen et al.). Finally, Schmidt et al. 2018a,b reports on an initial multi-area model where each area is represented by a microcircuit.

In **WP4.3**, major progress has been made on a Lagrangian formulation of synaptic plasticity rules that provide a biologically attractive alternative to the Back-propagation algorithm. Overall, the partners have worked towards translating synaptic plasticity rules to hardware and to explore biologically motivated learning paradigms and algorithms in software.

All tasks of **WP4.4** have shown satisfactory advances. At the macroscopic level, a model-based inference of stimuli propagation over large-scale brain activity was proposed. At the mesoscopic level, a model simulating brain activity of mice recorded via calcium imaging was developed, including adaptation to capture different brain states. Models of spatial navigation were also extended to include planning and memory. At the microscopic level, models of the retina are now being implemented at the population level; whilst the model of basal ganglia for motor control shifted from point-neurons to multi-compartment neuron models, thus allowing to capture empirical observations arising from dendritic plateau potentials.

WP4.5 has developed minimally invasive network interventions for stopping seizure propagation in epileptic patients. We also explained a specific seizure onset pattern observed using depth electrodes in some epileptic patients. Regarding the comparison of activity dynamics between models and living brains, a phenomenological model of delay-coupled oscillators was applied to identify underlying principles by which the spatio-temporal structure of the brain governs phase lags between distant brain regions. A validation process has also been established for network simulations, specifically against massively parallel activity data from experiments on a statistical level.

2. Introduction

SP4 is responsible for the theoretical neuroscience part of the HBP, and is involved in designing models at various scales, from cellular models up to whole-brain level. SP4 also develops strong interactions with all the platforms, from SP5 to SP10. It also has tight links with many of the experimental neuroscience data (SP1 to SP3). In this deliverable, we report the progress made in the different models developed in SP4, and how they connect to the key results of the HBP.

3. Key Result KR4.1: Develop models of single-cell and population levels

3.1 Outputs

3.1.1 Overview of Outputs

Table 1: Overview of outputs for Key Result KR4.1

Output	Component number(s)	Component name(s)	Additional information
Simplified dendritic models	C951	Complex to Simplified Models	T4.1.1
Input-Output Transfer function of detailed morphological models	C2453	Input-output "correlation" transfer properties in simplified, "ball-and-stick", multi-compartmental models	T4.1.2 Contributes to KR4.1 and KR4.5
	C2454 + C2455	Input-output "correlation" transfer properties in reconstructed multi-compartmental models of rodent + human cortical neurons	
	C951	Complex to Simplified Models	
	C1031	Mean-field models of interacting spiking neurons with dendritic compartment	
Mean-field and population models	C1031	Mean-field models of interacting spiking neurons with dendritic compartment	T4.1.3 Contributes to KR4.1 and KR4.5
	C2357	Slow-fast effects in mean-fields models	
	C1030	Mean-field models of interacting populations of rate and spiking neurons	
	C2742	Application of Mean-field simulations (MIIND)	
Biophysical models of brain signals	C1234	Model of calcium imaging signals	T4.1.4

3.1.2 Simplified dendritic models

Task T4.1.1

We derive simplified neuron and neural circuit models from biophysically and morphologically detailed models. We continued to study the correlation processing in neurons with simplified dendrites. We adjusted the parameters of our model to have a level of dendritic spikes activity similar to that observed in recent *in vivo* experiments (J. Moore et al. 2017). To better understand the mechanisms behind synaptic correlation processing, we also looked more specifically at dendritic firing rate responses to correlated synaptic input in addition to somatic firing rate responses. By doing this, we verified that interactions between dendritic spikes are responsible for the inverse correlation processing seen previously in somatic firing (**Fig. 1**-**2**, Gorski et al., 2018).

We also showed analytical estimation of the dendritic spikes collision rate. Assuming a constant velocity of dendritic spikes' propagation and a uniform distribution of dendritic spikes, the number of direct collisions is proportional to the length of the dendrite, while the sole effect of refractoriness does not scale with the length of a dendrite.

We are currently studying the correlation processing in more complex morphologies (**Fig. 3**). While inverse correlation processing is present in this kind of morphologies, here we can also analyse branch-specific synaptic correlations.

Implementation of our models on neuromorphic hardware involved re-writing our Hodgkin-Huxley model code in PyNN language. The AdEx mechanism will be implemented in PyNN by SP5, thus paving the way for running network model on BrainScaleS2 neuromorphic hardware.

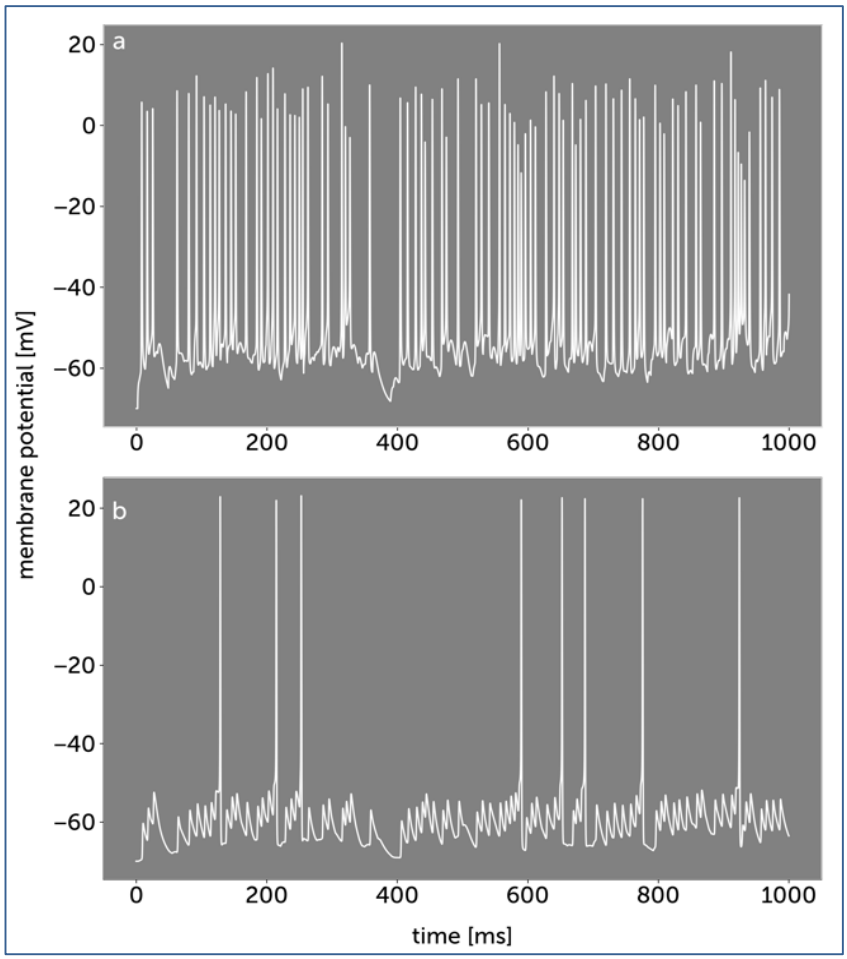

Figure 2: Comparison of dendritic and somatic spikes.

(a) Membrane voltage in the dendrite at 500 µm from soma. (b) Membrane voltage in soma. Most of the dendritic spikes cannot actively invade soma causing depolarizations with amplitudes of few millivolts.

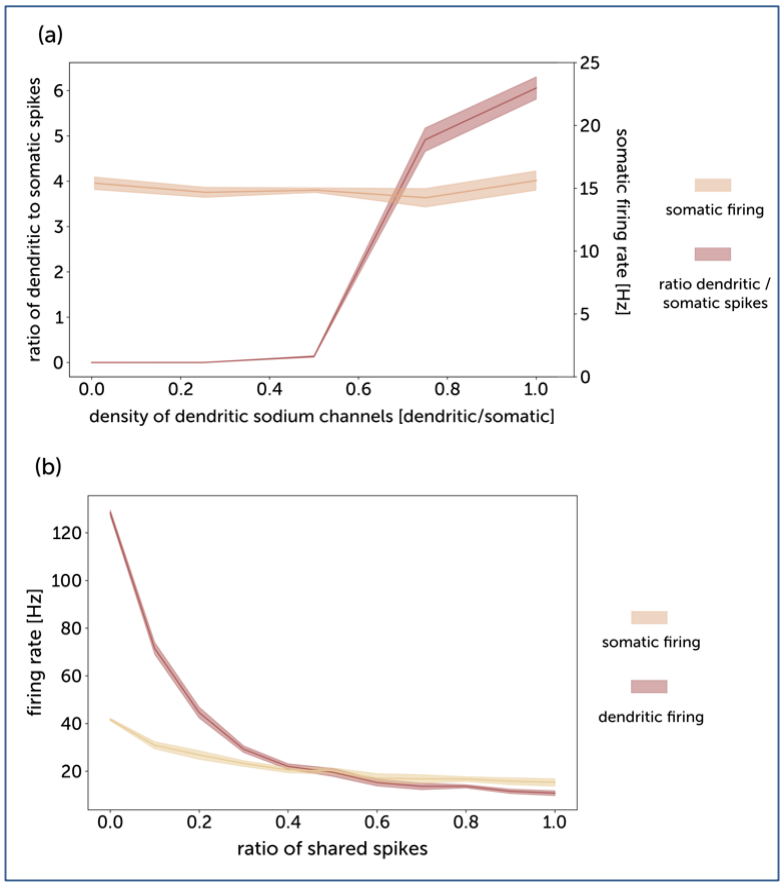

Figure 3: Somatic and dendritic spikes

(a) Ratio of dendritic spike firing to somatic spike firing as a function of the density of dendritic sodium channels. The somatic firing rate was kept at a constant level of 15 Hz by adjusting the input firing rate while changing channel densities. The input spike trains were uncorrelated. Dendritic spikes were detected in the middle at 500 µm from the soma. (b) Somatic and dendritic firing responses correlated with synaptic activity.

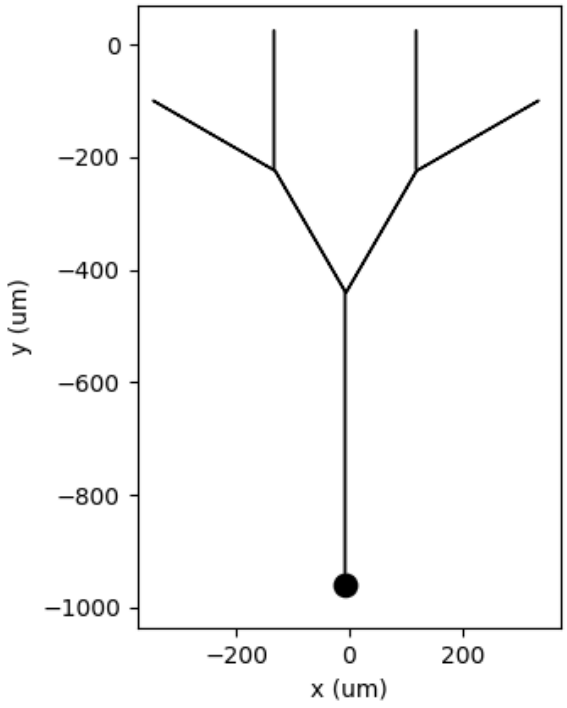

Figure 4: More complex dendritic morphologies affect synaptic correlations processing.

The **model can be interrogated on branch specific correlations.**

3.1.3 Input-Output Transfer function of detailed morphological models

Task T4.1.2

UA built spiking models from three-dimensional reconstruction of human neuronal morphologies from SP2 (H. Mansvelder). To explore the functional consequences of dendritic trees' size in these cells, we studied the dynamical transfer properties of multi-compartmental models based on these morphologies. We found that larger dendrites correlate 1) with more rapid action potential (AP) at the onset and 2) with a broader transmission bandwidth, extending well beyond 100 cycles/s (**Fig. 4**).

Within the same task, UA received data from in-house *in vitro* experiments in rodent cortical tissue. To extend the dynamical response characterization of the simplest microcircuits (i.e. pairs of neurons), UA focused on the somatosensory L5 microcircuits. We applied and validated for the first time a theoretical approach linking unique dynamical transfer properties of pyramidal cells, SOM-positive interneurons, and PV-positive interneurons to the spike-count covariance of pairs of cells receiving a known fraction of common inputs (**Fig. 5**).

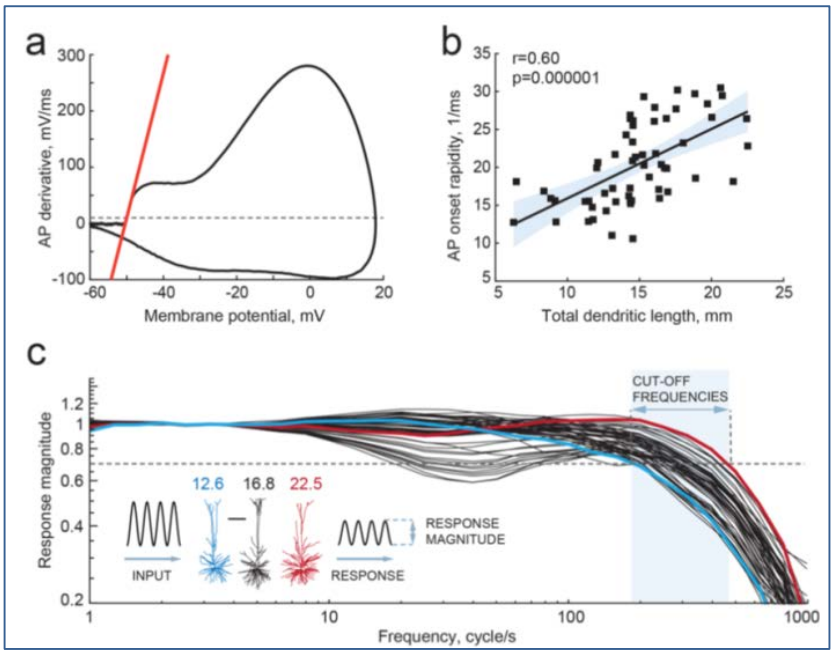

Figure 5: Higher total dendritic length results in faster AP at onset and wider transmission bandwidth

This work appeared in eLife at the end of 2018.

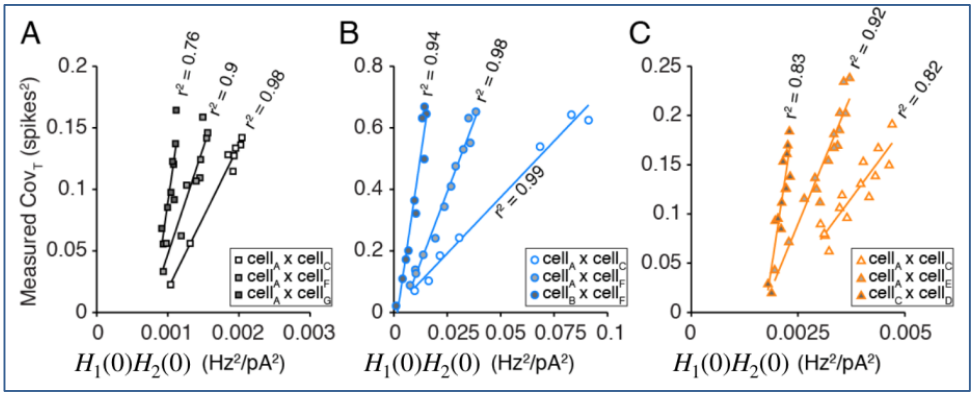

Figure 6: Predicted & measured spike-count covariance match, validating linear response theory

A manuscript has been submitted to the Journal of Neuroscience.

3.1.4 Mean-field and population models

Task T4.1.3

Mean-field models of a network of stochastic spiking neurons with dendritic compartment

The dendrites of many neurons are endowed with active mechanisms, which confer them properties of excitability and enable the genesis of local dendritic spikes. In this work, we consider the propagation of dendritic spikes in a single dendritic compartment. Because the dendrite morphology is modelled after a half-line, dendritic spikes propagate in both directions, although with possibly different speeds. Two dendritic spikes propagating in opposite directions will cancel out when they collide as in the case of the axon. We focus on an abstract description of this non-linear behaviour that is more amenable to analysis. This description reveals a rich mathematical structure that we study through the use of combinatorics. This also provides an algorithm for an efficient simulation. In passing, we link this description to the famous Ulam problem opening the door for a mean-field model.

We can now describe an isolated neuron as follows: whenever a dendritic spike reaches the soma, it triggers a depolarization. For simplicity, we put a spiking mechanism in the soma modelled after a generalized integrate-and-fire model. We call this a Ball-and-Stick (BaS) neuron. We then study the large N limit of networks of N excitatory BaS neurons. Among other findings, we are able to extract the right scaling for the synaptic weights, allowing for a large N limit which we derive. Intensive numerical simulations are presented for cases not covered by our mathematical results. This is one of the first pieces of work on mean-field limits of networks of spiking neurons with a dendritic branch (**Fig. 6**). Its significance is in demonstrating how to scale conductances when networks of neurons with dendritic compartments are considered. This work has been accepted for publication in Annales de l'Institut Henri Poincaré (B) Probabilités et Statistiques (2019).

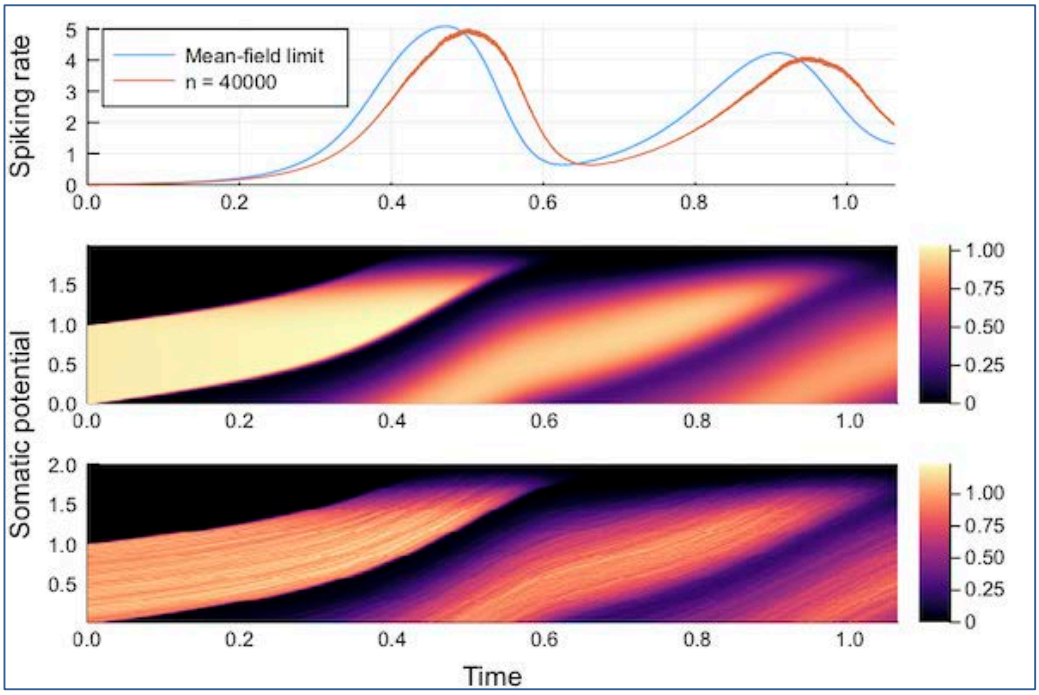

Figure 7: Mean-field limits of networks of spiking neurons with a dendritic branch.

Top: Comparison of the Firing rate in the finite size network and the mean-field limit. Middle: density plot of membrane potentials g(t,v) in the mean-field. Bottom: empirical density in the finite size network.

Study of a mean-field of network of spiking neurons with non-linear Integrate-and-Fire dynamics

The family of two-dimensional non-linear spiking neuron models (Gerstner et al. 2014) is efficient in reproducing the majority of observed membrane potential behaviour, such as bursting.

As described in previous studies (De Masi et al., 2015; Fournier et al., 2016), we use a stochastic firing mechanism of jump type with rate function *lambda* only depending on the membrane

potential, followed by a reset. We then considered a large number (N) of excitatory neurons each connected to randomly chosen N other ones. The firing of one neuron induces a size jump J/N of the membrane potential of the post-synaptic neurons. The goal of the present work is to analyze the (heuristic) mean-field limit. General studies of this problem are scarce.

The contributions of this work are two-fold: theoretical and numerical. The main theoretical advances are the proof of existence of invariant distribution, which is notoriously difficult for jump processes (Fig. 7). This is done by showing that an isolated neuron with arbitrary current is ergodic, thanks to the fact that the embedded Markov chain $(\bar v, w_n)_n$ is one-dimensional here. We then analyzed the PDE limit and analyzed its equilibrium and (linear) stability based on the analysis of the isolated neuron. This allows prediction of collective oscillations.

On the numerical side, we developed an adaptive implicit positive and conservative scheme, which has second-order accuracy in time in order to simulate the dynamics of the mean-field limit. Without this scheme, the simulation of the mean-field is extremely unstable due to the reset mechanism. Finally, we are able to perform numerical bifurcation analysis of the PDE and predict multi-stability and collective oscillations.

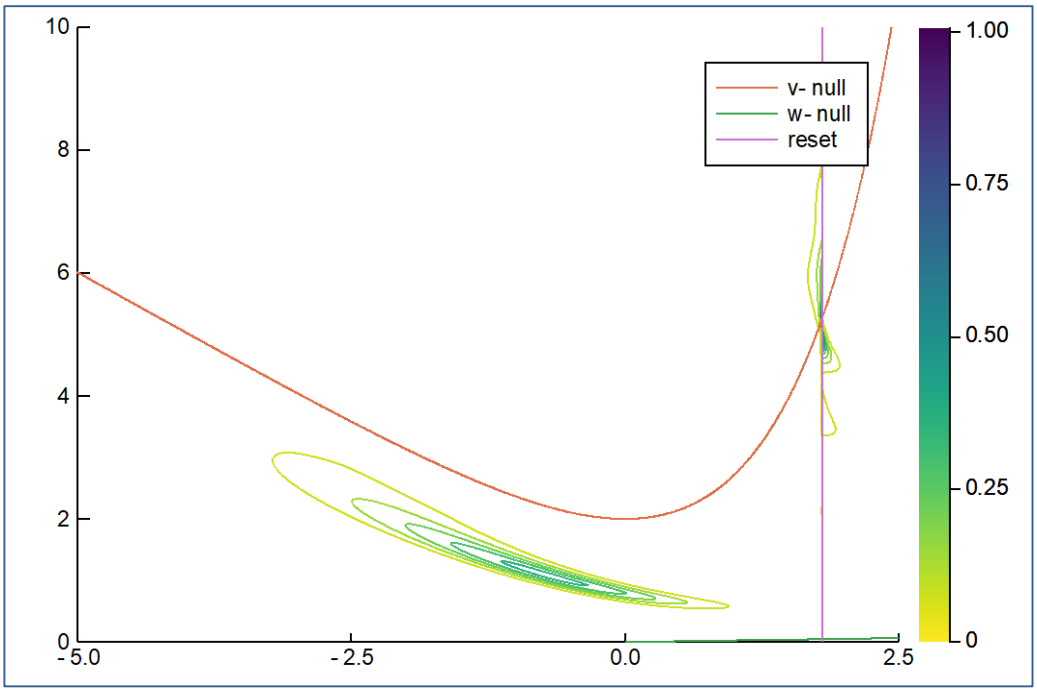

Figure 8: Example of invariant distribution for a neuron in a bursting firing regime

Example of invariant distribution for a neuron in a bursting firing regime, visible as the density present on the reset line.

Long-term behaviour of a mean-field model of interacting neurons

We model the steady-states of a network of integrate-and-fire neurons in interaction. The dynamics are as follows:

- between two spikes, the membrane potential of each neuron i evolves according to a deterministic one-dimensional equation
- a neuron spikes randomly at time t with a rate depending on its potential $f(V_t^i)$.
- when neuron i spikes, its potential is reset to a deterministic constant and the membrane potential of the post-synaptic neuron receives small kicks J^{ij}

We studied the long-term behaviour of the limit system when the number of neurons in the network approaches infinity.

First, the value of the synaptic weights is: $\frac{J}{\deg(j)}$, where the degree $\deg(j)$ of the neuron j is the number of incoming synapses. The mean-field equation is obtained when the size of the network

approaches infinity. The membrane potential of a typical neuron evolves according to a jumping non-linear McKean Vlasov equation.

We obtained the explicit Volterra equation satisfied by the spiking rate function of a typical neuron. We proved that for small synaptic weight *J,* a unique equilibrium exists to the McKean Vlasov equation and any solution converges exponentially fast to this equilibrium. For larger *J,* even in a pure excitatory (sub)-network, we observed spontaneous oscillation and a bi-stability phenomenon (Fig. 8).

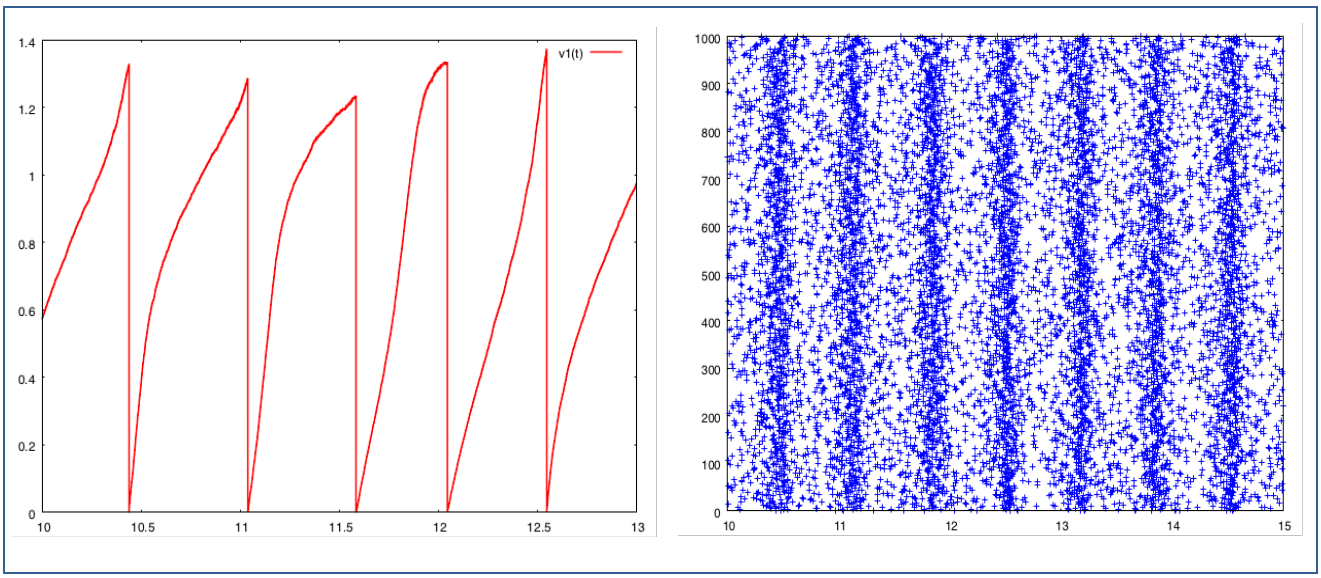

Figure 9: Mean-field model of interacting neurons.

Left: dynamics of a single neuron in the network. Right: example of Raster plot for the network.

Mean-field dynamics of networks with correlated synaptic weights

The mean-field effects are well-known in networks of interacting neurons with deterministic synaptic weights. In this work, we generalized the study to more realistic settings in which the unknown synaptic weights are modelled with correlated random variables.

We proved that the size of the synaptic weights can be of the order of $1/\sqrt{N}$ instead of $1/N$ in the deterministic setting. Moreover, the limit equation does not satisfy the propagation of chaos property. In other words, even in the mean-field limit, the activity of two typical neurons is still correlated. In the deterministic setting, the propagation of chaos property holds: two typical neurons have independent activities in the thermodynamic limit (Fig. 9).

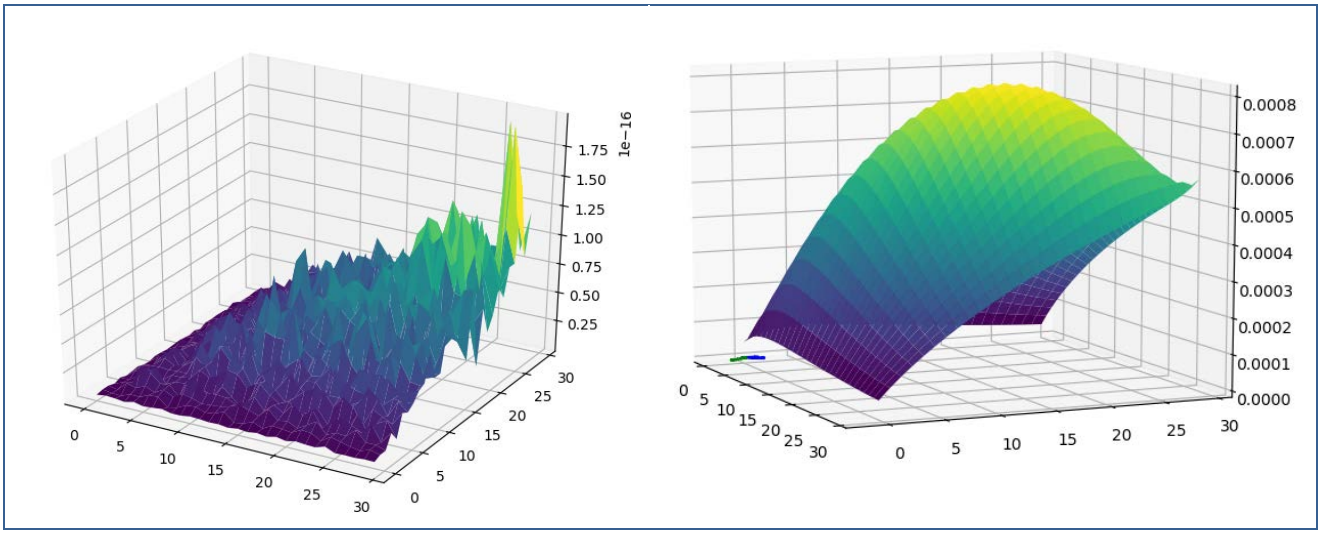

Figure 10: Mean-field and synaptic weight correlation.

Left: plot showing the absence of correlation between the activities of two typical neurons when synaptic weights are uncorrelated. Right: significant amount of correlation when they are.

Biologically realistic mean-field models

We extended our work on building mean-field models, which describe neural dynamics at the mesoscopic scale. Using few equations, these models predict the time-course of global quantities (e.g. a population spiking activity) of a network composed by a large number of interconnected neurons. We extended previous work (Zerlaut et al., 2018) by deriving a mean-field model that takes explicitly into account spike frequency adaptation, a very important property observed in excitatory neurons. This improvement makes the model biologically realistic and allows correct prediction of mean spontaneous activity in asynchronous irregular regimes, which are typical of wake states. Consistently, this was also possible in the previous version of the model, which considers adaptation as stationary, as it actually happens during spontaneous activity of asynchronous dynamical states. Nevertheless, by introducing spike frequency adaptation as a dynamical variable in the new version, we are also capable of correctly predicting transient responses to external stimuli. Figure 10 shows how the new mean-field version (*Mean-field*, green line) accurately captures the activity measured through a computer simulation of the corresponding network composed of 10,000 coupled neurons (*Network*, noisy green line), at variance with the previous version of the model (*Stationary MF*, red dashed line).

Moreover, by introducing adaptation as a dynamical variable, the present model is capable of quantitatively predicting network dynamics during slow oscillations, which are characterized by the alternation of low and high activity periods typically observed during anaesthesia or deep sleep. This can be appreciated by comparing direct simulations of the network (Fig. 11A-B) and mean-field model (Fig. 11C).

Furthermore, thanks to the simplicity of the model, we gained a mechanistic understanding of the processes yielding these oscillations, as interplay of neural noise and spike frequency adaptation acting on a bi-stable system characterized by a *down*- and an *up*-state (Fig. 11D).

We conclude that the new mean-field model is “biologically realistic” i.e. it can capture both spontaneous and evoked activity during wake and sleep states. Therefore, this model appears a suitable candidate for the design of very large-scale models involving multiple brain areas.

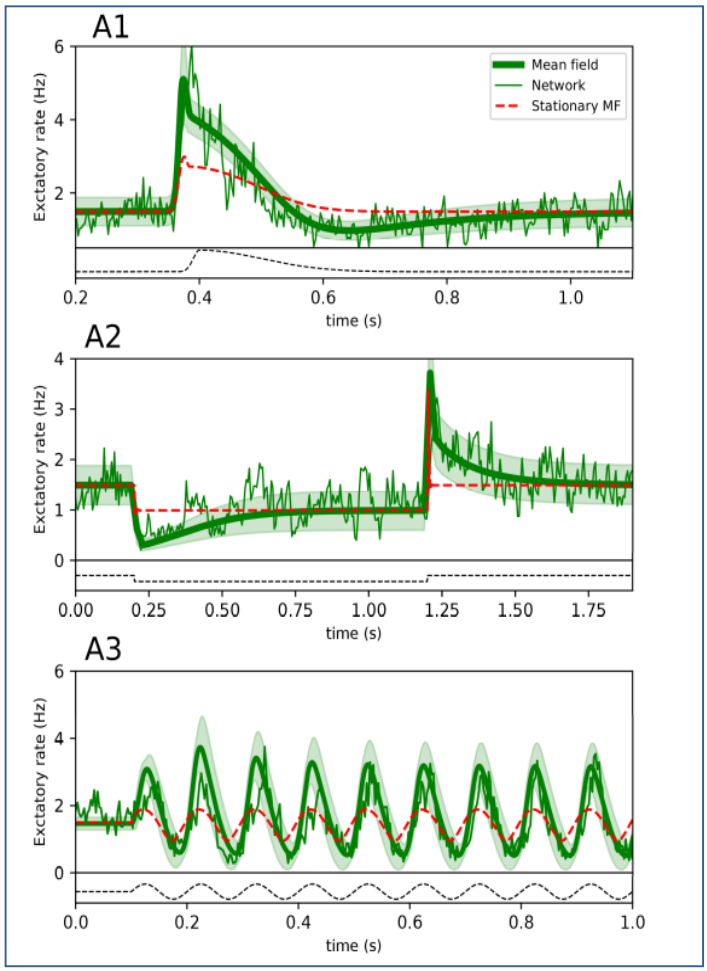

Figure 11: Population activity of excitatory sub-population of a network of N=10,000 neurons

Population activity of the excitatory sub-population of a network of N=10,000 neurons (noisy green line) in the presence of different time-varying external stimuli. Superimposed are the mean and standard deviation over time predicted by the mean-field model. Bottom panels represent the time-course of the external stimulus. Red dashed lines are the theoretical prediction based on the previous mean-field model version where the adaptation variable is fixed to its stationary value.

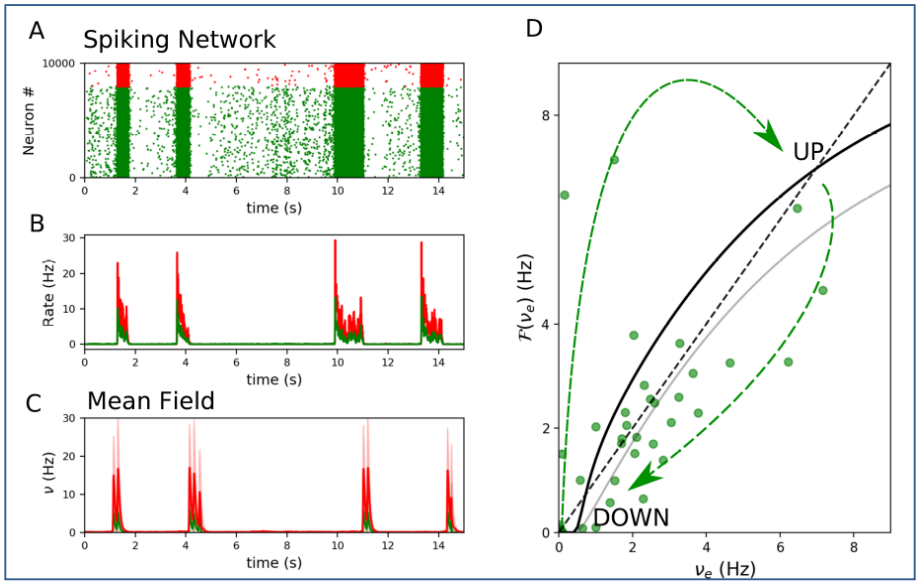

Figure 12: Raster plot of a spiking network of N=10,000 neurons

A) Each dot represents a spiking event from a specific neuron. B) Average firing rate (green=excitation; red=inhibition). C) Corresponding mean-field model dynamics. D) Phase-plane derived from mean-field with superimposed the firing rate (green dots) of the network dynamics (B). Green dashed arrows are used to guide the eyes through the spiking network trajectory during DOWN-UP cycle.

Application of mean-field simulations (MIIND)

We spent considerable effort parallelizing our code. In the end, a CUDA implementation was the most efficient, leading to simulation times comparable to NEST, but using an order of magnitude less memory, thereby allowing a large-scale 80GByte 16 thread OpenMP simulation to be moved from HPC cluster to PC, equipped with GPU. The version of MIIND with CUDA implementation has been installed on the JURON machine of the HBP cluster (Fig. 12). We are now ready to produce network models in MIIND and provide an example of work in progress on spinal cord circuitry.

Muscle synergies are canonical patterns of temporally-linked muscle activations and inhibitions, which are combined to produce the complexities of motor control. The role of proprioception in the muscle synergy hypothesis of motor control is unclear. The Chakrabarty group (University of Leeds) identified two synergies responsible for control of knee flexion accounting for >90% variation across participants.

Having demonstrated that static proprioceptive feedback influences muscle synergy recruitment, we then reproduced this pattern of activity in a neural population model. We used the MIIND neural simulation platform to build a network of populations of motor neurons and spinal interneurons with a simple Integrate-and-Fire neuron model. Two mutually inhibiting populations of both excitatory and inhibitory interneurons were connected to five motor neuron populations, each with a balanced descending input (Fig. 13). The synergies arise naturally from the connectivity of the network and afferent input. This suggests muscle synergies could be generated at the level of spinal interneurons wherein proprioceptive feedback is directly integrated into motor control.

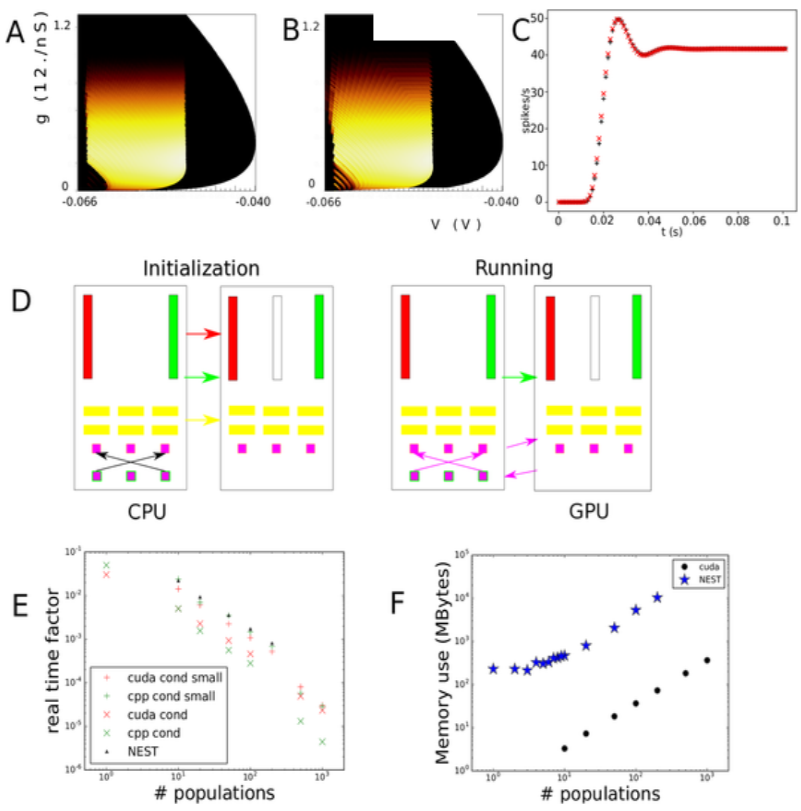

de Kamps M, Lepperød M, Lai YM (2019) Computational geometry for modeling neural populations: From visualization to simulation. PLOS Computational Biology 15(3): e1006729. https://doi.org/10.1371/journal.pcbi.1006729
https://journals.plos.org/ploscompbiol/article?id=10.1371/journal.pcbi.1006729

PLOS COMPUTATIONAL BIOLOGY

Figure 13: MIIND

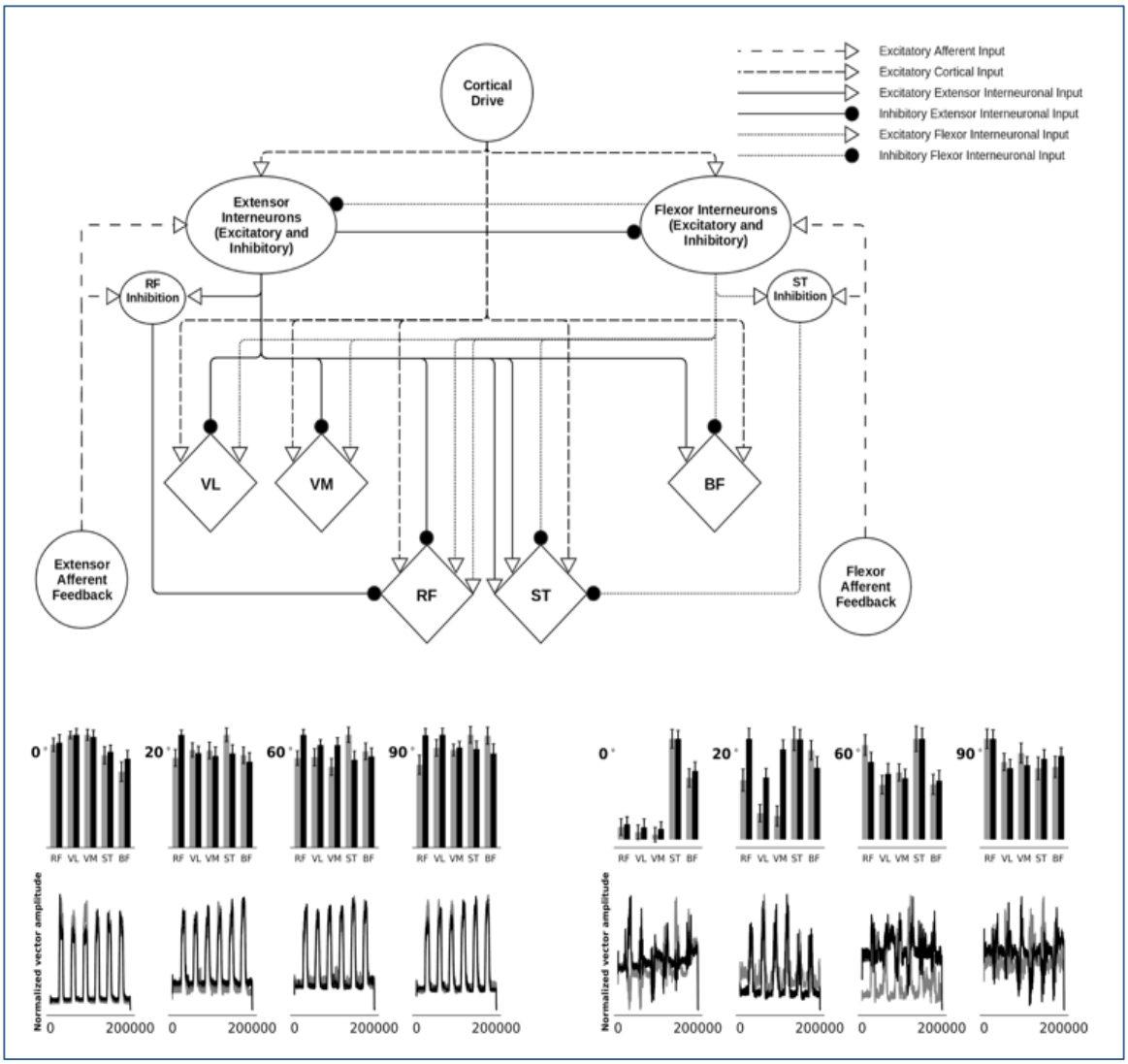

Figure 14: Application of MIIND.

Proprioceptive feedback effects muscle synergy recruitment during an isometric knee extension task.

3.1.5 Biophysical models of brain signals

Task T4.1.4

We aimed to model the calcium signal expected from the activity of a spiking network. We recorded the membrane potential (V_m) values of 10 neurons in each excitatory and inhibitory population during the simulations. Increases in the V_m lead to an inward calcium current through voltage-dependent channels. These currents increased the calcium concentration inside the cells, which had been previously loaded with a calcium indicator. Binding of the calcium ions to the calcium indicator produces a fluorescence F(t) signal, which is proportional to the amount of calcium ions. This is the measured signal (calcium, two-photon, **Fig. 14**). We modelled this signal for 10 cells in each population and then computed the average fluorescence, describing the dynamical changes observed at the spiking level (**Fig. 15**).

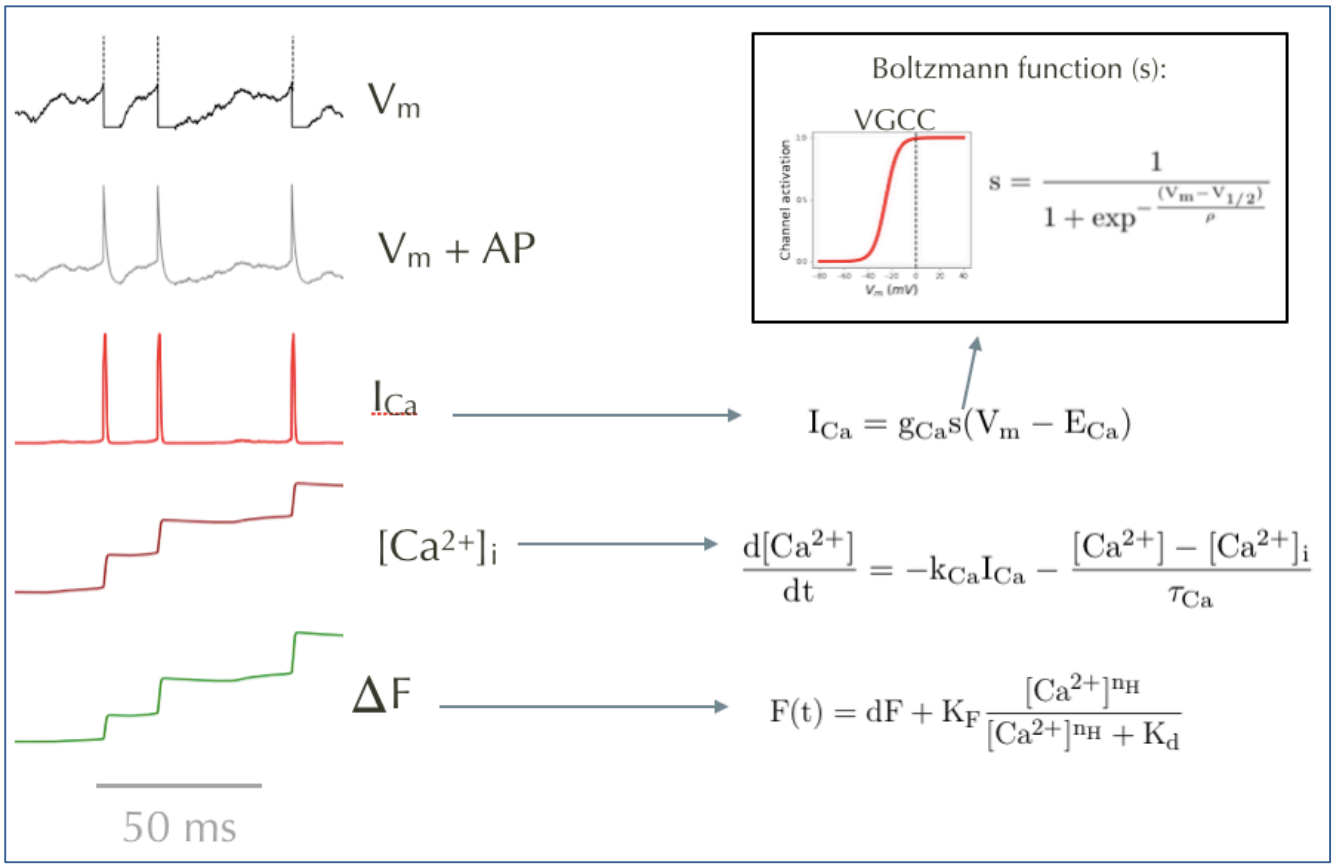

Figure 15: Computation of fluorescence (F) associated with increased V_m

Computation of fluorescence (F) associated with increased V_m and spikes or action potentials (AP) triggering the activation of calcium channels and producing intracellular calcium increase. Right: formulas used to calculate F.

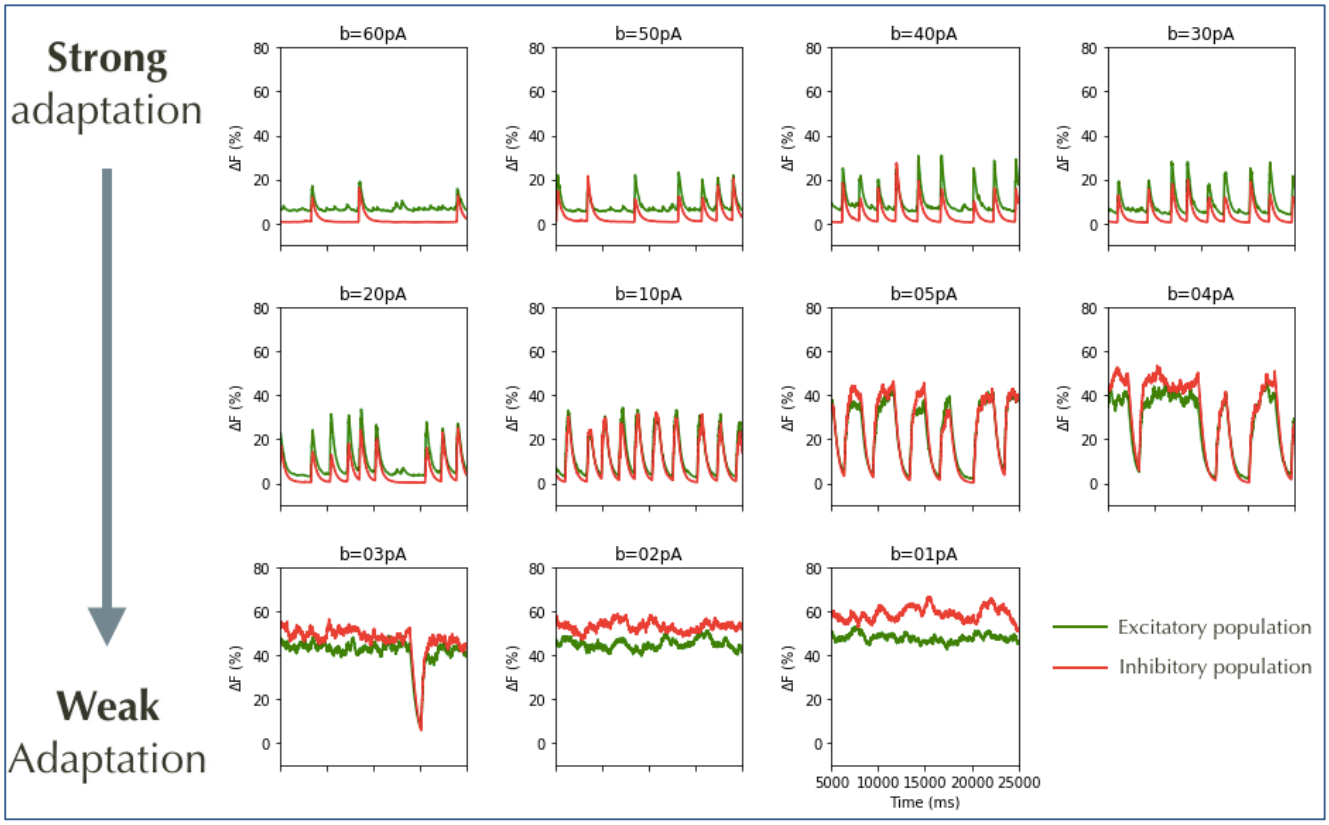

Figure 16: Average fluorescence in excitatory and inhibitory neuronal populations

Average fluorescence in excitatory and inhibitory neuronal populations at each level of adaptation. This reproduces changes in dynamics observed both experimentally (two-photon signals) and in the spiking network model.

Modelling of local field potentials

Action potentials (APs) are electric phenomena that occur both intracellularly and extracellularly. APs are usually initiated in the short segment of the axon called Axon Initial Segment (AIS). It was recently proposed that at onset of an AP the soma and the AIS form a dipole. We studied the extracellular signature (extracellular action potential, EAP) generated by this dipole. We first demonstrated the formation of the dipole and its extracellular signature in detailed morphological models of a reconstructed pyramidal neuron. Then, we studied the EAP waveform and its spatial dependence in models with axonal AP initiation and contrast it with the EAP obtained in models with somatic AP initiation. As shown in **Figure 16**, in models with axonal AP initiation, the dipole forms between somato-dendritic compartments and the AIS, and not between soma and dendrites, as in the classical models. The soma-dendrite dipoles are present only in models with somatic AP initiation. The two dipole configurations produce different extracellular potential (LFP) signatures. Thus, this study has consequences not only for interpreting extracellular recordings of single-neuron activity and determining electrophysiological neuron types, but also for validating models against experimental data.

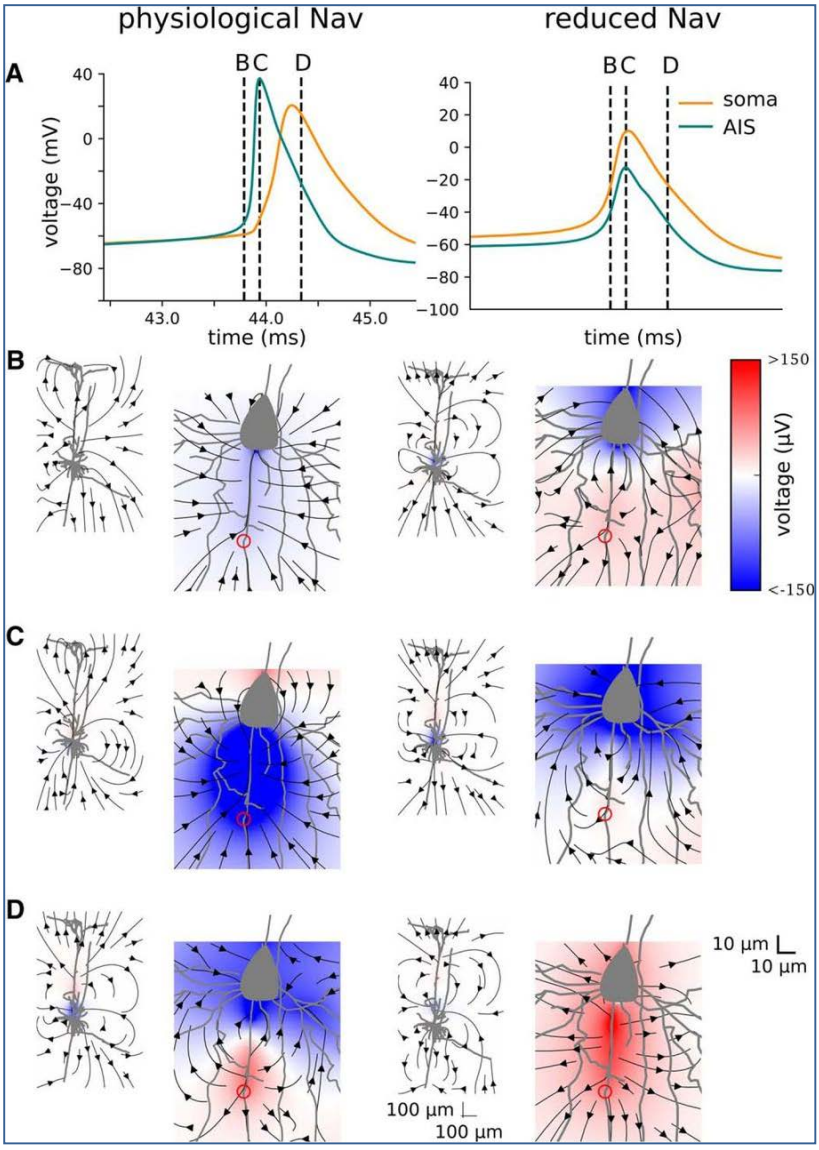

Figure 17: Comparison of the extracellular potentials generated by models with axonal (left) or somatic AP initiation (right).

A) Membrane potential in the soma (orange) and in the end of the AIS (blue). Dotted vertical lines show at which time points B-D are recorded. B-D) Extracellular potential (color-map: see color-bar on the right, red=positive and blue=negative) and electrical current (arrows) at different times of APs plotted for around whole morphology (left) and around the soma-AIS region (right). Recordings were made at: 0.15msec before the peak of the AP in the AIS (B), at the peak of the AP in the AIS (C), 0.4msec after the peak of the AP in the AIS (D). The two models give different dipole configurations, and this affects the extracellular potential. (From Telenczuk et al. eNeuro, 2018)

3.2 Validation and Impact

3.2.1 Actual Use of Output(s) / Exploitation

The MIIND simulation experiment has been performed in a virtual environment within the Neurorobotics Platform.

3.2.2 Potential Use of Output(s)

Task T4.1.2

The reconstructed human cortical pyramidal cells, turned into spiking neuron models, can be immediately incorporated in large scale simulation of the human cortex.

The computational analysis performed within this task can be applied and generalised to morphologically accurate models of biological neurons.

Our discovery of slow "intra-burst" oscillations emerging in simplified recurrent networks of excitatory neurons may be immediately translated in more accurate models of neocortical neuronal networks, bridging theoretical and experimental observations in a model of genetic disease (Moskalyuk, 2019).

Task T4.1.3

The biologically realistic mean-field model can be used for the design of large-scale models involving multiple brain areas.

3.2.1 Publications

- de Kamps M, Lepperød M, Lai YM (2019) Computational geometry for modeling neural populations: From visualization to simulation. PLoS Comput Biol 15(3): e1006729. https://doi.org/10.1371/journal.pcbi.1006729
    - **Significance:** The authors describe a new geometrical method to design population models and show that it is applicable to a wide variety of models.
- di Volo M, Romagnoni A, Capone C , Destexhe A (2019) Biologically realistic mean field models of conductance-based spiking neurons with adaptation, Neural Computation 31: 653-680.
    - **Significance:** The authors provide a mean-field model of unprecedented biological realism that can capture the response of a network to various inputs, as well as the dependency of the response to the state of ongoing network activity.
- Goriounova NA, Heyer DB, Wilbers R, Verhoog MB, Giugliano M, Verbist C, Obermayer J, Kerkhofs A, Smeding H, Verberne M, Idema S, Baayen JC, Pieneman AW, de Kock CPJ, Klein M, Mansvelder HD (2018) Large and fast human pyramidal neurons associate with intelligence, eLife 7:e41714, https://doi.org/10.7554/eLife.41714
    - **Significance:** Using a combined experimental and modelling approach, the authors show that human pyramidal neurons of individuals with higher IQ scores sustain fast action potential kinetics during repeated firing and display wide information transmission bandwidth.

Total number of publications: 10

3.2.2 Measures to Increase Impact of Output(s): Dissemination

- Results from MIIND (C2742) applications were presented at CNS2019 and will be uploaded as a paper on arXiv.

4. Key Result KR4.2: Plausible biological models of plasticity for large networks with non-trivial functionality

4.1 Outputs

4.1.1 Overview of Outputs

Table 2: Overview of outputs for Key Result KR4.2

Output	Component number(s)	Component name(s)	Additional information
Synaptic plasticity and learning	C1066	Plasticity models	T4.3.1
	C66 (completed)	Plasticity: STDP for structural plasticity	
Learning in networks of neurons	C2472	Plasticity: multifactor rule for deep networks	T4.3.2
Functional Plasticity for multi-compartment neurons in a multi-scale simulation framework	C2420	Plasticity: prototype implementations of rules and testing within and without the SP9 platforms	T4.3.3
Motor control model	C1025	Motor control model	T4.4.3 Contributes to CDP1 and CDP4

4.1.2 Synaptic plasticity and learning

Task T4.3.1

(UBern) The tag & capture rule and the natural gradient rule are currently in discussion with the Heidelberg group for implementation in the neuromorphic hardware. Both rules achieve improved performances as compared to standard gradient-based learning rules and even more so as compared to phenomenological rules, such as classical SDTP.

(EPFL) Model of Neurogenesis in hippocampus: Neurogenesis is part of the learning mechanism used by the brain to store novel data in the hippocampus. Adult neurogenesis of dentate granule cells (DGC) only concerns a small percentage of the dentate gyrus (DG) cell populations; yet, it has been shown to promote behavioural pattern separation from similar stimuli in a variety of tasks. The properties of new-born DGC evolve as a function of maturation: only cells that are well-integrated into the DG survive. This process critically depends on GABAergic input. The latter is excitatory in the early maturation phase and becomes inhibitory later in maturation. The modelling work of Olivia Gozel (EPFL-LCN) studies why the switch from excitation to inhibition in adult DG neurogenesis is crucial for proper integration. To our knowledge, we present the first model that can explain both how adult new-born DGC integrate into the pre-existing network and why they promote pattern separation of similar stimuli (C1066).

Eligibility Traces and 3-factor learning rules (C1066 and C2472): Synaptic eligibility traces are a major ingredient that enables the brain to link reward to the earlier activity of neurons. The basic idea is that joint activity of a pre-synaptic and a post-synaptic neuron leaves a trace at the synapses which is transformed into a weight change only if a neuromodulatory signal occurs in parallel or within the next few seconds. The neuromodulator could broadcast information on reward or surprise.

Structural Plasticity in Recurrent Networks (C66): Excitatory synaptic connections in the adult neocortex consist of multiple synaptic contacts, which are almost exclusively formed on dendritic spines. Mortiz Deger at EPFL-LCN developed a combined model of structural and spike-timing-dependent plasticity that explains the multi-contact configuration of synapses in adult neocortical networks under steady-state and lesion-induced conditions. Our plasticity rule with Hebbian and anti-Hebbian terms stabilizes both the post-synaptic firing rate and correlations between the pre- and post-synaptic activity at an active synaptic contact. Contacts appear spontaneously at a low rate and disappear if their strength approaches zero.

4.1.1 Learning in networks of neurons

Task T4.3.2

(UBern) We describe a concrete example of a spike sampling network which learns to dream handwritten digits (MNIST) and is amenable to implementation in neuromorphic hardware.

(EPFL) Combined unsupervised and supervised learning in Layered Networks (C2472): We investigated a simplistic network with one hidden layer and a single readout layer. The hidden layer weights are either randomly fixed or trained with an unsupervised, local learning rule implementing Sparse Coding. This achieves 98.1% test accuracy on MNIST, which is close to the optimal result achievable with error-back-propagation in non-convolutional rate networks with one hidden layer.

(Weizmann) Modeling of free recall of randomly assembled lists of words: Free recall of random lists of words is a standard way to probe human memory. We propose (Romani et al., 2013; Katkov et al., 2017) a deterministic step-by-step associative algorithm based on two basic principles: 1) memory items are represented in the brain by sparse neuronal ensembles in dedicated memory networks; 2) the next item to be recalled is the one having the representation with the largest overlap with the current one. This model predicts a simple analytical relation between the number of words acquired by subjects during the acquisition phase of the experiment (M), and the average number of words recalled (RC) (**Figure 17**).

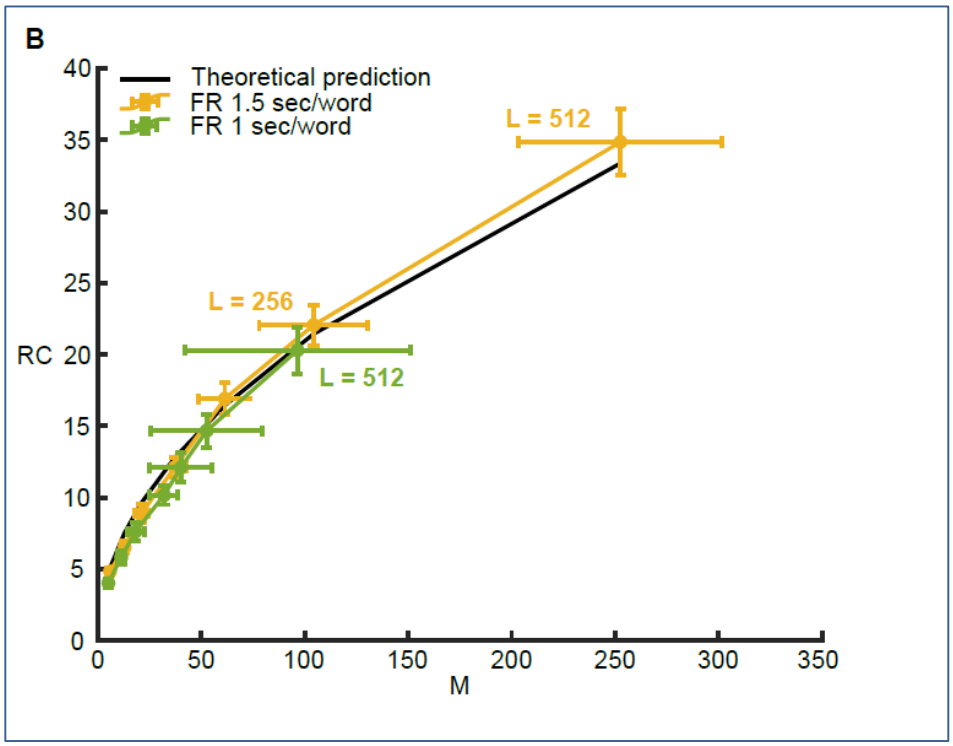

Figure 18: Average number of words recalled as function of average number of acquired words

Black line: theoretical prediction. Yellow line: experimental results for presentation rate 1.5 sec/word. Green line: experimental results for presentation rate 1 sec/word.

4.1.2 Functional Plasticity for multi-compartment neurons in a multi-scale simulation framework

Task T4.3.3

(UBern) Dendritic non-linearities distributed across multiple compartments are shown to be crucial to overcome random drifts in synaptic plasticity and to stabilize learning based on the dendritic prediction of somatic spiking. A new contrastive certainty coding model allows for a certainty-weighted dendritic integration.

4.1.5 Motor control model

Task T4.4.3

(Karolinska) During the last 12 months the previously built basal ganglia network model (Lindahl et al. 2017; doi: 10.1523/ENEURO.0156-16.2016) was used for testing hypotheses on basal ganglia role in "action selection", and to generate hypotheses on the underlying network mechanisms. In particular, the model has been used for studying stop-signaling tasks (**Fig. 18**).

In parallel, in collaboration with SP6, we have constructed a systems level rate-based model to investigate how the recently discovered populations in Globus Pallidus Externa could influence the action selection capabilities of the Basal Ganglia (Suryanarayana et al., 2018, 2019).

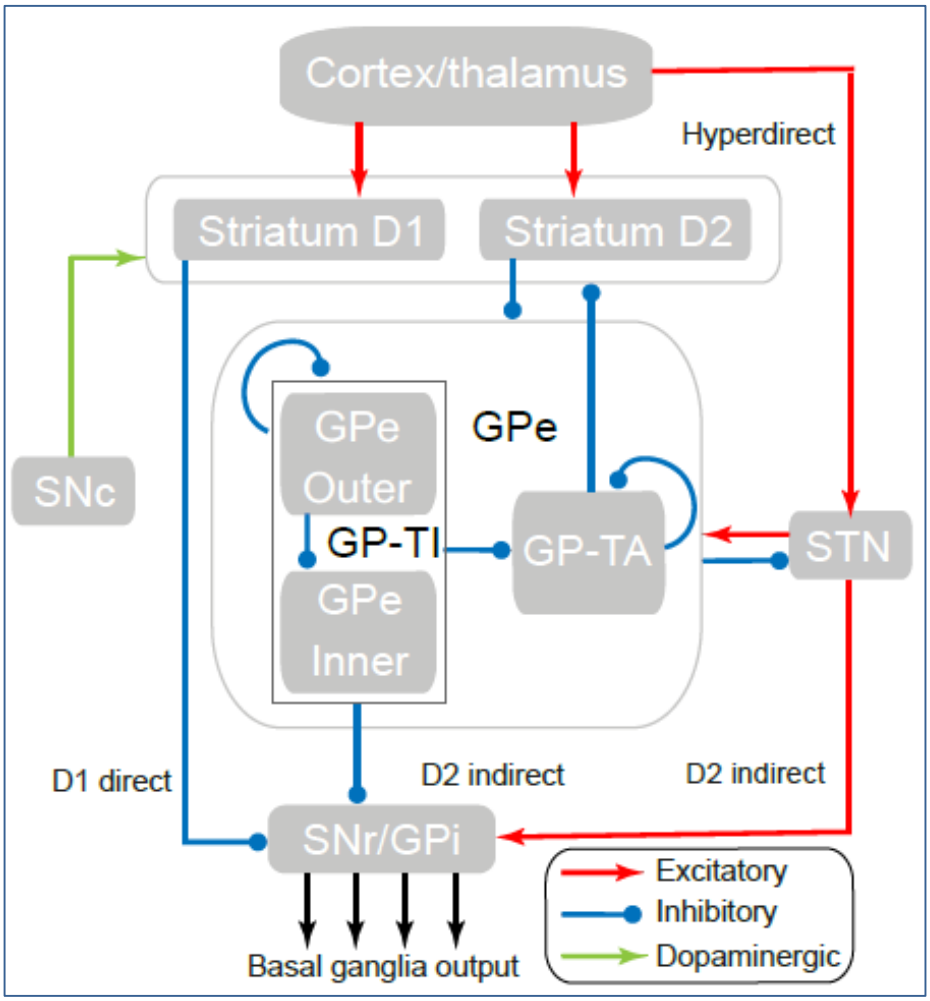

Figure 19: Intrinsic organization of GPe incorporated into the model.

In order to better define the role of the GPe in action selection, we incorporated the arkypallidal (GP-TA) and prototypical (GP-TI) neural sub-populations and their connectivity in the GPe. The arkypallidal neurons provide a massive striatal innervation. Another level of organisation of the prototypical neurons, as outer and inner GPe neurons, is also represented.

4.2 Validation and Impact

Task T4.3.1 (EPFL)

The interplay of single-neuron genesis and single-synapse plasticity in the model is now well understood, so that we can move on to networks. The relation of plasticity models with eligibility trace to synaptic plasticity data with delayed neuromodulators is now well understood.

Task T4.3.2 (EPFL)

The limits of MNIST as a benchmark for spiking neuron models with plasticity have been explored. The link between abstract models using eligibility traces and recent experimental data on synaptic plasticity under neuromodulation has been summarized in a review.

Task T4.3.3 (UBern)

We have validated our approach to spike-based supervised learning by comparison to standard ML benchmark tasks.

4.2.1 Actual Use of Output(s) / Exploitation

Task T4.3.3 (UBern)

Outputs are used in CDP5. They are also used to guide integration of learning rule templates in the neuromorphic platforms in SP9.2 and SP9.3. We are aware that the Loihi project has expressed interest in the rules developed within T4.3.3.

4.2.2 Potential Use of Output(s)

Task T4.3.1 and Task T4.3.2

The plasticity models developed in these Tasks are strongly inspired by the past and current work of Matthew Larkum (HUBERLIN, SP3).

- EPFL: The results with plasticity for spiking neurons that are established here are transferable to neuromorphic spiking chips. The transfer is ongoing and happens via CDP5.
- UBern: The plasticity rules developed in T4.3.1 (and tested in T4.3.2) are continuingly discussed with the Heidelberg group (SP9, through Mihai Petrovici) for their hardware implementation. The transfer happens via CDP5.

Task T4.3.3 (UBern)

The learning rules developed and I transformed to the NM platforms need to undergo another cycle of validation and need to be better integrated into the existing platforms to enable testing on a large scale.

The learning rules once fully adapted to the platforms offer the promise of competitive performance of spike-based neuromorphic computations with respect to standard AI approaches.

Rules are being integrated into the NM platforms of SP9.

4.2.3 Publications

- Wybo WAM, Torben-Nielsen B, Nevian T, Gewaltig MO (2019). *Electrical Compartmentalization in Neurons*. Cell Reports 26, 1759–1773, https://doi.org/10.1016/j.celrep.2019.01.074.
    - **Significance:** The paper presents a rigorous mathematical formalism to link the dendritic arborisation to an impedance-based tree graph and from there to functional dendritic subunits. It thus clarifies the putative role of neuronal dendrites.

- Leng L, Martel R, Breitwieser O, Bytschok I, Senn W, Schemmel J, Meier K, Petrovici MA. (2018), *Spiking neurons with short-term synaptic plasticity form superior generative networks.* Scientific Reports 8: 10651
    - **Significance:** This paper links the abstract idea of generative networks used in artificial intelligence research to specific neuronal properties, in particular short-term synaptic plasticity. It shows that sampling works better in networks with short-term depression because a larger fraction of the space becomes accessible.
- Katkov M., Romani S. & Tsodyks M. (2017) *Memory Retrieval from First Principles.* Neuron, 94:1027-1032.
    - **Significance:** This paper turns a very strong, parameter-free theoretical prediction into experiments at the level of psychophysics of free memory recall.

Total number of publications: 9

4.2.4 Measures to Increase Impact of Output(s): Dissemination

- Work on the model of neurogenesis in hippocampus (T4.3.1, C1066) has been presented at the Cosyne Conference 2019 (Lisbon, Portugal) as Poster Number II-17.
- Work on the model of unsupervised and supervised learning (T4.3.2, C2472) has been presented at the Cosyne Conference 2019 (Lisbon, Portugal) as Poster Number II-12.
- Suryanarayana SM, Kozlov A, Hjorth J, Hellgren Kotaleski J, Gurney K, Grillner S (2018) Investigating action selection in the basal ganglia – computational approaches at different levels of biological description, FENS abstract, 2018 (T4.4.3)

Total number of disseminations: 23

5. Key Result KR4.3: Develop models of brain activity and function

5.1 Outputs

5.1.1 Overview of Outputs

Table 3: Overview of outputs for Key Result KR4.3

Output	Component number(s)	Component name(s)	Additional information
Collective states in recurrent networks	C1030	Mean-field models of interacting populations of rate and spiking neurons	T4.1.3
	C1054	Population activity equations: finite-N mean-field model for interacting populations	
Models of spontaneous activity and sleep	C1235	Local network model of spontaneous activity in cortex	T4.4.1

Models of low-level vision	C2296	Network model of the retina responding to complex stimuli	T4.4.2 Contributes to KR4.1 KR4.3, KR4.5, and KRc4.1
Whole-brain model for propagation of spontaneous activity	C1859	Alteration of spontaneous activity and emergent dynamics under external stimuli	T4.4.4
	C999	Macroscopic model of spontaneous human brain activity	

5.1.2 Collective states in recurrent networks

Task T4.1.3

To perform complex tasks, our brains transform inputs in a complicated, non-linear manner. Such transformations are implemented by large recurrent networks. Corresponding neural network models exhibit a transition to chaotic activity if the overall coupling strength between neurons is increased. This transition is believed to coincide with optimal information-processing capabilities, such as short-term memory. Our work has shown that this coincidence is not valid for networks receiving time-varying inputs.

We analysed the stochastic non-linear dynamics of randomly coupled neural networks of rate units in the presence of fluctuating inputs and derived the dynamic mean-field theory using systematic methods from statistical physics (C1030). This approach reveals that fluctuating inputs shape the network's activity and suppress the emergence of chaos. We discover an unreported dynamical regime that amplifies perturbations on short time scales, but is not chaotic for longer times. In this regime, networks optimally memorize their past inputs (**Fig. 19**).

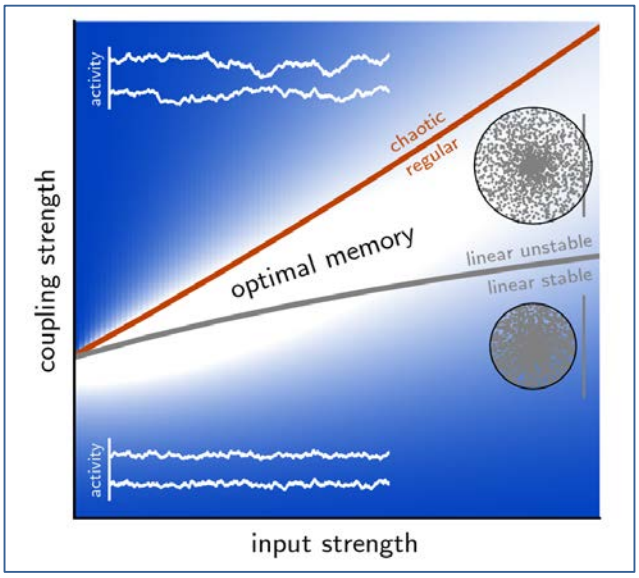

Figure 20: Phase diagram of a driven network

Gray curve: Loss of linear stability. Red curve: Transition to chaotic activity. Shading indicates memory capacity.

5.1.3 Models of spontaneous activity and sleep

Task T4.4.1

We developed a spiking network model capable of reproducing the spontaneous activity of a cortical network during anaesthesia. We decreased the strength of adaptation to reproduce the increase in

frequency of the slow oscillations observed from two-photon calcium signals when decreasing the level of anesthesia in Thy1-GCaMP6f mice (data from the collaboration with SP1, **Fig. 20**). The network consists of an excitatory population of regular spiking neurons (RS) and an inhibitory population of fast spiking neurons (FS). All neurons were modelled as adaptive exponential integrate-and-fire neurons (**Fig. 21**).

The membrane potential of RS neurons is affected by spike frequency adaptation, which we modelled with the variable *w*. At each spike, *w* is incremented by a value *b*, which regulates the strength of adaptation. In order to simulate different levels of adaptation to model fading of anesthesia, the parameter *b* varies between 60 and 1 pA in RS cells, while the inhibitory population (FS) has no adaptation (**Fig. 22**).

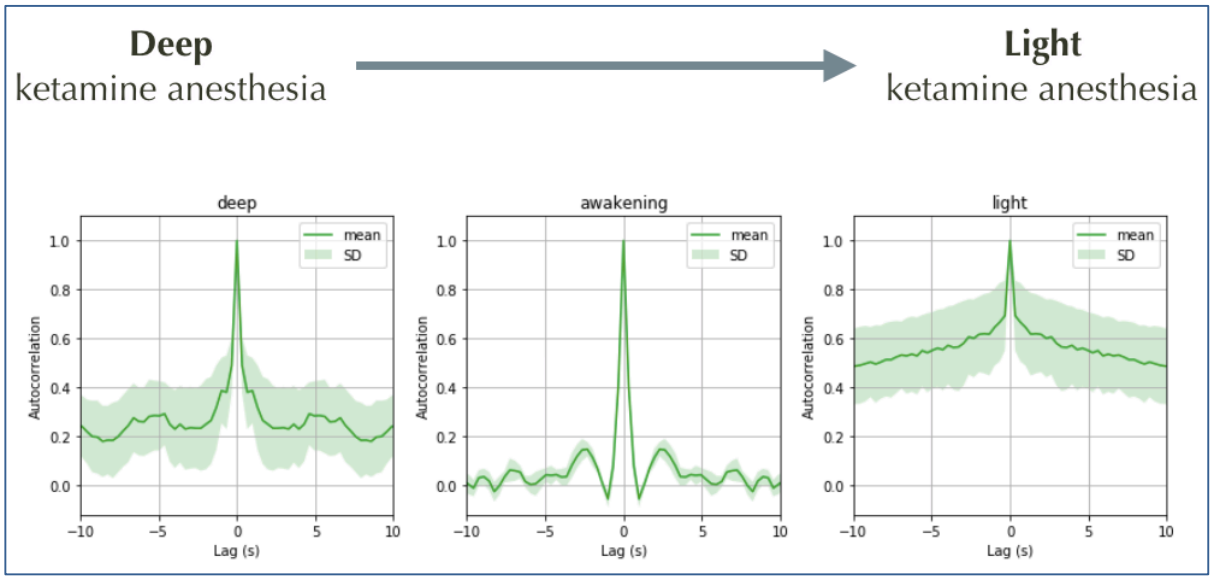

Figure 21: Spiking network model of spontaneous cortical activity during anaesthesia

Frequency of slow oscillations increased as the level of anaesthesia decreased (two-photon data).

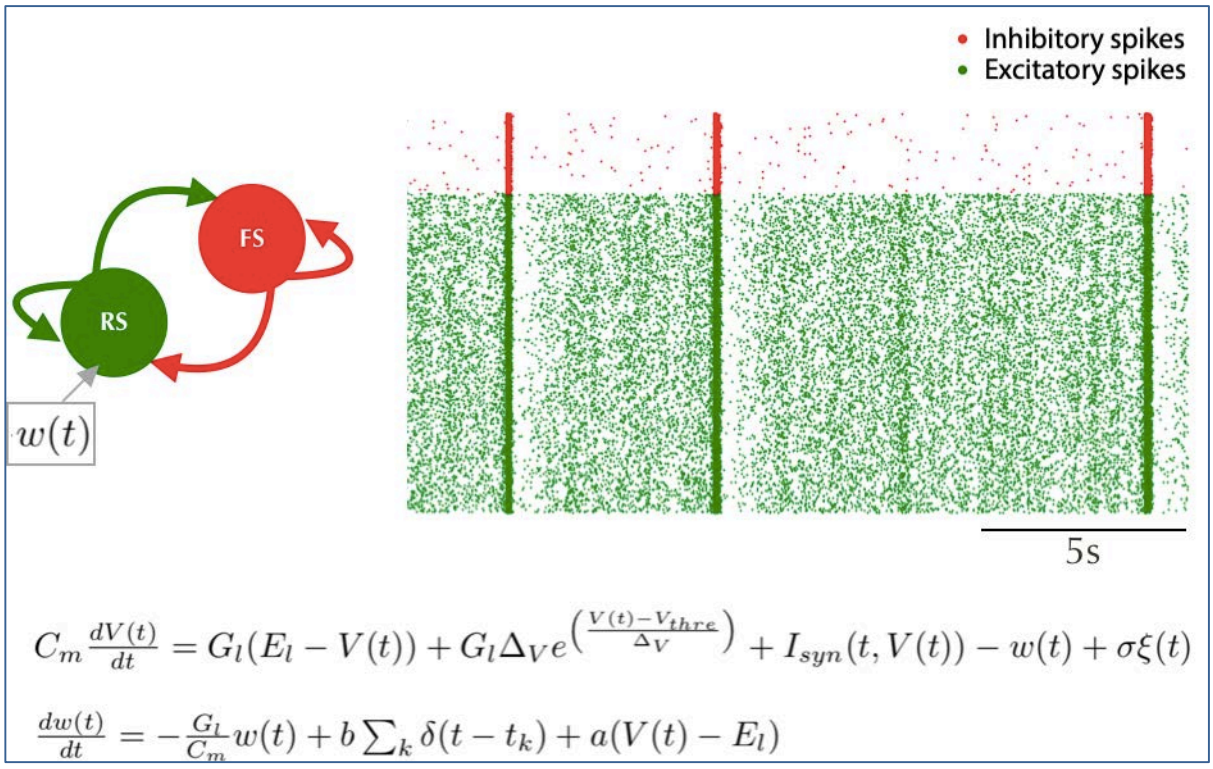

Figure 22: Schematic spiking network model indicating connections between two populations

Right: example of raster plot of neuronal spikes in a network showing slow oscillations. Bottom: equations driving the neuronal network dynamics.

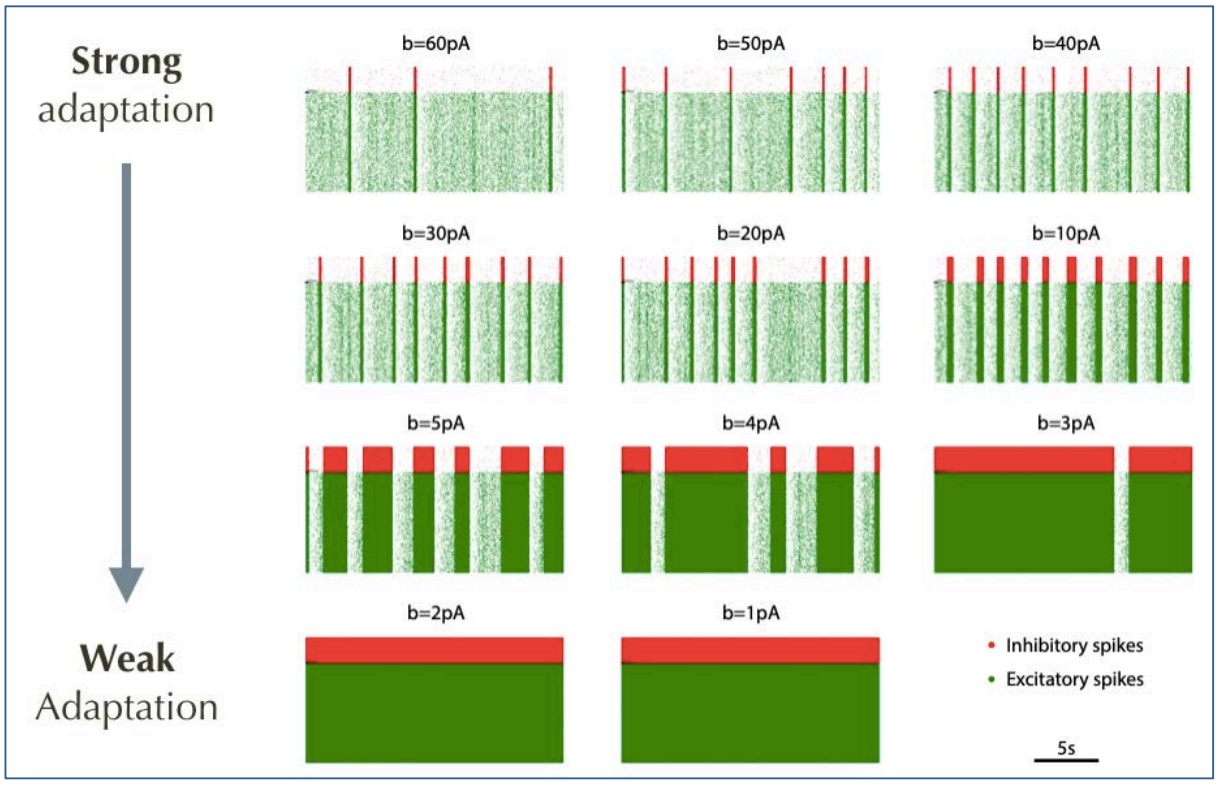

Figure 23: Model of spike frequency adaptation.

Raster plots show changes in spiking patterns in the network as adaptation strength (*b*) is progressively reduced to mimic changes observed experimentally.

5.1.4 Models of low-level vision

Task T4.4.2

We develop models of the retina that accurately predict retinal network responses to complex stimuli and ultimately natural scenes. Our work contributes to SP10 (models of retina-brain signals during visuo-motor tasks). We provide them with a realistic retinal input. To do this, we built on the single-cell model developed in SGA1 and extended it to an entire population of ganglion cells responding to complex stimuli.

Data from neuronal simultaneous recordings show that cells of the same type have specific fast-noise correlation, probably due to gap junction coupling. We have integrated this coupling in our model to predict how an entire neuronal population responds to dynamic stimuli.

We equipped an arbitrary model of single-neuron stimulus encoding with a network of couplings between output neurons. We developed a method for inferring both the parameters of the encoding model and the couplings between neurons from simultaneously recorded retinal ganglion cells (**Fig. 23**). The inference method fits the couplings to accurately account for noise correlations, without affecting the performance in predicting the mean response.

We have demonstrated that the inferred couplings are independent of the stimulus used for learning and can be used to predict the correlated activity in response to more complex stimuli.

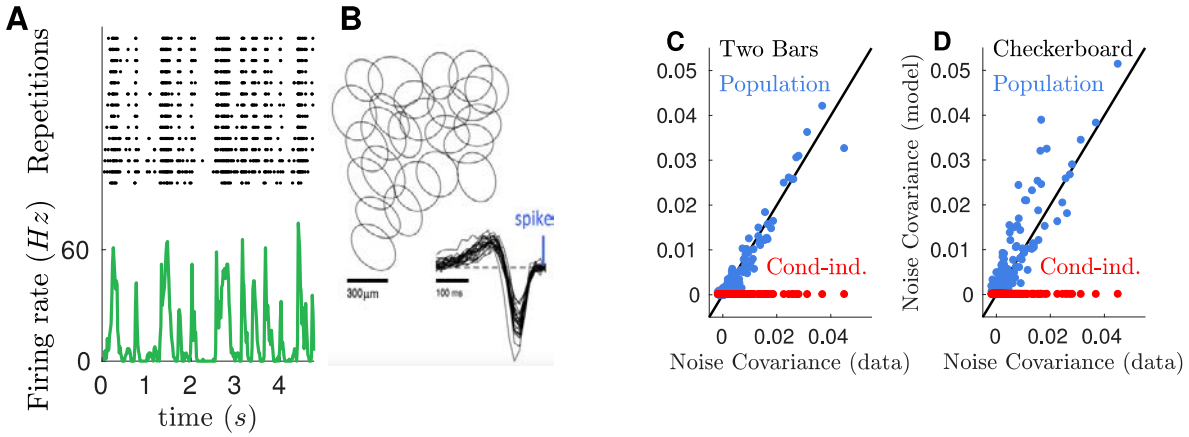

Figure 24: Inference method of neuronal couplings

A) Top: activity of one ganglion cell over repeated presentations of the same stimulus. Bottom: firing rate of the cell across time. B) Receptive field mosaic of the isolated OFF ganglion cells. C) Our model predicts empirical noise covariances when applied on a testing set (blue points). Conditionally-independent model predicts zero noise covariances (red). D) Same as C, but when the couplings are inferred from response to a different type of stimulation.

Model for high-level contributions to low-level vision

We develop functional and circuit models of integrating bottom-up with top-down processing in vision. We developed two main extensions of previous work: 1) we identified the contribution of activations proceeding from high-level visual areas, in particular IT areas, to lower-level areas, in particular V1. These allow the visual system to disambiguate the categorization of image features that cannot be reliably recognized without the top-down contribution. 2) We developed a network-level model including a bottom-up stream, a top-down stream and their interactions.

To reach the goal of categorizing image features which require the contribution from higher-level visual areas, we developed a model for the full interpretation of so-called “minimal images”. These are local image regions recognized with high accuracy by human observers, which become unrecognizable with any reduction in size or resolution. We first showed that current feed-forward models, including leading models based on deep-network models, cannot perform this task and their performance is far below human level. We next developed a functional model allowing the categorization of minimal images and their internal features through integration of top-down with bottom-up processing.

The model uses a two-stage computation: an initial processing by a feed-forward network, followed by a top-down process. The top-down process uses an object model stored in long-term memory to search for a specific configuration of image contours.

We recently applied this to challenging images showing people in close interaction. Images were significantly better interpreted than with alternative schemes using bottom-up processing alone (Fig. 24).

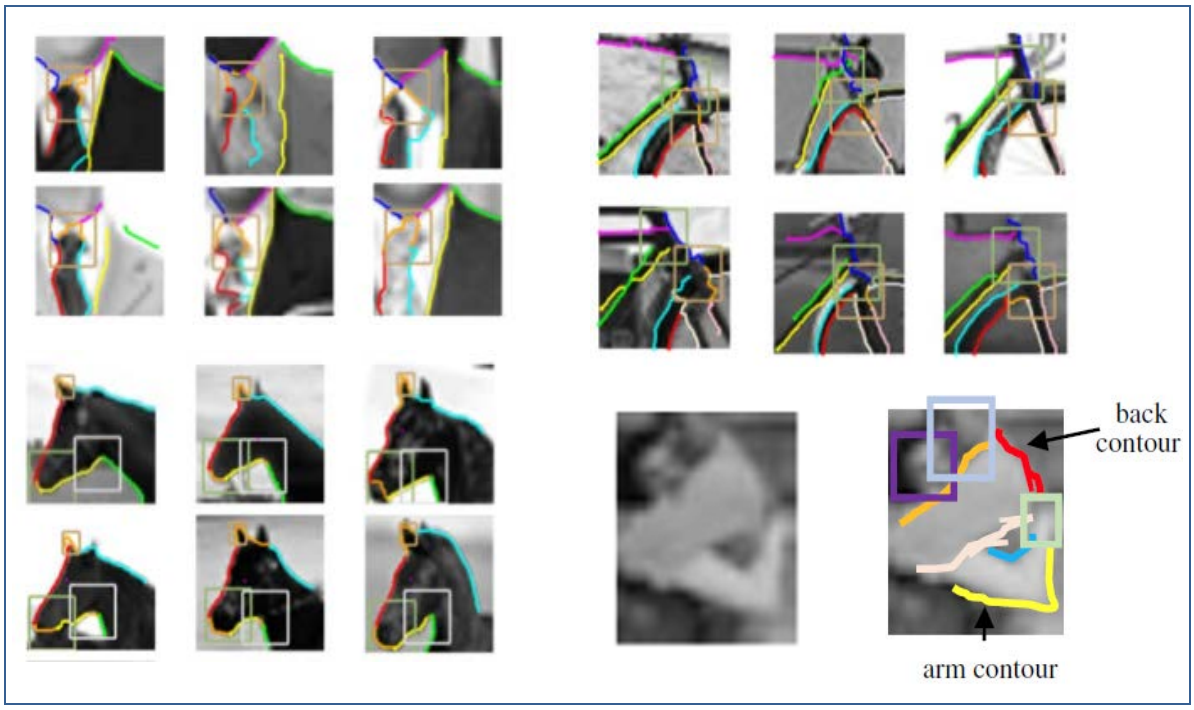

Figure 25: Outputs of the algorithm integrating top-down with bottom-up processing.

The model was asked to recognize the internal contours of difficult images, such as a human torso, bicycles, a horse-head, and people interacting. These contours, which are not detected by feed-forward models, are detected in the current model at nearly human-level performance.

5.1.5 Whole-brain model for propagation of spontaneous activity

Neuroimaging techniques (fMRI) have been widely used to explore the associations between brain areas. Structural connectivity (SC) captures the anatomical pathways across the brain and functional connectivity (FC) measures the correlation between the activity of brain regions. However, the application of network theory is only a "static" representation despite the dynamic nature of time series obtained from fMRI. Here, we tune a multivariate Ornstein-Uhlenbeck (MOU) process:

$$\dot{x}_i = -\frac{1}{\tau}x_i + \sum_{i=1}^{N} A_{ij}x_j + \xi_i$$

to reproduce the statistics of the whole-brain resting-state fMRI signals. The dynamic communicability is defined as the Green function of the MOU on the network. It describes the elementary and transient network response to an external impulse applied to all nodes. Formally, dynamic communicability is defined as:

$$\mathscr{C}(t) = |J^o| \left(e^{Jt} - e^{J^o t}\right)$$

where J is the Jaccobian of the networked MOU and J^0 is the Jaccobian of the intrinsic leakage. In contrast to classical graph theory, our model-based framework stresses the importance of taking the temporal aspect of fMRI signals into account, which allows us to identify a separation of time-scales and of individual roles of brain regions (**Fig. 25**). Two publications have been submitted (Gilson M. et al.).

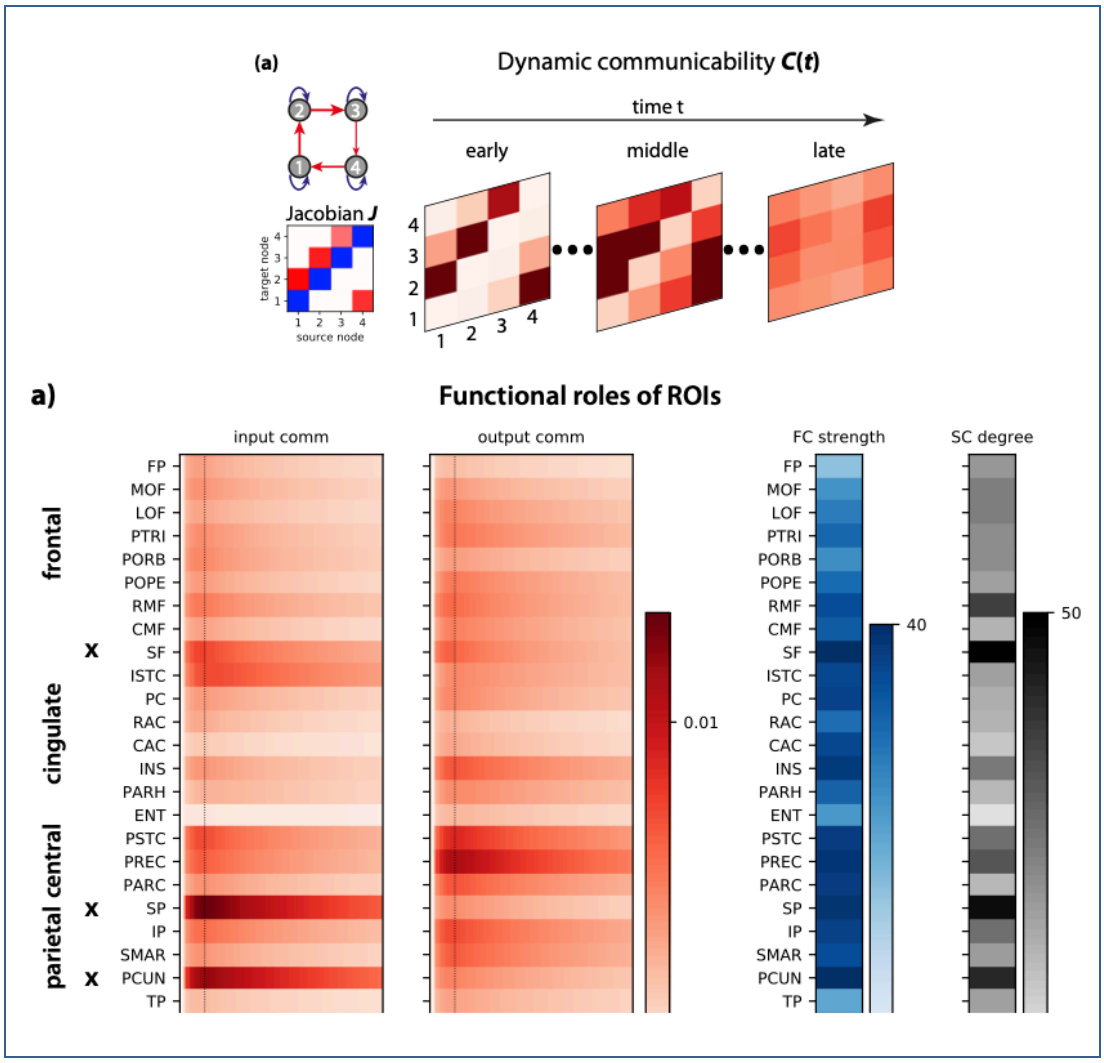

Figure 26: Dynamic communicability

(Top) A perturbation applied to all network nodes generates a collection of states. At early times it resembles the underlying connectivity, but over time the local effects of the perturbation homogenize. (Bottom) Dynamic communicability allows to study the temporal role of each ROI on the propagation of the perturbation.

5.2 Validation and Impact

Task T4.1.3

The *Collective states in recurrent networks* output develops a toolbox of methods allowing the prediction of parameters that are optimal for the computational performance of neuronal networks. This toolbox opens the study of recurrent neural networks to the rich, powerful and mature set of methods that have been developed over decades in statistical physics. These tools will have a substantial impact on the design, control, and understanding of biological and artificial neural networks with finite numbers of units (C1054). Importantly, they go beyond the known limitations of mean-field theory, which lacks finite-size fluctuations and requires homogeneous network architectures.

Task T4.4.2

The low-level vision model offers a powerful and precise tool for assessing the impact of noise correlations on the encoding of sensory information. We have tested quantitatively our models and found the parameters for several major cell types of the retina. This model will also provide a realistic input when no stimulation is presented, and will be a realistic input to thalamus model.

5.2.1 Actual Use of Output(s) / Exploitation

Task T4.1.3

These methods are used by T4.5.1 within the HBP to constrain recurrent network models by the statistics of massively parallel recordings from macaque monkeys.

Task T4.4.2

Our work was used to study and improve recognition in deep neural network models and make them more stable [1]. The approach is also being used in an ongoing study by Gilbert and Freiwald at the Rockefeller on the recognition of local image features in the macaque monkey [2].

[1] Srivastava et al. Minimal Images in Deep Neural Networks: Fragile Object Recognition in Natural Images (International Conference on Learning Representations 2019).

[2] Altavini TS, et al. Object recognition in the Macaque based on informative components of familiar objects (SfN Abstract 2017)

The model for high-level contributions to low-level vision has applications to Neurorobotics in SP10 for *in silico* models of behaviour, cognition and motor control.

5.2.2 Potential Use of Output(s)

Task T4.1.3

This output will be useful to analyse and understand how recurrent networks transform time-dependent signals into network states. These results will allow us to impose functional constraints in the network models, e.g. in paradigms such as reservoir computing.

Task T4.4.2

It will help to understand the role of top-down inputs to area V1. It will improve recognition of local image regions in artificial vision systems.

5.2.3 Publications

Task T4.1.3

- Schuecker, Goedeke, Helias (2018) *Optimal Sequence Memory in Driven Random Networks*. Phys Rev X 8, 041029
- Owaki T, Vidal-Naquet M, Nam Y, Uchida G, Sato T, Câteau H, Ullman S, Tanifuji M. (2018) *Searching for visual features that explain response variance of face neurons in inferior temporal cortex*. PLoS one, 13, 1-27.
    - **Significance:** This study combined physiological recordings and computational modelling to model object representation in high-level areas (specifically face-parts in inferior temporal cortex), which are potentially involved in the top-down, bottom-up integration.
- Ullman S. (2019) Using neuroscience to develop artificial intelligence. Science, 363 (6428), 692-693.
    - **Significance:** This is an opinion paper with a general significance for the HBP project. A large part of the HBP project centres around the development of realistic neural models for perceptual and cognitive tasks. The paper compares recent AI deep-net based models with biological cortical circuitry and argues that aspects of the biological circuitry are likely to prove crucial for future AI cognitive and perceptual models.

Total number of publications: 4

5.2.4 Measures to Increase Impact of Output(s): Dissemination

Task T4.1.3

- The developments of Output 1 (Collective states in recurrent networks) will be released as an overview monograph, which is currently in preparation (Helias, Dahmen 2019).
- In addition, at the upcoming CNS*2019 conference, D. Dahmen, A. Crisanti, and M. Helias are going to give a tutorial to introduce students and postdocs to these methods: https://www.cnsorg.org/cns-2019-tutorials#T6.
- A similar tutorial will also be held by Dahmen and Helias at the EITN Spring School 2019 (Helias, Dahmen, 2019) Statistical field theory for neural networks. ArXiv:1901.10416 [cond-mat.dis-nn]).

6. Key Result KR4.4: EITN Postdoctoral programme

6.1 Outputs

6.1.1 Overview of Outputs

Table 4: Overview of outputs for Key Result KR4.4

Output	Component number(s)	Component name(s)	Additional information
State-dependent Mean Field	C1024	EITN Postdoctoral Fellows Programme	T4.6.2
Slow Oscillations			
Integration of models in The Virtual Brain			

6.1.2 State-dependent Mean-Field

Mean-field theories aim at understanding how population dynamics are generated by the designed parameters of the networks. Despite analytic solutions for the mean-field dynamics already proposed for current based neurons (CUBA, **Fig. 26A-B**), a complete analytic description has not yet been achieved for more realistic neural properties, such as conductance-based (COBA, **Fig. 26C-D**) network of adaptive exponential neurons (AdEx). Here, we propose a novel principled approach to map a COBA on a CUBA. This approach provides a state-dependent approximation capable of reliably predicting the firing rate properties of an AdEx neuron with non-instantaneous COBA integration.

One of the major challenges of this model is the evaluation of the transfer function for neurons provided with COBA signal integration, which generates a complicated and bidirectional interaction between input statistics and membrane potential statistics. The mean-field model obtained was tested against numerical simulations of the network. As shown in **Fig. 26E**, the average firing rate of the population is well-predicted by the theoretical transfer function. Our approach is particularly effective when applied to investigate the biologically relevant regimes of the population dynamics, i.e. *asynchronous irregular* (AI) and *slow oscillating* dynamics (SO).

We considered a network based on two different cell types, excitatory (E), also known as "regular spiking" (RS) and inhibitory (I) or "fast spiking" (FS) neurons (**Fig. 27A**). The mean-field model of RS-FS networks was based on a Master Equation Formalism proposed previously (El Boustani-Destexhe, 2009), while the method for evaluating the transfer function is inspired to (Brunel, 2000). The dynamics of the system can be described by the following equations:

$$\begin{cases} \tau_E \frac{d\nu_E}{dt} = TF_E[\nu_E, \nu_I, W(t)] - \nu_E \\ \tau_I \frac{d\nu_I}{dt} = TF_I[\nu_E, \nu_I] - \nu_I \\ \frac{dW}{dt} = -\frac{W}{\tau_W} + b\nu_E - a(\mu_V^E - E_l) \end{cases}$$

where $\nu_E(t)$ and $\nu_I(t)$ are the excitatory and inhibitory population activities, and $W(t)$ the level of adaptation, whose dynamics is defined by parameters *a* and *b*.

Here, we show our mean-field model, successfully describing the dynamics of RS-FS networks (**Fig. 27B-C**, phase space with nullclines and time-course of dynamics respectively), as observed in the spiking network (**Fig. 27D**) for different regimes (top: AI; bottom: SO models). These results show that a state-dependent approximation can be successfully introduced to take into account the subtle effects of COBA integration and to deal with a theory capable of correctly predicting the activity in regimes of alternating states like slow oscillations.

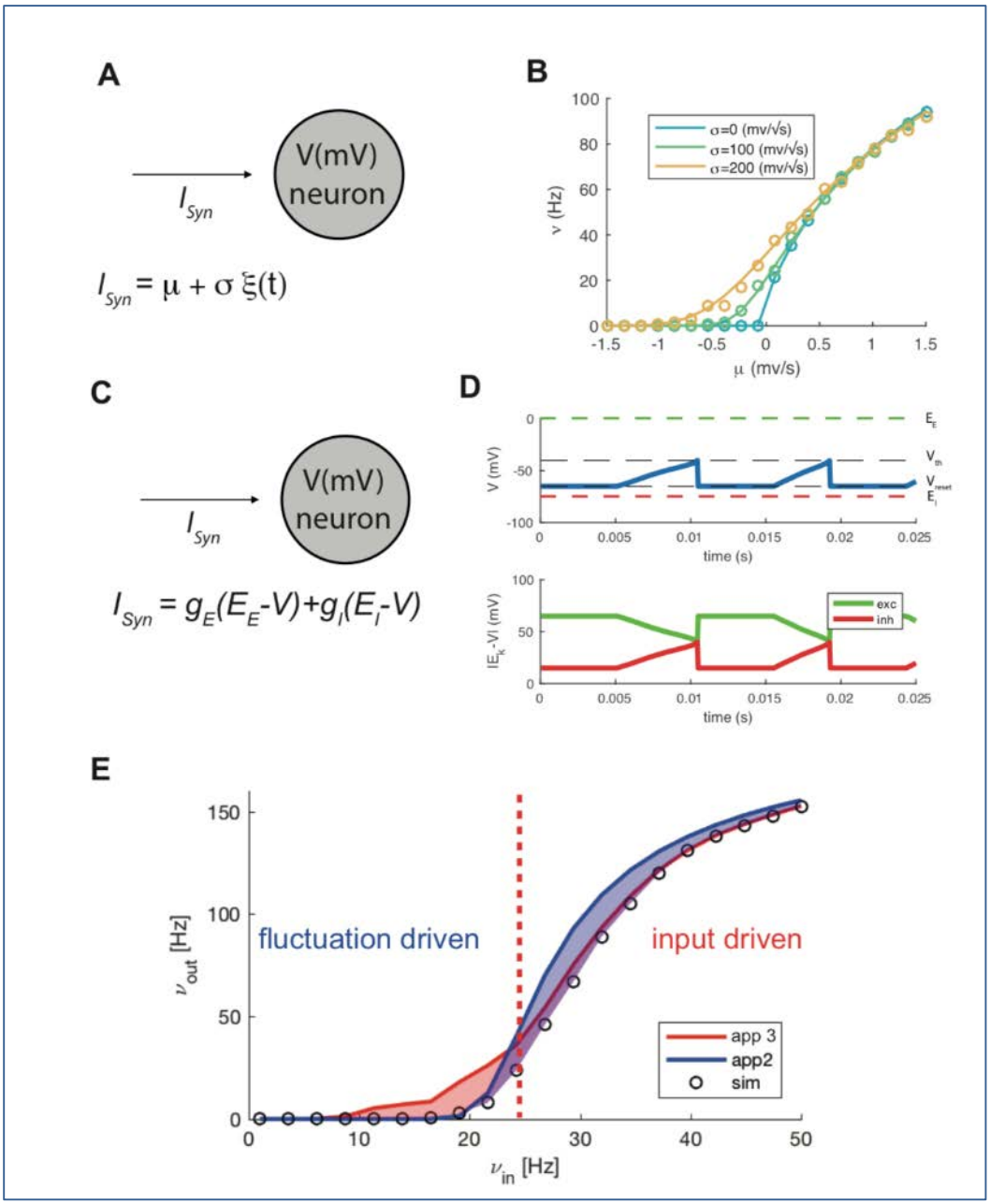

Figure 27: Current-to-rate gain function for AdEx neurons with conductance-based input

A different approximation is applied according to the input regime of the neuron.

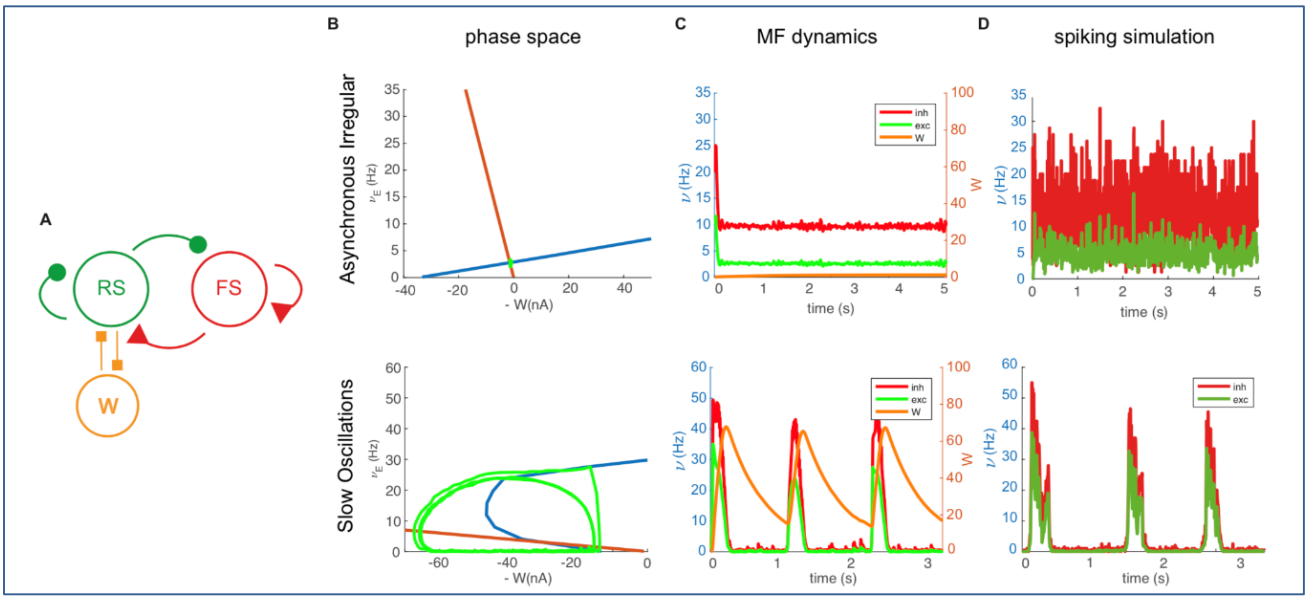

Figure 28: Mean-field dynamics in RS-FS network.

Application of the state-dependent formalism to obtain a mean-field model of alternating Up- and Down-state regimes.

6.1.3 Slow Oscillations

We study how neuromodulation affects dynamics of spontaneous slow wave oscillations in brain slices. We first asked how cholinergic stimulation could affect statistical properties of slow waves (durations of up/down-states and correlations between durations of subsequent up- and down-states). We analysed extracellular recordings in brain slices exhibiting spontaneous slow waves in entorhinal cortex.

Carbachol, a cholinergic agonist, was dissolved in an artificial cerebrospinal fluid (ACSF) to activate cholinergic receptors. Carbachol addition increased slow wave frequency which became more irregular (**Fig. 28**). Down-states disappear for concentrations above 0.1μM. The correlation between durations of subsequent down- and up-states also changes: while without carbachol the correlation is positive i.e. long up-states follow long down-states and short up-states follow short down-states, during cholinergic stimulation the correlation becomes negative (**Fig. 29**).

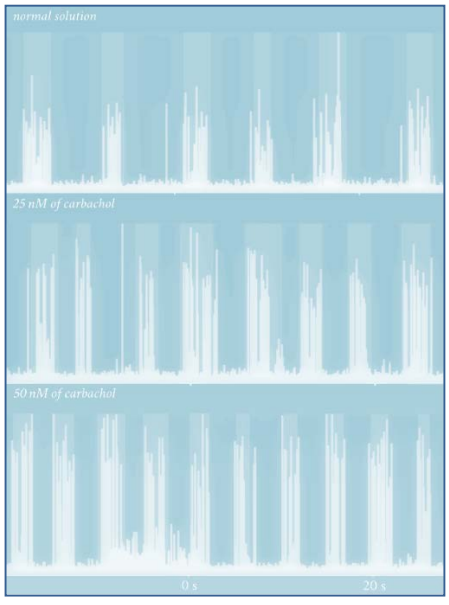

Figure 29: Extracellular recordings of spontaneous slow waves in brain slices with normal ACSF, or Carbachol 25nM and 50nM.

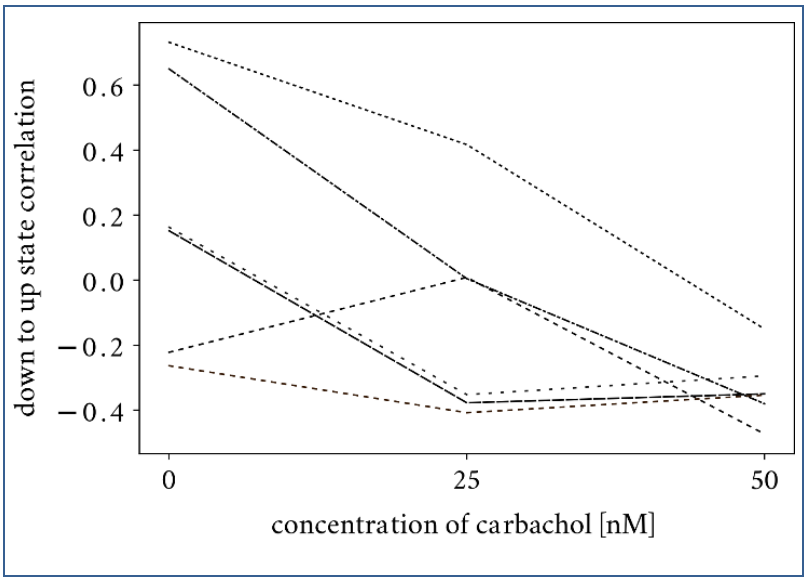

Figure 30: Correlation between UP-state and previous DOWN-state duration

Correlation between UP-state and previous DOWN-state duration as a function of carbachol concentration

The activation of cholinergic receptors is known to decrease spike frequency adaptation in pyramidal neurons (McCormick et al., 1989). To understand how the change of spike frequency adaptation can affect slow wave dynamics, we simulated random directed network of 10^4 neurons with 5% probability of connection. 80% of neurons were regular spiking excitatory cells, 20% were fast spiking inhibitory cells. We used adaptive exponential integrate-and-fire model introduced in (Brette et al., 2005).

Depending on parameters of adaptation or input noise fluctuations, our network can be in asynchronous state or synchronous oscillating state. For high adaptation parameter, the frequency of slow waves is low and waves are regular. The correlation between durations of subsequent down- and up-state is positive. For lower adaptation parameter, frequency increases and for stronger noise fluctuations waves can become irregular and the correlation negative (**Fig. 30**). This behaviour of computational network is in accordance with dynamics of slow waves in brain slices before and after cholinergic stimulation.

Currently, we work on serotonergic modulation of slow waves dynamics. The aim is to adjust the computational model by adding further levels of complexity, by taking into account changes of spike-frequency adaptation, leak conductance of pyramidal neurons and fast spiking inhibitory neurons, and synaptic quantal conductance.

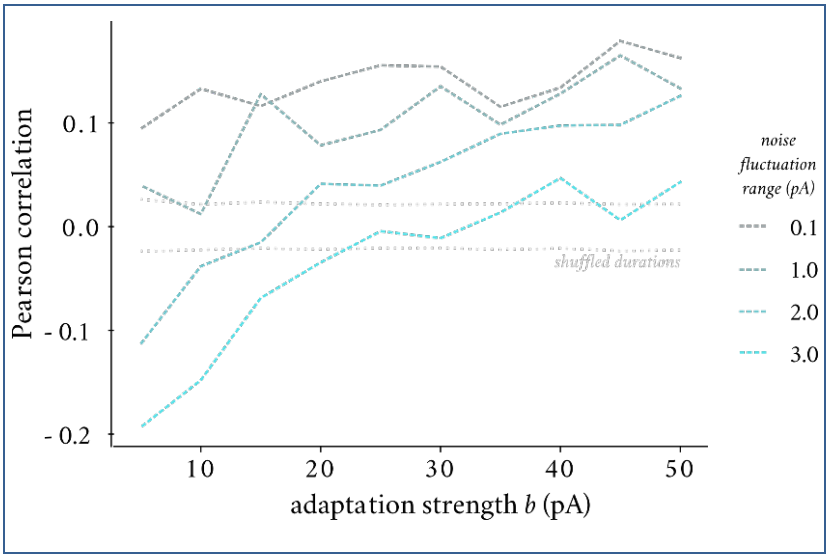

Figure 31: Correlation between DOWN- and subsequent UP-state

Correlation between DOWN- and subsequent UP-state as a function of adaptation (parameter b in the model).

6.1.4 Integration of models in The Virtual Brain

The Virtual Brain (TVB) is a powerful tool for personalized brain-wide modelling, capable of taking into account space-time dynamics over multiple scales by simulating each node of the brain network as a mean-field model (Sanz-Leon et al., 2015; Jirsa et al., 2017). It has, however, remained impossible to study the mechanisms regulating pathological and normal brain states, regulated by changes in spike-frequency adaptation, bursting dynamics, and cellular conductances using the TVB due to a lack of a mean-field model incorporating these parameters.

We have recently developed a mean-field model of adaptive exponential integrate-and-fire neuron networks, with which it is possible to take into account biological differences between brain states (di Volo et al., 2018; Brette and Gerstner, 2005). Using this model, we have found that changing the level of spike frequency adaptation, conductance, and noise results in dynamics associated with the brain state space empirically associated with differing levels of arousal and consciousness. Studying fixed points of the model, we find naturally occurring quasi-stable states attributed to normal brain states including sleep and waking activity, but also aberrant states similar to epileptic seizure.

In collaboration with the laboratory of Prof. Viktor Jirsa, we have prepared the AdEx mean-field model for integration into the framework of TVB. We begin now to explore the mechanisms regulating changes in neural dynamics with brain state for networks of mean-field models constrained by biological data including patch and dynamic clamp electrophysiology; Utah array; voltage and calcium imaging; local field potential (LFP); diffusion weighted magnetic resonance imaging (dw-MRI); electro-encephalography (EEG); and magneto-encephalography (MEG).

We had previously found that spectral energy and entropy vary coherently even between subtly different brain states, dependent on the level of phenomenological coupling in the Kuramoto sense of coupled oscillators (Nghiem et al., 2018), as shown in **Figure 31**. However, biological mechanisms underlying brain state-dependent changes in coupling remained mysterious, necessitating biophysical features from single cells to connected neural networks spanning whole brain circuits. This becomes possible with the AdEx mean-field in TVB. Preliminary evidence from the TVB AdEx suggests that increasing spike frequency adaptation regulates the level of coupling in neural networks, promoting synchronous, regular dynamics found at the level of single cells, reduced spectral entropy, and enhanced spectral energy found in whole brain networks (**Fig. 32**). Using this new tool, mechanisms underlying the differing capacities for processing, encoding, and learning between brain states will be studied through the analysis of spatio-temporal codes within native person-specific neural anatomy.

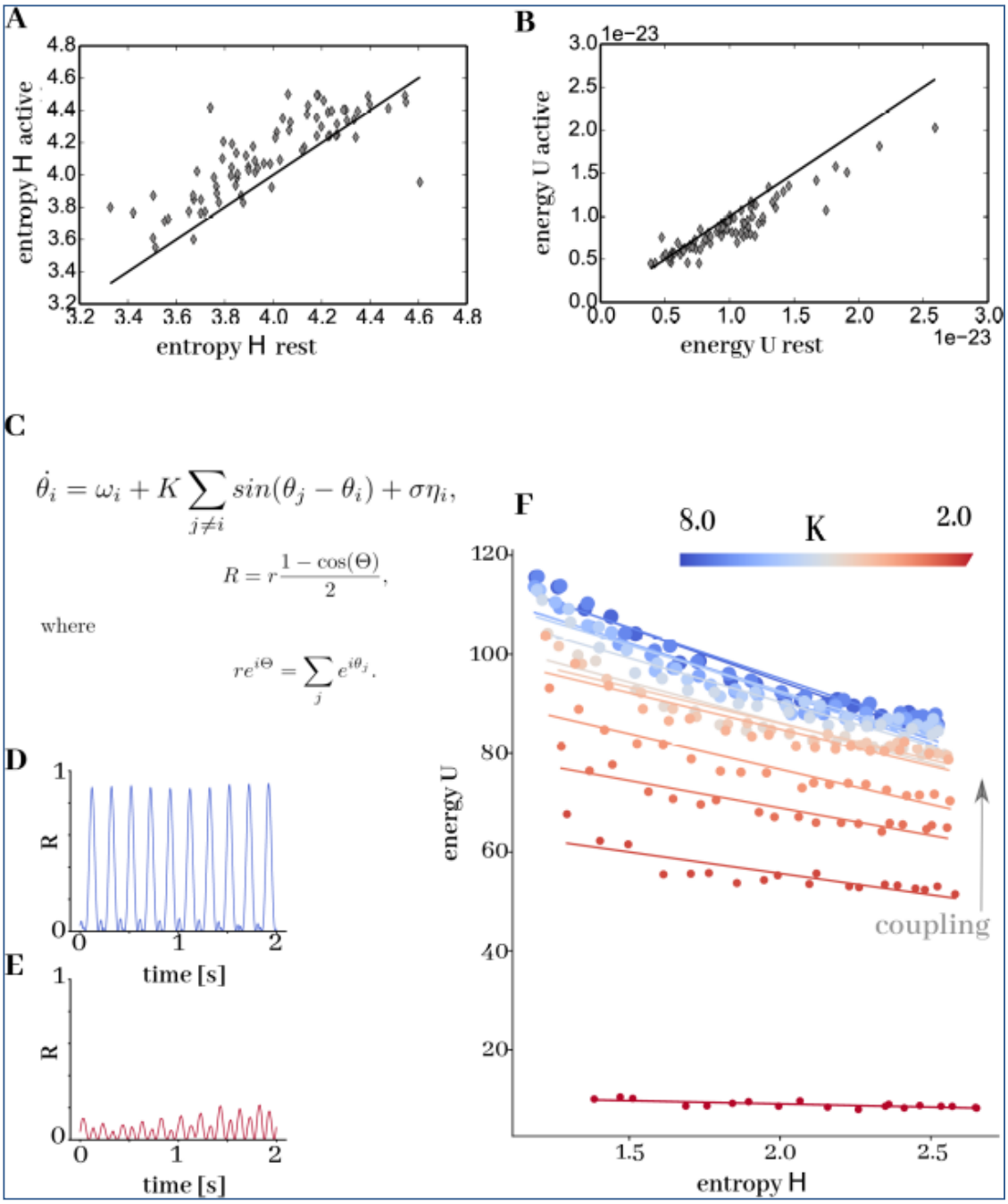

Figure 32: Variation of the spectral energy-entropy relation between brain states is robust across subjects

Mean spectral entropy (A) and mean spectral energy (B) are represented.

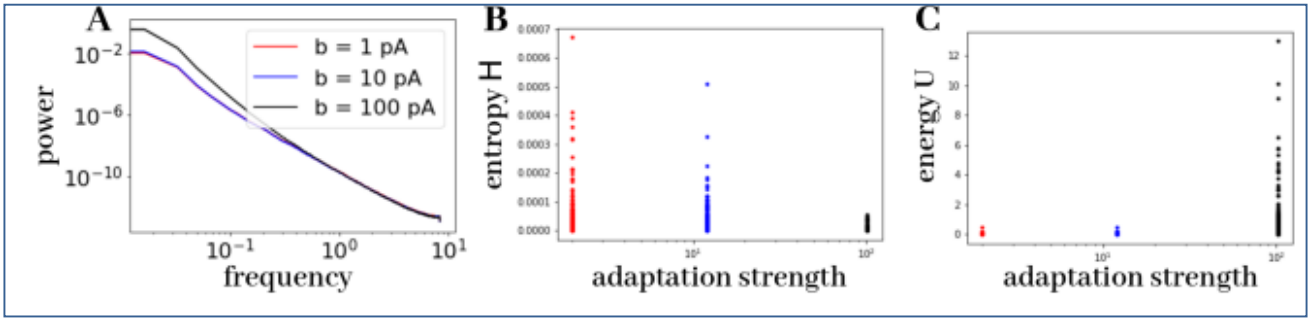

Figure 33: Bridging scales: cellular spike frequency adaptation regulates spectral properties of brain wide neural networks

The adaptive exponential mean-field model (di Volo et al. 2018) was adapted for use in The Virtual Brain (TVB).

6.2 Validation and Impact

Mean-field models, the effect of controlling adaptation, and implementation in the Virtual Brain contribute to our understanding of the mechanisms supporting brain states, their transitions, and computational capacities, with the potential to explain inter-subject differences in neural coding between brain states

6.2.1 Actual Use of Output(s) / Exploitation

The mean-field models are already integrated in TVB, so they participate to the whole-brain models in HBP.

6.2.2 Potential Use of Output(s)

We would like mean-field models to be ported to platforms in the next years, but some work is needed to implement such models in SpiNNaker (a voucher was asked for this, but it was not obtained).

6.2.2 Publications

- Nghiem TAE, Tort-Colet N, Gorski T, Ferrari U, Moghimyfiroozabad S, Goldman JS, ... & Destexhe A (2018). *Cholinergic switch between two different types of slow waves in cerebral cortex.* BioRxiv, 430405.
- Gorski T, Veltz R, Galtier M, Fragnaud H, Goldman JS, Telenczuk B and Destexhe A (2018) *Dendritic sodium spikes endow neurons with inverse firing rate response to correlated synaptic activity.* J. Computational Neurosci. 45: 223-234.
- di Volo M, Romagnoni A, Capone C and Destexhe A. *Biologically realistic mean-field models of conductance-based networks of spiking neurons with adaptation* (2019) Neural Computation 31: 653-680. https://doi.org/10.1101/352393.

Total number of publications: 3

6.2.3 Measures to Increase Impact of Output(s): Dissemination

At the moment, the dissemination is through publications, and pre-prints that are openly available (bioXiv, arXiv).

7. Key Result KR4.5: Validation of spiking network model against experimental data

7.1 Outputs

7.1.1 Overview of Outputs

Table 5: Overview of outputs for Key Result KR4.5

Output	Component number(s)	Component name(s)	Additional information
Tool for Validation Testing on the Level of Network Activity	C1680	Python libraries for structured model validation tests	T4.5.1
Publications on conceptual implementation of model validation in simulation neuroscience	C1863	Concepts for comparison of massively-parallel electrophysiological data	T4.5.1
Mesocircuit model	C2418	4x4mm spatially organised model of a single area	T4.2.1
Biophysical models of brain signals	C2339	Hybrid Schemes for combining point-neuron network simulations in NEST with biophysically detailed NEURON simulations	T4.1.4 Contributes to KR4.1 and KR4.5
	C2340	Biophysical modelling of population signals (LFP, ECoG, EEG, MEG, LMF), with detailed reconstructed neurons	

7.1.2 Tool for Validation testing on the Level of Network Activity

In order to assess the validity of a model, its features must be validated against experimental findings on multiple levels in a rigorous and reproducible fashion. For brain simulations of the scale of neuronal networks and beyond, a key way to assess models' validity is to reproduce the features of population activity dynamics observed in recordings of brain dynamics, e.g. in electrophysiological experiments. The Python library NetworkUnit, which is central to the back-end libraries for validation testing (C1680), represents a tool to formalize the validation process on the level of statistical features of network activity. It is based on the SciUnit framework, making it compatible with complementary validation libraries (i.e. NeuroUnit to validate single neuron models) and easy to integrate into the HBP validation framework. A first release (v0.1.0) of the library was published (https://github.com/INM-6/NetworkUnit), featuring 10 different tests in addition to various scores. In addition to both standard validation models against experimental data, it implements substantiation scenarios where models are compared against other models and/or simulation engines. The library, built on the functionality of the Elephant analysis toolbox (C348) and the generic Neo data model (C361), therefore, represents the technical basis for validation tests for spiking neural network models.

7.1.3 Publications on conceptual implementation of model validation in simulation neuroscience

The concepts of model validation (assessing the validity of models based on experimental data) and model substantiation (assessing the equivalence of models and simulators) have not received as much attention in neuroscience as in other computationally strong sciences. In an initial step, we laid the foundations to transfer concepts of validation testing to the domain of neural network simulations. The results of our work were published in two papers (Trensch et al., 2018 and Gutzen et al., 2018) and include (i) a comprehensive transfer of validation concepts to the domain, including a suggested terminology in line with existing literature and a discussion on differences to validation in other disciplines; (ii) a complete worked example of a substantiation scenario to compare models running on the NEST simulator against implementations on the SpiNNaker neuromorphic hardware; and (iii) an overview of the implementation of the validation process using NetworkUnit (part of C1680). Building on these results, we extended this work to experimental data (Gutzen et al., 2018). Further investigations will include, for example, formalizing the process of relating specific experimental data records to the correct counterparts in the simulation (Fig. 33).

Theoretical work published in preprint format in Dahmen et al. (ArXiv:1711:10930) investigated the intrinsic distribution of covariance statistics in balanced network states. These results are in the process of being validated by experimental data, and will provide a further conceptual aspect in validating activity dynamics based on mathematical understanding. A peer-reviewed publication of the work is in progress.

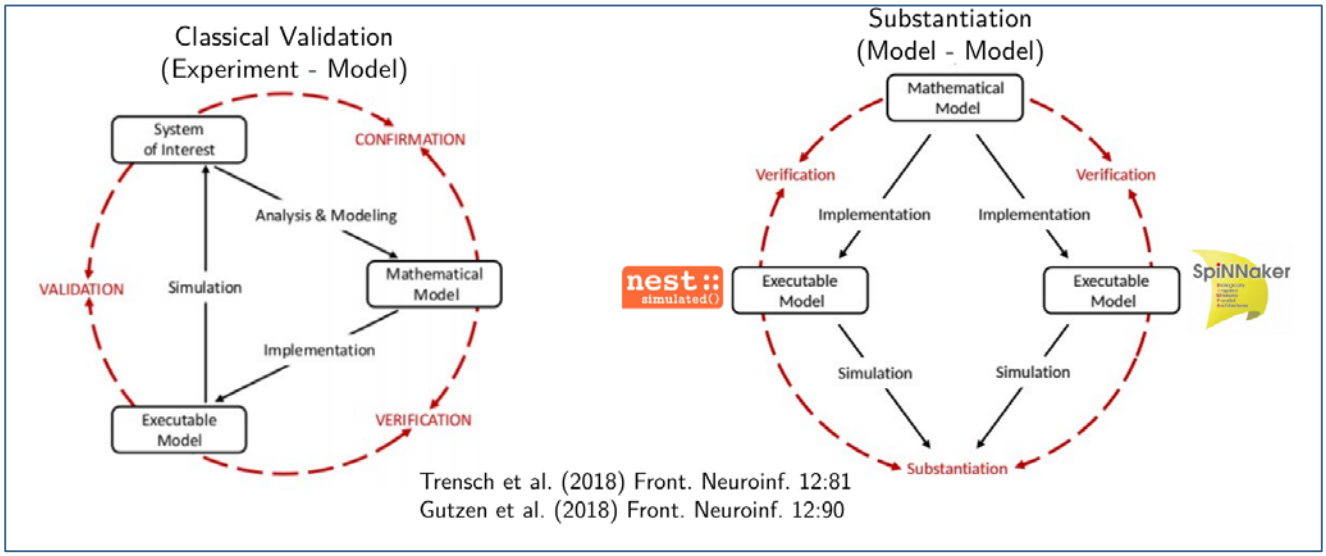

Figure 34 Formalization process of experimental-to-simulated data relationship

7.1.4 Mesocircuit model

We aim to validate simulated model data and experimental data from electrophysiological measurements. This goal requires a network model representing the experimental conditions both in network size and measurement modalities. We have extended a cortical microcircuit model to cover the same surface area as the 4x4 mm² Utah multi-electrode array with 10x10 electrodes. The mesocircuit model accounts for spiking activity and local field potentials. Both signals are accessible in corresponding experiments and the results are published in Senk et al., 2018a (ArXiv:1805.10235).

7.1.5 Biophysical models of brain signals

Our main result is the release and corresponding publication of the open-source software LFPy 2.0 (Hagen et al., 2018, **Fig. 34**) (http://github.com/LFPy/LFPy). This software can simultaneously calculate many different brain signals from arbitrary neural activity, such as the local field potential

(LFP), electro-corticography (ECoG), electro-encephalography (EEG) and magneto-encephalography (MEG), which makes it possible to directly compare simulated results with experimental measurements of many different kinds. Together with collaborators, we have used LFPy in several projects to elucidate the origin and interpretation of LFP signals.

LFPy 2.0 is a vital part of our two components C2339 and C2340, and contributes towards Key Results 4.1 and 4.5. We will make LFPy 2.0 an integrated part of the Brain Simulation Platform and other HBP simulation infrastructure, so that it can be easily used by the research community.

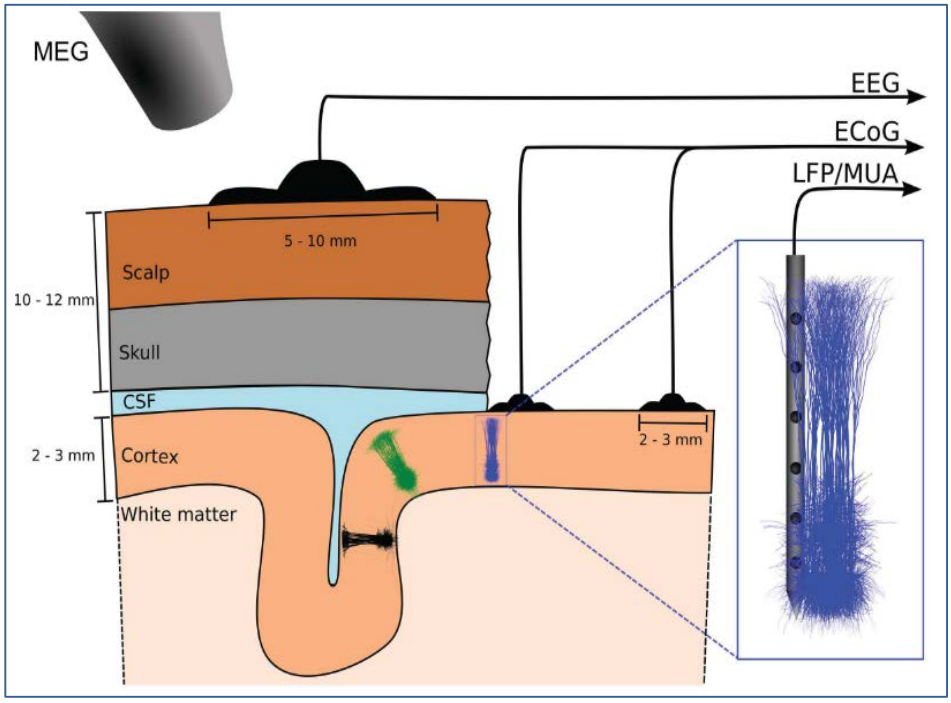

Figure 35: Multimodal modelling of brain signals.

Simultaneous calculation of several brain signals stemming from neural activity can be done with the software LFPy 2.0 (Hagen et al., 2018), ensuring that simulated neural activity can be directly compared with experimental data.

An efficient analytical reduction of detailed non-linear neuron models (Neuron_Reduce)

Detailed conductance-based non-linear neuron models consisting of thousands of synapses are key to the understanding of computational properties of single neurons and large neuronal networks, and for interpreting experimental results. Simulations of these models are computationally expensive, considerably curtailing their utility.

Neuron_Reduce is a new analytical approach to reduce the morphological complexity and computational time of non-linear neuron models (Fig. 35). Synapses and active membrane channels are mapped to the reduced model preserving their transfer impedance to the soma. Synapses with identical transfer impedance are merged into one NEURON process while still retaining their individual activation times. *Neuron_Reduce* accelerates the simulations by 40 to 250 folds for a variety of cell types and realistic number (10,000-100,000) of synapses while closely replicating voltage dynamics and specific dendritic computations.

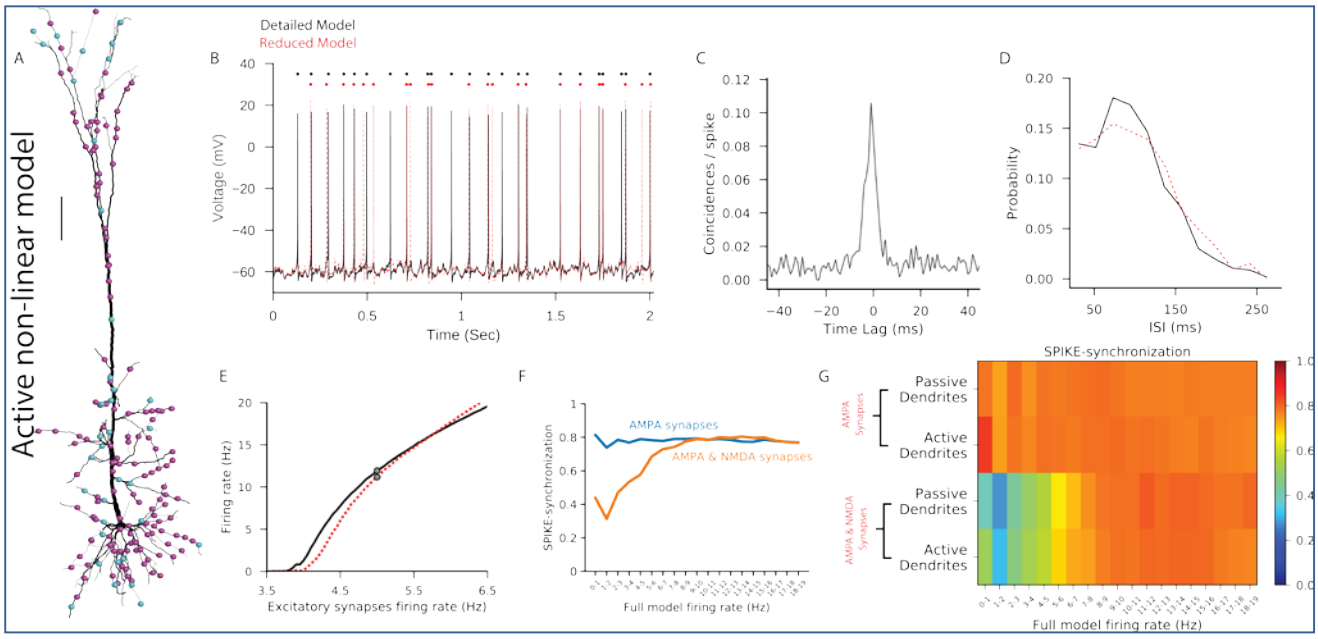

Figure 36: *Neuron_Reduce*, a novel analytical method for reducing neuron model complexity.

Reduction method that faithfully replicated the I/O properties of a detailed non-linear neuron model. A) Layer 5 pyramidal cell model with excitatory (magenta dots) inhibitory synapses (cyan dots. B) An example of the voltage dynamics at the soma of the detailed model (black trace) and the *Neuron_reduced* model (red trace). C) Cross-correlation between spikes in the reduced versus the detailed models. D) Inter-Spike Interval distributions for the two models. E) Output firing rate of the reduced (red) versus the detailed (black) models. F, G) SPIKE-synchronization measure between the two models.

7.1.6 Overview of released components

Table 6: Overview of major Component updates and releases related to Key Result KR4.5

ID	Component Name	Contact	Info on releases and major updates
C2418	4x4mm spatially organised model of a single area	Markus Diesmann	Senk et al. 2018a
C1680	Python libraries for structured model validation tests	Michael Denker	NetworkUnit 0.1.0 (6th Nov 2018) https://github.com/INM-6/NetworkUnit
C1863	Concepts for comparison of massively-parallel electrophysiological	Michael Denker Sonja Gruen	Trensch et al. 2018 Gutzen et al. 2018

7.2 Validation and Impact

Task T4.5.1

The initial release of NetworkUnit was presented at conferences through posters and tutorials, and its impact is strengthened by the accompanying publication.

Task T4.2.1

The mesocircuit model allows direct comparison between simulated and experimental data, which can help to restrict network parameters and explain experimental observations.

Task T4.1.4

We released the software LFPy 2.0 with relative publication. This open-source Python package has proven to be a very useful tool for calculating brain signals from simulated neural activity, and has been used in many scientific publications.

The reduced neuron-models (Neuron_Reduce) will enable realistic simulations of neural networks at unprecedented scale, including networks emerging from micro-connectomics efforts and biologically-inspired "deep networks". *Neuron_Reduce* is publicly available and straightforward to implement (https://www.biorxiv.org/content/10.1101/506485v1).

7.2.1 Actual Use of Output(s) / Exploitation

Task T4.5.1

The NetworkUnit library (within C1680) has been released following validation through extensive validation/substantiation scenario outlined and fully published in Trensch et al., 2018 and Gutzen et al., 2018. The library is currently being further co-designed, in particular in the context of validating spatial dynamics of UP/DOWN-state transitions in experiment and simulation within the HBP (WaveScalES, C2051, C2053), and with respect to development of the 4x4mm spatially organised model of a single area (C2418). In this process, the library will also become more integrated into the developing Validation Framework services of the HBP (e.g. C722). The published results of C1863 directly relate to the NetworkUnit library by providing conceptual and practical blueprints for formalizing model validation and substantiation into a rigorous process, and currently hold an average view rank of 38% in comparison to all articles published in the Frontiers Journals.

Task T4.2.1

A generic version of the mesocircuit model has been published in Senk et al., 2018a. The model is currently further refined to better match experimental data.

Task T4.1.4

LFPy is extensively used within SP4 in our group (NMBU; Gaute Einevoll) for better understanding Local Field Potentials (LFPs). We are currently using LFPy in combination with the large-scale Hippocampus model from SP6 (Michele Migliore). LFPy is used by the group of Markus Diesmann (T4.2.1), in combination with large-scale point-neuron network simulations. Results from LFPy has been used by the group of Hans Ekkehard Plesser (SP7) to calculate Local Field Potentials (LFPs) directly from point-neuron simulations in the NEST Instrumentation App. LFPy is used in a wide range of research projects world-wide. For a list of publications using LFPy see: http://goo.gl/nKuRRE.

We are not aware of any current uses of LFPy by medical or industrial bodies, but we have recently been approached by the developers of a commercial software intended for medical use, who are interested in using LFPy in combination with their product.

We have received very positive feedback from the community. The first publication on LFPy (2014) currently has 88 citations (https://goo.gl/nktaEn). LFPy has been used in more than 20 scientific publications, from both computational and experimental neuroscientists. For a list of publications using LFPy see https://goo.gl/nKuRRE.

7.2.2 Potential Use of Output(s)

Task T4.5.1

The NetworkUnit library represents a first stable initial release ready for use in validation scenarios. However, several changes are expected in the future. In particular: additional tests, improved documentation, inclusion of standard result data types, and a more sophisticated formalization of experimental data based on metadata. The library will become a standard component of HBP's validation framework to enable statistical comparisons of network activity in four areas: 1) to validate models against recordings of activity data from the brain; 2) to compare different models; 3) to substantiate one model implementation against another (e.g. on a different simulation engine); and 4) to contrast dynamics features of different experimental datasets. The library also plays a major role in defining a set of standard data types for the results of activity data analysis, as developed in the HBP Voucher Program. This is to further formalize the connection between the type of results obtained from a validation test and fitting scores, thus allowing to quantify the difference between the two datasets.

Task T4.2.1

The mesocircuit model appears as a component in the long-term roadmap for the construction of multi-area models with spatial resolution in the individual areas.

Once the manuscript on the mesocircuit is accepted by a peer-reviewed journal, an open source repository will be opened as we did in SGA1 for the microcircuit model. We expect that the model will then be used by a larger number of researchers as a building block for more complex models and a test-bed for mean-field and field-theoretical approaches.

Task T4.1.4

LFPy 2.0 is a relatively mature scientific software, ready to be used by the general scientific community. The recently implemented capability of LFPy 2.0 to calculate electro-encephalography (EEG) and magneto-encephalography (MEG) signals makes LFPy valuable for a new group of researchers who work on non-invasive human experiments. LFPy 2.0 will become an integrated part of the Brain Simulation Platform.

7.2.3 Publications

- Pesaran, Vinck, Einevoll, Sirota, Fries, Siegel, Truccolo, Schroeder & Srinivasan (2018). Investigating large-scale brain dynamics using field potential recordings: Analysis and interpretation. *Nature Neuroscience*, 21, 903–919.
    - **Significance:** This paper is a primer on the recording, analysis and interpretation of various types of electrical recordings, specifically recordings of extracellular potentials such as local field potentials and EEG signals. The paper describes both the principles of physics-type forward modelling as well as statistical analysis techniques.
- Ness, Remme & Einevoll (2018). h-Type Membrane Current Shapes the Local Field Potential from Populations of Pyramidal Neurons. *Journal of Neuroscience*, 38(26), 6011–6024.
    - **Significance:** Several previous modelling studies have addressed how populations of neurons with passive dendrites give rise to recorded local field potentials. Here, the authors investigate the putative effects of sub-threshold active dendritic conductances on the generation of local field potentials from populations of pyramidal cells. It is found that in particular the so called h-current can have strong effects on the generated local field potential.
- Luo, Macias, Ness, Einevoll, Zhang & Moss (2018). Neural timing of stimulus events with microsecond precision. *PLoS Biology*, 16(10), 1–22.
    - **Significance:** In this combined experimental and modelling study on the auditory system, the extracellular potential recorded in a midbrain nucleus is used to probe the temporal precision of sound stimuli processing in bats. A remarkable microsecond precision, thought to stem from synchronized neuronal firing in the nucleus, is observed.

Total number of publications: 11

7.2.4 Measures to Increase Impact of Output(s): Dissemination

- JUELICH will participate in the EITN Spring School in Computational Neuroscience 2019 (T4.2.1).
- JUELICH will lead the third annual 2½ week Spring School on Advanced Neural Data Analysis (ANDA) for young scientists, which will feature a demonstration of the NetworkUnit library and potentially practical work based upon it (T4.5.1).
- NetworkUnit has been featured at multiple demos at the German Neuroscience meeting in March 2019 (T4.5.1).

Total number of disseminations: 5

8. Key Result KR4.6: Parameter space confinement of mesocircuit model for the reproduction of experimental data

8.1 Outputs

8.1.1 Overview of Outputs

Table 7: Overview of outputs for Key Result KR4.6

Output	Component number(s)	Component name(s)	Additional information
Spiking mesoscale cortical models with spatial organisation	C2418	4x4mm spatially organised model of a single area	T4.2.1 Contributes to KR4.6, KR4.7, and KR4.9
Comparing activity dynamics of models and living brains	C1574	Structural and functional connectivity at different scales	T4.5.1

8.1.2 Spiking mesoscale cortical models with spatial organisation

The developed mesocircuit model of 4x4mm extends the microcircuit model by Potjans & Diesmann (2014) and introduces distance-dependent connectivity. The model integrates anatomical and electrophysiological data and produces activity comparable to experimental measurements. To date, not enough detailed structural data is available to fully constrain the network parameters. We ran parameter scans within biologically plausible bounds to assess the resulting network activity and found network states that differ qualitatively. Results are published in Senk et al., 2018a.

To visually explore spatio-temporal activity data as emerging in the 2D layers of the mesocircuit model, we implemented the interactive tool VIOLA (VIsualization Of Layer Activity). This joint work with WP7.3 is published in Senk et al., 2018b.

We investigated the origin of spatio-temporal patterns in spiking activity with a simplified 1D model using linear stability analysis and published the results in Senk et al., 2018c.

8.1.3 Comparing activity dynamics of models and living brains

We have used phenomenological models of delay-coupled oscillators with increasing degree of topological complexity to identify underlying principles by which the spatio-temporal structure of the brain governs the phase lags between oscillatory activity at distant regions (**Fig. 36**). Besides in-phase, we have shown that clustered delays can induce anti-phase synchronization for certain frequencies, while lags' sign is determined by natural frequencies and inhomogeneous network interactions. Faster oscillators always phase lead, while stronger connected nodes lag behind the weaker during frequency depression, which consistently arises for *in-silico* results.

We have also shown that the choice of surrogates does not affect the mean of the observed phase lags, but higher significance levels decrease their variance and might fail to detect the generally weaker coherence of the inter-hemispheric links.

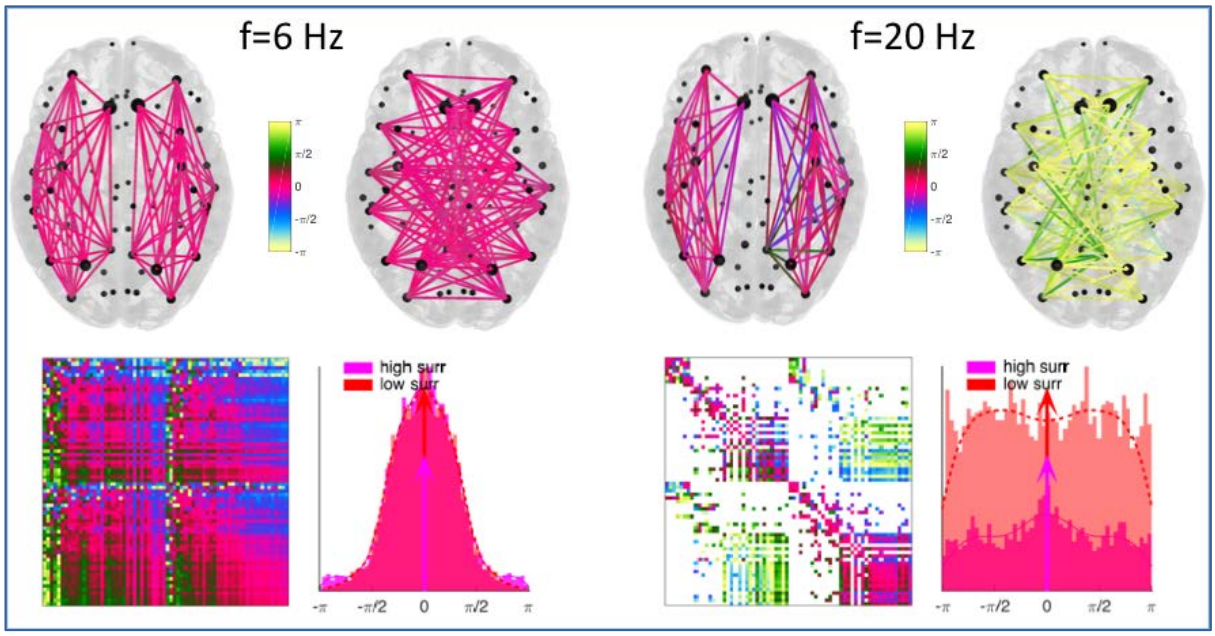

Figure 37: In-phase (left) and anti-phase (right) synchronization between brain hemispheres

Upper plots show sub-networks of 10 strongest regions in each hemisphere, with their internal and external links (left and right). Bottom plots are matrices of phase lags between brain regions ordered by strength within hemisphere, and the overall distribution of phase lags, using two different levels of significance.

8.1.4 Overview of released components

Table 8: Overview of major Component updates and releases related to Key Result KR4.6

ID	Component Name	Contact	Info on releases and major updates
C2418	4x4mm spatially organised model of a single area	Markus Diesmann	Senk et al. 2018a

8.2 Validation and Impact

Task T4.2.1

The mesocircuit model allows for systematic parameter investigations. We make use of simulations with parameter scans, visualization and analytical derivations to explore spatio-temporal features in the network activity.

Task T4.5.1

Our results uncover mechanisms through which the spatio-temporal structure of the brain renders phases to be distributed around 0 and π.

8.2.1 Actual Use of Output(s) / Exploitation

Task T4.2.1

The mesocircuit model can be validated against experimental data (T4.5.1) as it covers the same surface area as the 4x4mm² Utah array and accounts for spiking activity and local field potentials.

The microcircuit has meanwhile been used in 17 peer-reviewed publications and the respective article is cited by 71 peer-reviewed publications. We hope for a similar success for the mesocircuit model. For the publication of the executable model description we will use the latest technology as developed in T4.2.3 for the multi-area model (see KR4.7).

8.2.2 Potential Use of Output(s)

Task T4.2.1

Once the manuscript on the mesocircuit is accepted by a peer-reviewed journal, an open source repository will be opened as we did in SGA1 for the microcircuit model. We expect that the model will then be used by a larger number of researchers as a building block for more complex models and a test-bed for mean-field and field-theoretical approaches.

The mesocircuit model is an essential milestone on the long-term roadmap towards a multi-area model with spatial resolution in the individual areas. Furthermore, the connectivity could be adapted to a specific brain area, e.g. motor cortex, to facilitate the comparison with experimental data (Task T4.5.1).

8.2.3 Publications

- Petkoski S, Palva JM and Jirsa VK. (2018) Phase-lags in large scale brain synchronization: Methodological considerations and in-silico analysis. PloS CB.
    - **Significance:** Functional connectivity and, in particular, phase coupling between distant brain regions may be fundamental in regulating neuronal processing and communication. We use a model of oscillatory dynamics superimposed on the space-time structure defined by the connectome. We show that stronger connected nodes phase lag behind the weaker and we derive the conditions for in- and anti-phase synchronization of brain hemispheres.
- Senk J, Carde C, Hagen E, Kuhlen T, Diesmann M, Weyers B (2018b) *VIOLA - A multi-purpose and web-based visualization tool for neuronal-network simulation output.* Frontiers in Neuroinformatics 12:75
    - **Significance:** We implemented the interactive tool VIOLA (VIsualization Of Layer Activity) to visually explore spatio-temporal activity data as emerging in the 2D layers of the mesocircuit model.

Total number of publications: 6

8.2.4 Measures to Increase Impact of Output(s): Dissemination

Task 4.2.1

A poster of the mesocircuit model was presented at the Bernstein Conference 2018: Senk J; Hagen E; van Albada SJ; Diesmann M (2018d) A mesoscopic layered cortical network model for spiking activity and local field potentials; Bernstein Conference 2018 (T28).

9. Key Result KR4.7: Release of multi-area model of macaque visual cortex, improved using new connectivity and activity data

9.1 Outputs

9.1.1 Overview of Outputs

Table 9: Overview of outputs for Key Result KR4.7

Output	Component number(s)	Component name(s)	Additional information
Multi-area multi-layer spiking cortical models	C730	Multi-area model of cortical network at neuronal resolution	T4.2.3
	C944	Full-density model of cortical microcircuit	T4.2.3

9.1.2 Multi-area multi-layer spiking cortical models

JUELICH finished and published work on a multi-area layered spiking model of all vision-related areas in one hemisphere of macaque cortex (Schmidt et al., 2018a,b; C730). The model represents each area by a 1mm^2 microcircuit with the full density of neurons and synapses, using leaky integrate-and-fire neurons. It reproduces microscopic spiking activity in V1, and fMRI functional connectivity between areas in the resting state, predicated on the system being poised at the edge of stability (**Fig. 37**).

Furthermore, JUELICH with UMAN completed a comparison of the cortical microcircuit model of Potjans and Diesmann (2014) between NEST and SpiNNaker (van Albada et al., 2018; C944). This work demonstrated that SpiNNaker is able to accurately simulate models of this type despite its fixed-point arithmetic, and lays the groundwork for porting even larger models to SpiNNaker. Another JUELICH publication (Maksimov et al., 2018) quantitatively and qualitatively characterizes excitatory-inhibitory balance, membrane potential and neural input stability, and local excitability of cortical networks, enabling computational neuroscientists to constrain their models accordingly.

The described microcircuit and multi-area models have a number of simplifications and limitations that JUELICH has started to address. In the microcircuit, the role of separate somatostatin (SOM), parvalbumin (PV), and vasoactive intestinal peptide-expressing (VIP) interneuron populations and their specific connectivity are being investigated. With the help of this refinement, JUELICH has started to model cell-type-specific neuromodulation by acetylcholine in the microcircuit. In the context of CDP4, the multi-area model is being extended with motor-related cortical areas, which will enable visuo-motor interactions to be investigated. The cortico-cortical connectivity is taken from axonal tracing data from the CoCoMac database and complemented with predictive connectomics. A motor cortex microcircuit model taking into account its specific architecture and connectivity is under development. In collaboration with TUGRAZ, JUELICH has started to bring together anatomical constraints with functional performance of cortical microcircuits using the learning-to-learn framework (Bellec et al., 2018). Finally, JUELICH has started collaborating with KU Leuven on modelling covert visual spatial attention and relating the model activity to V6/V6A recordings in macaque.

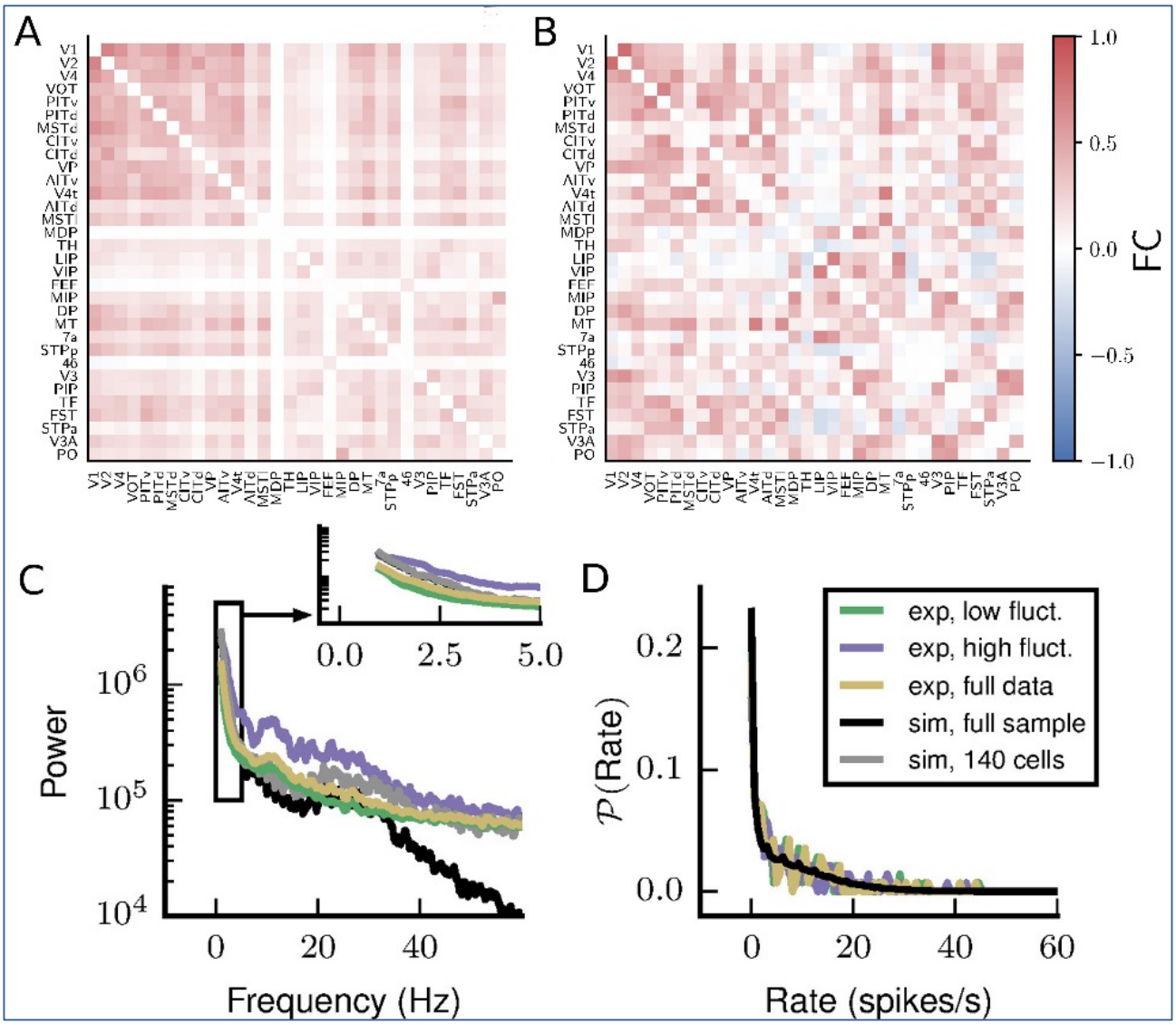

Figure 38: Dynamics of the multi-area model of macaque vision-related cortex

A) Simulated inter-area functional connectivity. B) Resting-state fMRI functional connectivity, averaged across 6 monkeys. C) Spectra of experimental and simulated V1 spiking activity. D) Distribution of spike rates across single neurons in V1. Green and purple curves, statistics of experimental spiking data in phases with a low resp. high level of fluctuations in the population activity. Yellow curves, statistics for low- and high-fluctuation phases combined. Black curves, statistics for the simulated spiking activity of V1. Gray curves, statistics for 140 neurons randomly sampled from V1 in the model.

9.1.3 Overview of released components

Table 10: Overview of major Component updates and releases related to Key Result KR4.7

ID	Component Name	Contact	Info on releases and major updates
C730	Multi-area model of cortical network at neuronal resolution	Sacha van Albada	Schmidt et al. 2018a,b
C944	Full-density model of cortical microcircuit	Sacha van Albada	van Albada et al. 2018

9.2 Validation and Impact

Task T4.2.3

The multi-area model of macaque vision-related cortex serves as a platform for further model developments: refinements; extensions with further brain areas; application of the methods to build models of the cortex of other species; and incorporation of functional properties to yield models that can solve behavioural tasks. Current efforts in this direction include modelling of human cortex in DFG SPP 2041; extension with motor areas in the context of CDP4; and combination of the learning-to-learn framework (Maass, SP9) with anatomical constraints of the cortical microcircuit. The multi-area model further serves as a key use-case for HPC and as a key planned use case for SpiNNaker. The microcircuit model serves as a use-case for the BrainScaleS hardware.

9.2.1 Actual Use of Output(s) / Exploitation

Task T4.2.3

An executable formal model description of the multi-area model of all vision-related areas of macaque cortex (Schmidt et al., 2018a,b) was made available on GitHub (https://inm-6.github.io/multi-area-model/), enabling others to build on the code. So far, it is watched by 2 external users, starred by 9 external users, and forked by 6 external users (outside JUELICH INM-6). The total number of external users interacting with the repository so far is 16. This includes people both inside and outside the HBP.

A tutorial video was published on YouTube (https://www.youtube.com/watch?v=YsH3BcyZBcU), available also in the HBP Education channel (https://www.youtube.com/watch?v=NGAqe78vmHY) and via the NEST simulator website (http://www.nest-simulator.org/), and has already received >1200 views. The videos have so far received 27 up-votes and no down-votes.

The publications on the multi-area model (Schmidt et al., 2018a,b; Schmidt et al., arXiv 2015) have been cited 25 times to date. The NEST-SpiNNaker comparison of the microcircuit model (van Albada et al. 2018) has been cited 10 times to date. The publication was already viewed 18,262 times and ranks in the top 2% of papers viewed in the journal.

9.2.2 Potential Use of Output(s)

Task T4.2.3

Estimated Technology Readiness Level (TRL) is 4 for the multi-area model and 8 for the microcircuit model.

Besides the uses already started or planned, mentioned above, the multi-area model could form a “growth nucleus” for increasingly integrated and validated models of the primate brain, including sub-cortical structures such as thalamus and basal ganglia, and validated on a wider range of experimental data, from spiking data to LFP, EEG, and fMRI, to support an integrated multi-scale understanding of the brain.

9.2.3 Publications

- Schmidt M, Bakker R, Hilgetag CC, Diesmann M, van Albada SJ (2018a) *Multi-scale account of the network structure of macaque visual cortex*, Brain Struct Func 223(3):1409-1435.
  - **Significance:** This publication describes the first derivation of an area-, layer-, and population-resolved connectivity map for all vision-related areas in one hemisphere of macaque cerebral cortex, which can serve to define neural network models for simulation.
- Schmidt M, Bakker R, Shen K, Bezgin G, Diesmann M, van Albada SJ (2018b) *A multi-scale layer-resolved spiking network model of resting-state dynamics in macaque visual cortical areas*, PLoS CB 14:e1006359.
  - **Significance:** In this work, the connectivity map from Schmidt et al., 2018a is used as the basis for spiking neural network simulations of all vision-related areas in one hemisphere of macaque cortex, forming the first neural network simulation of this scope using the full

density of neurons and synapses. The network dynamics is shown to conform to multi-scale experimental findings, so that the model can serve as a platform for further models of mammalian cerebral cortex.

- van Albada SJ, Rowley AG, Senk J, Hopkins M, Schmidt M, Stokes AB, Lester DR, Diesmann M, Furber SB (2018) Performance comparison of the digital neuromorphic hardware SpiNNaker and the neural network simulation software NEST for a full-scale cortical microcircuit model, Front Neurosci 12:291.
    - **Significance:** This paper describes the porting of a cortical microcircuit model with the full density of neurons and synapses to SpiNNaker and characterizes the performance of the neuromorphic hardware in comparison with NEST, thus guiding the development of SpiNNaker to make it available for large-scale neural network simulations with short biological time scales.

Total number of publications: 3

9.2.4 Measures to Increase Impact of Output(s): Dissemination

Task T4.2.3

- The multi-area model was made available via GitHub and a corresponding tutorial video was posted on YouTube, as described above.
- The publication van Albada et al., 2018 (Front Neurosci) on the SpiNNaker-NEST comparison of the cortical microcircuit model of Potjans & Diesmann (Cereb Cortex, 2014) was disseminated extensively, both locally and in the media (e.g. Frontiers Communications, TOP500, DNA India, HPCwire, Science Friday radio show, Science Node magazine, TheScienceBreaker, Forschungszentrum Jülich and University of Manchester websites). As of January 2019, the paper was viewed more than 17,000 times and it ranks among the 2% most viewed papers in the respective journal.
- The microcircuit and multi-area models were presented at various conferences and workshops (e.g. Netherlands Institute for Neuroscience, Amsterdam; 13th Neural Coding Conference, Torino; CNS 2018 (Seattle) and Bernstein conference 2018 (Berlin) workshops; SBMT 15th Annual Congress, Los Angeles; SpiNNaker 1 million event, video here; RWTH Aachen University; KTH Stockholm; Brain Research Center, Bar-Ilan University; Universidad de Chile, Santiago; Road to Reality Symposium, video here; workshops in Ischia and Sao Paulo)

10. Key Result KR4.8: Release of draft implementation of generic network model with glial contribution

10.1 Outputs

10.1.1 Overview of Outputs

Table 11: Overview of outputs for Key Result KR4.8

Output	Component number(s)	Component name(s)	Additional information
Neuronal-glial network model	C2359	Prototype spiking neuronal network model, including simplified version of the astrocyte-neuron interaction model to explain *in vitro* cell culture data	T4.2.2
Order reduction for network models	C2358	Simplified, generic astrocyte-neuron interaction model, with built-in model order reduction	T4.2.2

10.1.2 Neuronal-glial network model

Understanding the role of glial cells in brain functions is of fundamental interest to neuroscience and theoretical neuroscience. This includes the regulation of information propagation by astroglial cells. We implement key mechanisms of astrocytes modulating the information propagation in generic neuronal network models (C2359). The astrocyte component of interest is the so-called 'Slow Inward Current' (SIC), an excitatory current via post-synaptic NMDA receptors (Pirttimaki et al., 2017; Manninen et al., 2019). We additionally constrain the astrocyte influences using unpublished data on astrocyte locations and morphologies, produced by SP1 (DeFelipe group). The first version of the model is implemented to test the role of SIC on information propagation and network synchronization. The generic neuronal network model with glial contribution will be extended to Potjans-Diesmann model (Potjans and Diesmann, 2014) which maps the realistic distribution of excitatory and inhibitory neurons across cortical layers as well as the connectivity within and between layers.

10.1.3 Order reduction for network models

The current trend in theoretical and computational neuroscience is to incorporate multiple physical levels of the brain into mathematical models, which often results in large networks of interconnected neurons and other brain cells, i.e. high-dimensional numerical models that correspond to equally high computational demand. Model order reduction methods, adapted from control and systems theory, have not been extensively used in the field. We performed bench-marking of five different variants of POD (Proper Orthogonal Decomposition) and DEIM (Discrete Empirical Interpolation Method) methods. As a test case, we used a network of 50 compartmental Hodgkin-Huxley cells, based on a neuron model with dendritic and somatic compartment (Pinsky and Rinzel, 1994), resulting in a system of 500 coupled non-linear ordinary differential equations. The results showed that the reduced order model consumes a smaller amount of computational resources than the original model (Fig. 38, Lehtimäki et al., submitted; C2358). The population behaviour of

the reduced model starts to change with lower dimensions. We conclude that the work shows the potential benefits of the POD+DEIM method, while also giving insights into the limitations of the method.

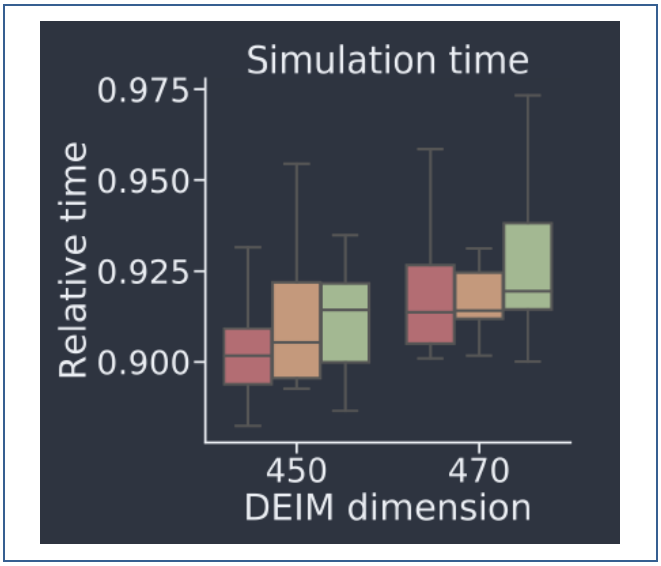

Figure 39: Reduction of simulation time with different POD and DEIM dimension (POD dimensions: Green 480; Yellow 460; Red 420).

10.1.4 Overview of released components

Table 12: Overview of major Component updates and releases related to Key Result KR4.8

ID	Component Name	Contact	Info on releases and major updates
C2358	Simplified generic astrocyte-neuron interaction model with built-in model order reduction	Marja-Leena Linne	Lehtimäki et al. (submitted publication)

10.2 Validation and Impact

Task T4.2.2

The neuronal-glial network model will have an impact on understanding the influence of glial cells in information propagation in the brain (scientific impact). Order reduction for network models provides an alternative approach to simplify models and has a potential to impact the development of neural simulators.

10.2.1 Actual Use of Output(s) / Exploitation

Task T4.2.2

Neuronal-glial network model (output 1) and order reduction for network models (output 2) are used by SP6 Simulation Platform, and other platform developers such as NEST and SpiNNaker (network models with glial influence; MS4.2.2.). None of these tools currently have the capacity to incorporate the influence from glial cells. The bioscience community outside the HBP is also very interested in applying the models developed by us to their work. The models developed will also be used in the EU Era-Net Neuron project on understanding the causes of schizophrenia.

10.2.2 Potential Use of Output(s)

Task T4.2.2

We are in the specification and implementation phase, in which we are testing various implementational approaches and methodologies for both the glial modelling and model order reduction. We expect a large exploitation of the components.

10.2.3 Publications

- Manninen T, Havela R, Linne ML (2019) *Computational models of astrocytes and astrocyte-neuron interactions: Categorization, analysis, and future perspectives*, Computational Glioscience, editors M. De Pitta and H. Berry, Springer. (Neuronal-glial network model)
    - **Significance:** The study provides detailed analysis of existing computational models of astrocytes. This analysis forms the basis for selecting the biological mechanisms linking astrocytes to neuronal networks functions. HBP SGA2 T4.2.2 is using these results to create new modules for the generic astrocyte-neuron network models.

Total number of publications: 3

10.2.4 Measures to Increase Impact of Output(s): Dissemination

Task T4.2.2

The results have been disseminated in the following meetings:

- Organization for Computational Neuroscience Conference (Seattle, USA, July 2018);
- Society for Neuroscience (San Diego, USA, November 2018);
- 3rd HBP Student Conference (Ghent, Belgium, February 2019; best poster prize).

11. Key Result KR4.9: Release of draft multi-layered cortical network model with spatially organised connectivity

11.1 Outputs

11.1.1 Overview of Outputs

Table 13: Overview of outputs for Key Result KR4.9

Output	Component number(s)	Component name(s)	Additional information
Mesocircuit model	C2418	4x4mm spatially organised model of a single area	T4.2.1 Contributes to KR4.6, KR4.7, and KR4.9

11.1.2 Mesocircuit model

We released the implementation of the mesocircuit model corresponding to Senk et al., 2018a internally in the HBP Collaboratory. The model accounts for spiking activity and local field potentials.

11.1.3 Overview of released components

Table 14: Overview of major Component updates and releases related to Key Result KR4.9

ID	Component Name	Contact	Info on releases and major updates
C2418	4x4mm spatially organised model of a single area	Markus Diesmann	Senk et al. 2018a

11.2 Validation and Impact

The mesocircuit model allows for systematic parameter investigations. We make use of simulations with parameter scans, visualization and analytical derivations to explore spatio-temporal features in the network activity.

11.2.1 Actual Use of Output(s) / Exploitation

See KR4.5

11.2.2 Potential Use of Output(s)

See KR4.5

11.2.3 Publications

- Upscaling of the spiking cortical microcircuit model by Potjans & Diesmann (2014) to the mesocircuit model, parameter investigation and forward modelling of local field potentials: Senk J, Hagen E, van Albada S, Diesmann M (2018a), Reconciliation of weak pair-wise spike-train correlations and highly coherent local field potentials across space. ArXiv:1805.10235
    - **Significance:** The developed mesocircuit model of 4x4 mm² extends the microcircuit model by Potjans & Diesmann (2014) and introduces distance-dependent connectivity. The model integrates anatomical and electrophysiological data and produces activity comparable to experimental measurements. To date, not enough detailed structural data is available to fully constrain the network parameters. We ran parameter scans within biologically plausible bounds to assess the resulting network activity and found network states that differ qualitatively.

Total number of publications: 1

11.2.4 Measures to Increase Impact of Output(s): Dissemination

See KR4.6.

12. Key Result KR4.10: Demonstration that brain personalised network models have predictive value for epileptogenic zones of individual patients

12.1 Outputs

12.1.1 Overview of Outputs

Table 15: Overview of outputs for Key Result KR4.10

Output	Component number(s)	Component name(s)	Additional information
Human brain function from structure	C1861	Improving identification of the epileptogenic zone	T4.5.3
	C1862	Personalised brain models for predicting seizure propagation	

12.1.2 Human brain function from structure

Task T4.5.3

Within this task, AMU group has worked on minimally invasive network interventions for stopping the seizure propagation in epileptic patients, and on explaining specific seizure onset pattern observed on a depth electrode in some epileptic patients. To do this, we have built human whole-brain network models based on personalized DTI-derived connectome data using Epileptor neural mass model and its extension for wave propagation for the study of epileptic activity, as well as 2D oscillator close to Hopf bifurcation for the study of healthy activity propagation.

The extended Epileptor has been used to demonstrate by means of numerical simulation that the features of the so-called theta-alpha activity at seizure onset pattern observed on a depth electrode in a specific epileptic patient can be plausibly explained by the seizure propagation across an individual folded cortical surface. The results also indicate that the spectral content and dynamical features might differ in the source space of the cortical gray matter activity and among the intracranial sensors, questioning the previous approaches to classification of seizure onset patterns done in the sensor space, both based on spectral content and on dynamical features.

With respect to the network interventions, we have studied two approaches: 1) the most invasive lesion of the direct links to the epileptogenic zone (EZ), and 2) targeting nodes or links outside the EZ (**Fig. 39**). For the former, linear stability analysis was applied to the reduced Epileptor, uncovering significant reduction of the necessary lesions needed to stop the seizure compared to other possible strategies. In addition, the importance of the individualized connectome was also demonstrated. The second approach is relevant for a considerable number of patients who have EZs that are distributed across multiple brain regions and may involve eloquent areas that cannot be removed due to the risk of neurological complications. Based on the clinically identified EZ, we employ modularity analysis to identify target brain regions and fiber tracts involved in seizure propagation. In addition, we assess safety via electrical stimulation for pre- and post-surgical condition to quantify the impact on the signal transmission properties of the network.

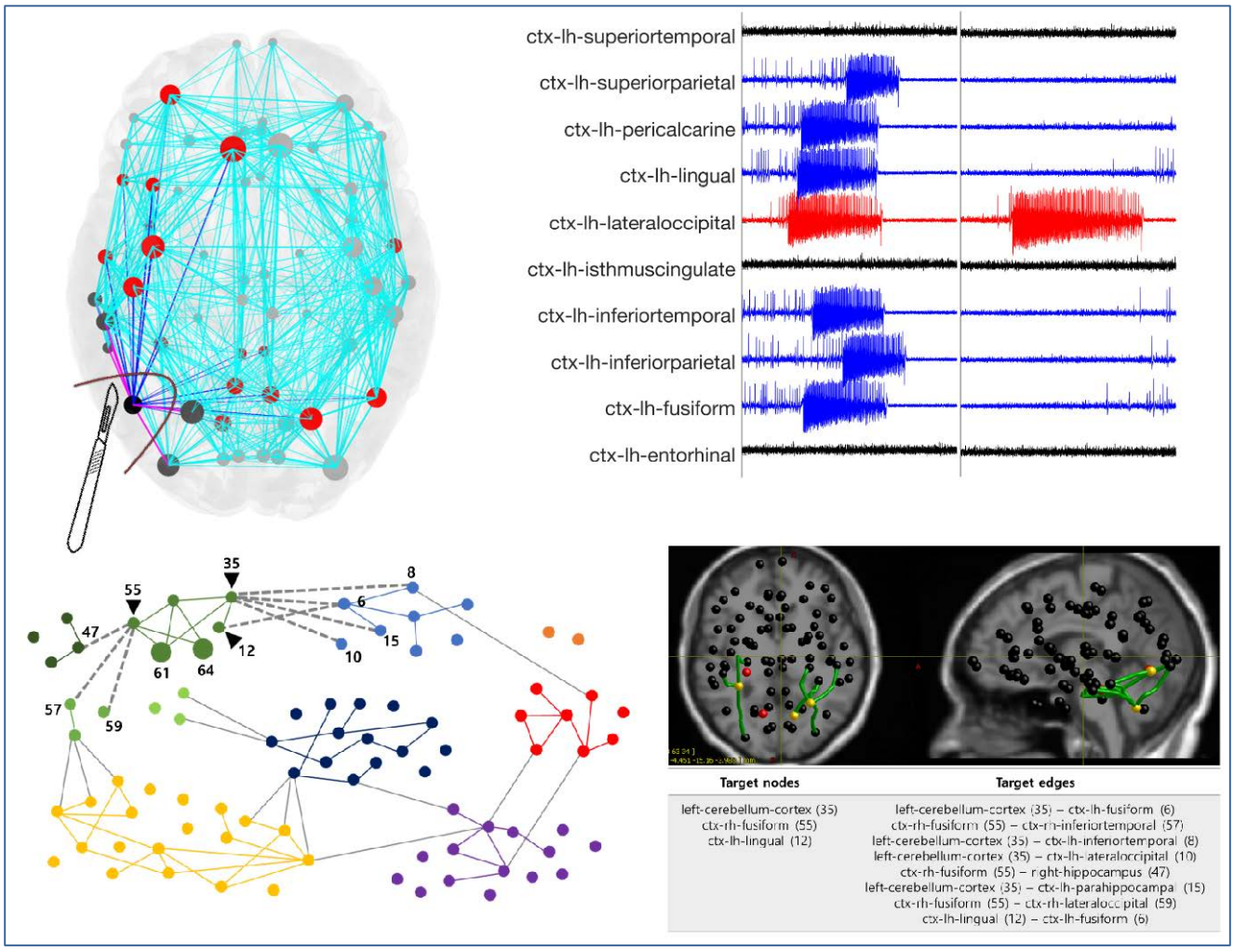

Figure 40: Minimally invasive resections for epileptic patients.

Top: scheme of standard resection (removal of the entire EZ) versus lesioning minimal number of links (left) and the epileptic activity before and after the intervention (right). Bottom: TZs derived from the modularity analysis when setting EZs to inoperable zones. The brain network is divided into seven modules and the EZ (nodes 61 and 64, large circles), based on which three nodes (triangles) and eight edges (dotted lines) are derived as target nodes and edges. Anatomical locations and list of the newly obtained TZs are shown on the bottom right.

12.2 Validation and Impact

The newly developed resections techniques should lead to much less invasive surgical procedures for epileptic patients, compared to the current procedures. Moreover, they can be applied to patients who have EZs involving areas that cannot be removed due to the risk of neurological complications. For the latter, a safety assessment procedure involving electrical stimulation has also been developed.

12.2.1 Actual Use of Output(s) / Exploitation

The results will be used by the computational and theoretical neuroscience community, as well by clinicians working with epileptic patients.

12.2.2 Potential Use of Output(s)

The proposed procedures have clinical application potential for performing surgical procedures on epileptic patients.

12.2.3 Publications

- Olmi S, Petkoski S, Guye M, Bartolomei F, & Jirsa V (2019). *Controlling seizure propagation in large-scale brain networks*. PLoS computational biology, 15(2), e1006805.
  - **Significance:** Epilepsy is characterized by perturbed dynamics that originate in a local network before spreading to other brain regions. For patient-specific brain network models of epilepsy we developed a seizure control strategy that is significantly less invasive than traditional surgery. Being entirely based on structural data, our approach allows creation of a brain model based on purely non-invasive data prior to any surgery.

Total number of publications: 3

12.2.4 Measures to Increase Impact of Output(s): Dissemination

- Poster presentation and a tutorial at SfN meeting 2018, San Diego, USA.
- Tutorial at ICT 2018, Wien, Austria.
- Poster presentation at a Brain Initiative Investigators meeting, Rockville, USA.

13. Key Result KR4.11: Demonstration of explanatory value of large-scale brain network mouse models with impaired connectivity and dysfunctional network

13.1 Outputs

13.1.1 Overview of Outputs

Table 16: Overview of outputs for Key Result KR4.11

Output	Component number(s)	Component name(s)	Additional information
Mouse brain function from structure	C1606	Mouse stroke brain network model	T4.5.2
	C2495	Compare experimental and theoretical data: mouse resting state functional connectivity	
	C998	Allen Mouse Brain Atlas-based brain network	T4.5.2

13.1.2 Mouse brain function from structure

Task T4.5.2

AMU has continued the work on a Mouse Brain Model for simulating the rehabilitation experiment defined in CDP1: calcium analysis for 5 mice during 5 weeks (one week before stroke, and 4 weeks

of rehabilitation on the M platform). The brain network model for the resting state activity is built using the open source tracer dataset of the Allen Institute that was implemented into The Virtual Brain (TVB), thus allowing detailed Structural Connectivity (SC) to be obtained. Experimental calcium data are used in a close loop validation system to model the cortical activity of the mouse, as reflected in the Functional Connectivity (FC) between distant brain regions. Compared to the SGA1 results, the experiment also contains the activity of several regions in the healthy hemisphere, thus allowing better modelling of the dynamical network reorganization during stroke and recovery (**Fig. 40**).

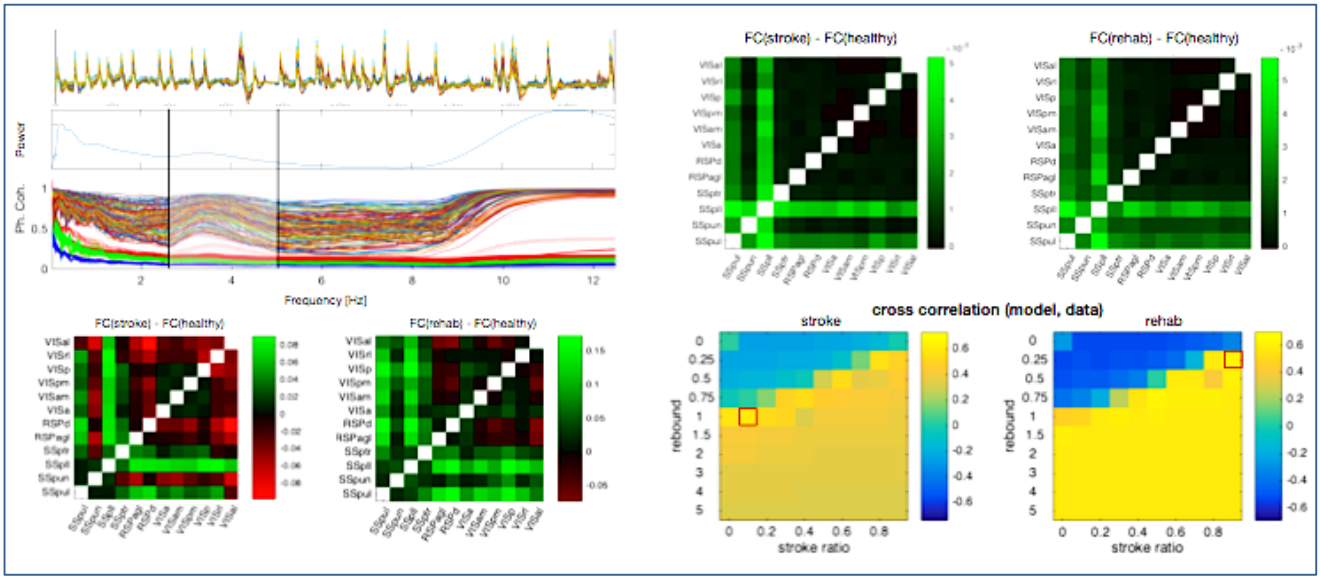

Figure 41: Comparison of empirical versus simulated FC.

Time-series, phase coherence and FC from calcium imaging empirical data (left), and FC from the model and cross-correlation between the model and the data (right). Relative changes of the FC are shown at stroke and after the rehabilitation compared to the healthy control for frequency band f=2.5-5Hz.

13.2 Validation and Impact

13.2.1 Actual Use of Output(s) / Exploitation

The model is built as part of our collaboration in CDP1. It is used by experimental neuroscientists who conduct experiments in rodent stroke models and calcium imaging. It has also a wider application for the computational neuroscientists working on rodent whole-brain modelling.

13.2.2 Potential Use of Output(s)

In line with CDP1's objectives, we plan to integrate both the model's output and the experiment within the Neurorobotic Platform, thus building a closed-loop for validation of different hypotheses in stroke research.

Additionally, it could be used for novel and improved strategies for rehabilitation after stroke.

13.2.3 Measures to Increase Impact of Output(s): Dissemination

- Poster presentation at a Brain Initiative Investigators meeting, Rockville, USA.
- Oral presentation at Stroke meeting in Florence, Italy

- Oral presentation at lab retreat, INS retreat 2018.

14. SP4 Tasks contributing to other SPs or to CDPs

The following Key Results contribute to tasks relevant to work done in SP4, without being mapped to any Key Result in SP4. These Key Results are part of other SPs or of CDPs that involve SP4.

15. Key Result KR3.3: Acquisition of brain imaging and electrophysiological recording, models of multisensory integration and spatial memory and navigation, and brain-inspired robots (i.e. visual-tactile rodent-like robot and a humanoid robot)

15.1 Outputs

15.1.1 Overview of Outputs

Table 17: Overview of outputs for Key Result KR3.3

Output	Component number(s)	Component name(s)	Additional information
Models of spatial memory	C984	Hippocampal and striatal model of navigation, extended to planning and memory	T4.4.4
	C2408	Simulated spatial neural firing patterns in freely moving rodents during spatial navigation and planning, for comparison with electrophysiological data	
	C2409	High-level (firing rate) model of visuo-spatial episodic memory	
	C2500	High-level model of spatial navigation for guiding autonomous agents	

15.1.2 Models of spatial memory

C984 from SGA1, continued as C2500 in SGA2

We developed a network model of firing-rate coded neurons in hippocampus and striatum which performs spatial navigation (C984). This model is used to investigate the different learning rules (temporal difference in striatum, incidental in hippocampus) and representations (e.g. sensory/action in striatum, and place cells etc. in hippocampus) involved in spatial navigation, and how they combine to guide action. The output is behaviour in classic navigation tasks used in rodents, neural firing characteristics, effects of lesions and behaviour. These outputs are compared with data from the literature. In C2500 this model is extended to general (non-spatial) decision-making and planning, and compared with classic tasks such as the 'two-step task' (Daw, Gershman, Seymour et al., 2011). The manuscript is being prepared for publication (Geerts, Chersi, Stachenfeld, Burgess, in preparation).

C2408

We are developing a simulation of the neural firing patterns in freely moving rodents during spatial navigation, to examine how self-motion information and environmental sensory information are combined in neural representations of self-location. This model is based on the principals of Simultaneous Localisation and Mapping (SLAM) in robotics. The outputs (neural firing patterns) are compared with electrophysiological data in situations where the influences on neural firing of self-motion and environmental inputs can be separated (with SP3 Episense, Cacucci lab, recently published: Chen et al., Nature Comms, 2019 10: 630). A manuscript is being prepared for publication (Evans & Burgess, in preparation).

C2409

We have developed a model of the neural representations of spatial scenes in population firing rates in medial temporal, retrosplenial and medial parietal areas, simulating encoding of locations of objects encountered within familiar environments, and retrieval of the spatial context of these events into visuo-spatial imagery. The initial sets of simulations are compared to classic data from the literature, and have recently been published (Bicanski & Burgess, eLife 2018; 7:e33752, **Fig. 41**).

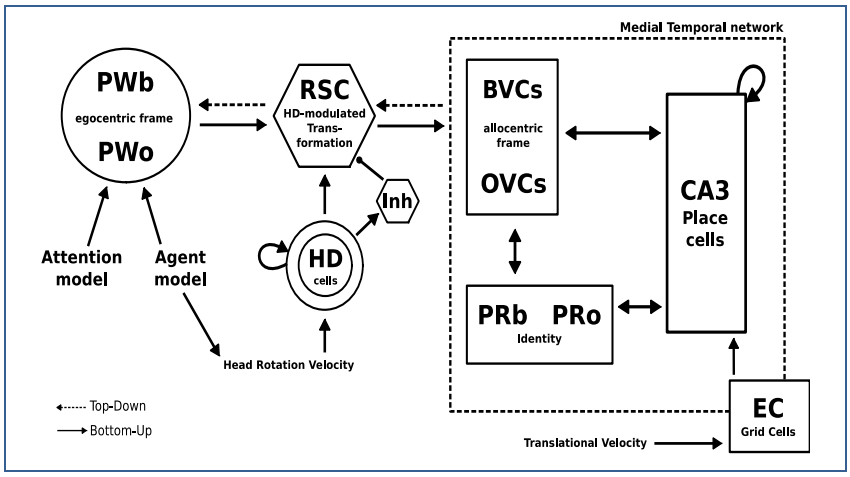

Figure 42: Model summary of the BB model

(Bicanski and Burgess, ELife 2018). Parietal representations (PWb/o) encode the egocentric position of extended boundaries and objects relative to an agent. These are transformed on retrosplenial cortex (RSC, modulated by head direction (HD) signals) to yield allocentric representations in the medial temporal lobe (boundary/object vector cells; BVCs/OVCs). These representations are associated with the positional code of place cells and grid cells.

15.2 Validation and Impact

15.2.1 Actual Use of Output(s) / Exploitation

Modelling in C2500 helped to design the experimental conditions used in SP3 Episense (Cacucci) – published in Chen et al., Nature Comms (2019) 10: 630.

15.2.2 Potential Use of Output(s)

C2408 will be used for comparison with electrophysiological data by SP3 Episense (Cacucci) and will be entered into the Neural Activity Resource

C2500 can be used to guide more detailed implementations on neurorobotic or neuromorphic platforms.

15.2.3 Publications

- Chen G, Lu Y, King JA, Cacucci F, Burgess N (2019) Differential influences of environment and self-motion on place and grid cell firing. Nature Comms. 10: 630.
  - **Significance:** Using a sophisticated virtual reality setup for mice the authors show for the first time that while mice are navigating, place cells represent the mouse location predominantly using environmental sensory cues while grid cells are more strongly driven by self motion.
- Bicanski A, Burgess N. (2018) A neural-level model of spatial memory and imagery, Elife, 2018 Sep 4;7:e33752.
  - **Significance: A** systems-level account of spatial memory (for both encoding and recall/visuo-spatial imagery) is presented for the first time. We can account for the function and interaction of all major spatially selective cell types (place cells, grid cells, head-direction cells, boundary, and predicting object vector cells) in one model.
- Bicanski A, Burgess N. A Computational Model of Visual Recognition Memory via Grid Cells. Current Biology – in press
  - **Significance:** The authors present a novel explanation for the hitherto puzzling existence of visual grid cells. In part analogous to grid cells in navigation studies, visual grid cells are hypothesized to calculate movement vectors for the focus of gaze (i.e. for saccades). The relative distances between any two features of a stimulus are embodied in corresponding pairs of grid cell population vectors, allowing the model to sample features in sequence and to accumulate evidence for stimulus identity.

Total number of publications: 3

15.2.4 Measures to Increase Impact of Output(s): Dissemination

Results from C2408 were presented by Dr. Talfan Evans at Cosyne 2019

16. Work carried out by the National Research Council (partner Pezzulo) under CDP7

16.1 Development of novel computational approaches to spatial navigation

Our research activities focus on the development of novel computational approaches to 1) understand goal-directed spatial cognition and hierarchical planning during navigation, and 2) to analyze the neuronal underpinnings of these abilities in rodents and humans, in particular in relation to the role of the hippocampus and surrounding structures.

The main hypothesis under scrutiny is that hippocampal- (and map-) based spatial cognition and planning can be modeled in terms of probabilistic inference using generative models (Pezzulo et al., 2014 and 2017). More specifically, we hypothesize that 1) the hippocampus (HC) / medial temporal lobe (MTL) acts as a compressed and hierarchically organised map for spatial navigation and 2) it interacts with prospective goal and sub-goal codes (PFC) to derive hierarchical plans.

In a first research stream (T4.5.4), we developed novel computational methods for the data analysis of HC / MTL neural codes (to be provided by our CDP7 partners: Pennartz, Spiers and Summerfield) to test the idea that they encode latent (hierarchical) structure that may support hierarchical planning. We leveraged on two existing methods, one (developed in our lab) based on algorithmic complexity theory (Donnarumma et al. 2016) and one based on the notion "successor representations" in reinforcement learning (Stachenfeld et al., 2017), to realize a novel integrated approach to test hierarchical spatial structure in neural codes (paper in preparation).

In a second research stream (T4.3.4), we developed a novel computational model of how the neural circuit formed by the hippocampus and the ventral striatum supports spatial cognition (Stoianov et al., PLoS 2018, **Fig. 42**). Specifically, we compared the internal variables of a certain class of (model-based) reinforcement learning model to neural data in the hippocampus (HC) and ventral striatum (vStr) and found that latent states emerging in the state-transition and state-value models of the model-based agent show key coding properties of HC and vStr neurons, respectively. The computational model was realized in collaboration with Cyriel Pennartz (partner of CDP7 and SP3) and his lab, and has led to a publication acknowledging HBP.

In a third research stream (T4.4.6), we extended the computational approach of (Stoianov et al., PLoS 2018) to model the formation of hierarchical spatial codes and their usage for inference, prediction and planning during spatial navigation, using deep belief networks (manuscript in preparation). Furthermore, in collaboration with SSSA (SP10), we performed preliminary tests for the integration of our computational models for spatial navigation and planning in the Neurorobotic platform. We intend to extend them to novel scenarios (e.g. four-room scenario) that will be used by our partners in CDP7.

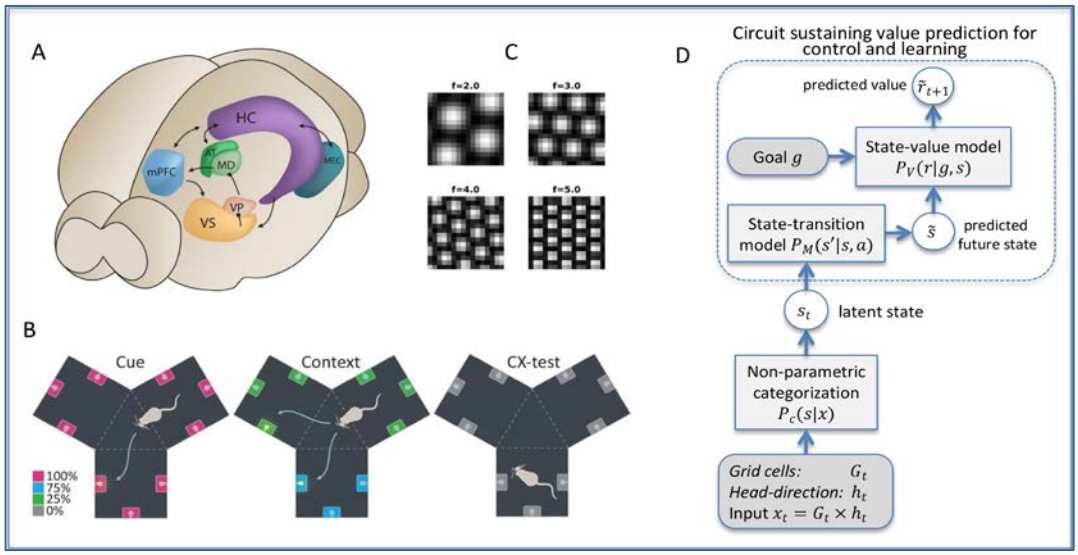

Figure 43: Schematic of the computational model of the hippocampus-ventral striatum circuit.

The computational model (a) mimics computations in the hippocampus and ventral striatum; (b) was tested in a Y-maze rodent navigation scenario developed by Prof. Pennartz (SP3 and CDP7); (c) uses simulated grid cells as inputs and (d) implements goal-directed spatial navigation and planning in terms of probabilistic inference, which uses components whose functioning can be mapped to neural substrate of (a). (Stoianov et al., PLoS 2018).

16.2 Validation and Impact

16.2.1 Actual Use of Output(s) / Exploitation

Our tasks have mainly a scientific impact. The results produced by task T4.5.4 are being used for the design (and successive analysis) of rodent and human tasks by the other partners of CDP7 (Hugo Spiers at UCL, Cyriel Pennartz at the University of Amsterdam, Christopher Summerfield in Oxford). Furthermore, the results of task T4.3.4, in particular the computational model that we published https://doi.org/10.1371/journal.pcbi.1006316, are being used by our partner in SP10 SSSA (Scuola Superiore Sant'Anna, under the supervision of Egidio Falotico) to realize a robotic implementation of spatial navigation and planning within the neurorobotic platform.

16.2.2 Publications

- Stoianov IP, Pennartz CM, Lansink CS, Pezzulo G. (2018) *Model-based spatial navigation in the hippocampus-ventral striatum circuit: A computational analysis,* PLoS computational biology, 14(9):e1006316. https://doi.org/10.1371/journal.pcbi.1006316.
    - **Significance:** This paper introduces a novel computational model of goal-directed spatial navigation. Our systems-level model reproduces rodent data during a cue conditioning task, at both behavioural and neuronal levels. It contributes to clarify the ways the hippocampus-ventral striatum circuit contributes to goal-directed spatial decisions.

17. Conclusion and Outlook

In conclusion, this interim report of SGA2 shows that there is good progress made in all models developed in SP4, and there is a large number of publications resulting from this work. The code of many of the models are already publicly available, and it is our plan to make all codes available in open access once the corresponding papers are accepted for publication.

Interaction of SP4 models with the HBP platforms is high, and many models also interact with the neuroscience data produced in HBP. As requested by the reviewers, SP4 should be more tightly integrated with the neuroscience part of the HBP (SP1 to SP3), and we are making constant effort to achieve such an integration. We will report about this integration next year.

Annex A: Component Details

Table 18: Component details contributing to Key Result KR4.1

ID	Component Name	Type	Contact	Additional information
C951	Complex to Simplified Models	Model	Guy Eyal	T4.1.1 (Simplified dendritic models)
C2453	Input-output "correlation" transfer properties in simplified, "ball-and-stick", multi-compartmental models	Model	Michele Giugliano	T4.1.2 (Input-Output Transfer function of detailed morphological models)
C2454	Input-output "correlation" transfer properties in reconstructed multi-compartmental models of rodent cortical neurons	Model	Michele Giugliano	T4.1.2
C2455	Input-output "correlation" transfer properties in reconstructed multi-compartmental models of human cortical neurons	Model	Michele Giugliano	
C1030	Mean-field models of interacting populations of rate and spiking neurons	Model	Olivier Faugeras	T4.1.3 (Mean-field and population models)
C1031	Mean-field models of interacting spiking neurons with dendritic compartment	Model	Romain Veltz	T4.1.3
C2357	Slow-fast effects in mean-fields models	Model	Etienne Tanré	T4.1.3
C1234	Model of calcium imaging signals	Model	Alain Destexhe	T4.1.4 (Biophysical models of brain signals)
C2742	Application of Mean-field simulations (MIIND)	Model	Marc De Kamps	T4.1.3

Table 19: Component details contributing to Key Result KR4.2

ID	Component Name	Type	Contact	Additional information
C66	Plasticity: STDP for structural plasticity	Model	Wulfram Gerstner	T4.3.2 (Learning in networks of neurons)
C1066	Plasticity models	Model	Wulfram Gerstner	T4.3.1 (Plasticity Algorithms)
C1025	Motor control model	Model	Jeanette H. Kotaleski	T4.4.3 (Models of motor control)
C2472	Plasticity: multifactor rule for deep networks	Model	Wulfram Gerstner	T4.3.2
C2420	Plasticity: prototype implementations of rules and testing within and without the SP9 platforms	Model	André Gruening	T4.3.3 (Functional plasticity for multi-compartment neurons in a multi-scale simulation framework)

Table 20: Component details contributing to Key Result KR4.3

ID	Component Name	Type	Contact	Additional information
C1030	Mean-field models of interacting populations of rate and spiking neurons	Model	Olivier Faugeras	T4.1.3 (Mean-field and population models)
C1054	Population activity equations: finite-N mean-field model for interacting populations	Model	Wulfram Gerstner	T4.1.3
C1235	Local-network model of spontaneous activity in cortex	Model	Alain Destexhe	T4.4.1 (Models of spontaneous activity and sleep)
C2296	Network model of the retina responding to complex stimuli	Model	Olivier Marre	T4.4.2 (Models of low-level vision)
C1859	Alteration of spontaneous activity and emergent dynamics under external stimuli	Model	Gustavo Deco	T4.4.1
C999	Macroscopic model of spontaneous human brain activity	Model	Gustavo Deco	T4.4.1

Table 21: Component details contributing to Key Result KR4.4

ID	Component Name	Type	Contact	Additional information
C1024	EITN Postdoctoral Fellows Programme	Service	Alain Destexhe	T4.6.2 (EITN programme)

Table 22: Component details contributing to Key Result KR4.5

ID	Component Name	Type	Contact	Additional information
C1680	Python libraries for structured model validation tests	Software	Andrew Davison	T4.5.1 (Comparing activity dynamics of models and living brains)
C1863	Concepts for comparison of massively-parallel electrophysiological experimental and model data	Report	Sonja Gruen	T4.5.1
C2418	4x4mm spatially organised model of a single area	Model	Markus Diesmann	T4.2.1 (Spiking mesoscale cortical models with spatial organisation)
C2339	Hybrid Schemes for combining point-neuron network simulations in NEST with biophysically detailed NEURON simulations	Model	Gaute Einevoll	T4.1.4 (Biophysical models of brain signals)
C2340	Biophysical modelling of population signals (LFP, ECoG, EEG, MEG, LMF), with detailed reconstructed neurons	Model	Gaute Einevoll	T4.1.4

Table 23: Component details contributing to Key Result KR4.6

ID	Component Name	Type	Contact	Additional information
C2418	4x4mm spatially organised model of a single area	Model	Markus Diesmann	T4.2.1 (Spiking mesoscale cortical models with spatial organisation)
C1574	Structural and functional connectivity at different scales	Model	Viktor Jirsa	T4.5.1 (Comparing activity dynamics of models and living brains)

Table 24: Component details contributing to Key Result KR4.7

ID	Component Name	Type	Contact	Additional information
C730	Multi-area model of cortical network at neuronal resolution	Model	Sacha van Albada	T4.2.3 (Multi-area multi-layer spiking cortical models)
C944	Full-density model of cortical microcircuit	Model	Sacha van Albada	T4.2.3

Table 25: Component details contributing to Key Result KR4.8

ID	Component Name	Type	Contact	Additional information
C2358	Simplified, generic astrocyte-neuron interaction model, with built-in model order reduction	Model	Marja-Leena Linne	T4.2.2 (Network models including neuro-glial interactions)
C2359	Prototype spiking neuronal network model, including simplified version of the astrocyte-neuron interaction model to explain *in vitro* cell culture data	Model	Marja-Leena Linne	T4.2.2

Table 26: Component details contributing to Key Result KR4.9

ID	Component Name	Type	Contact	Additional information
C2418	4x4mm spatially organised model of a single area	Model	Markus Diesmann	T4.2.1 (Spiking mesoscale cortical models with spatial organisation)

Table 27: Component details contributing to Key Result KR4.10

ID	Component Name	Type	Contact	Additional information
C1861	Improving identification of the epileptogenic zone	Model	Viktor Jirsa	T4.5.3 (Human brain function from structure)
C1862	Personalised brain models for predicting seizure propagation	Model	Viktor Jirsa	T4.5.3

Table 28: Component details contributing to Key Result KR4.11

ID	Component Name	Type	Contact	Additional information
C998	Allen Mouse Brain Atlas-based brain network	Model	Viktor Jirsa	T4.5.2 (Mouse brain function from structure)
C1606	Mouse stroke brain network model	Model	Viktor Jirsa	T4.5.2
C2495	Compare experimental and theoretical data: mouse resting state functional connectivity	Model	Viktor Jirsa	

Table 29: Component details contributing to Key Result KR3.3

ID	Component Name	Type	Contact	Additional information
C984	Hippocampal and striatal model of navigation, extended to planning and episodic memory	Model	Neil Burgess	T4.4.4 (Models of spatial memory)
C2408	Simulated spatial neural firing patterns in freely moving rodents during spatial navigation and planning, for comparison with electrophysiological data	Model	Neil Burgess	T4.4.4
C2409	High-level (firing rate) model of visuo-spatial episodic memory	Model	Neil Burgess	T4.4.4
C2500	High-level model of spatial navigation for guiding autonomous agents	Model	Neil Burgess	T4.4.4

Appendix I: Key Results in SGA2 Amendment 2

Key Result	Name	Work Packages and Tasks	Responsible
KR4.1	Develop models of single-cell and population levels	T4.1.1, T4.1.2, T4.1.3, T4.1.4	Alain Destexhe
KR4.2	Plausible biological models of plasticity for large networks with non-trivial functionality	T4.3.1, T4.3.2, T4.3.3, T4.4.3	Wulfram Gerstner
KR4.3	Develop models of brain activity and function	T4.1.3, T4.4.1	Moritz Helias (in-kind)
KR4.4	SP4 EITN Postdoctoral Fellows Programme	T4.6.2	Alain Destexhe
KR4.5	Validation of spiking network model against experimental data	T4.1.1, T4.1.2, T4.1.3, T4.1.4 T4.2.1, T4.5.1	Alain Destexhe, Markus Diesmann, Sonja Gruen
KR4.6	Parameter space confinement of mesocircuit model for the reproduction of experimental data	T4.2.1	Markus Diesmann
KR4.7	Release of multi-area model of macaque visual cortex, improved using new connectivity and activity data	T4.2.3	Sacha van Albada
KR4.8	Release of draft implementation of generic network model with glial contribution	T4.2.2	Marja-Leena Linne
KR4.9	Release of draft multi-layered cortical network model with spatially organised connectivity	T4.2.1	Markus Diesmann
KR4.10	Demonstration that brain personalized network models have predictive value for epileptogenic zones of individual patients	T4.5.3	Viktor Jirsa
KR4.11	Demonstration of explanatory value of large-scale brain network mouse models with impaired connectivity and dysfunctional network	T4.5.2	Viktor Jirsa
KR3.3	Acquisition of brain imaging and electrophysiological recording, models of multisensory integration and spatial memory and navigation, and brain-inspired robots (i.e. visual-tactile rodent-like robot and a humanoid robot)	T4.4.4	Neil Burgess

Appendix II: Milestones Status

Note that the milestones (4.1.3/4.3.1/4.4.3, in red) which have been achieved after the first submission of the deliverable will be reported in the Month 18 report.

Work Package	Milestone	Milestone title	Status	Achievement date
WP21	MS170	MS4.1.1 "Neuroreduce" an open source automated reduction scheme for any complex neuron model (T4.1.1)	Achieved	30.09.18 (M06)
WP21	MS171	MS4.1.2 Find the good scalings for synaptic connections in order to have a mean field limit.(T4.1.3)	Achieved	26.04.19 (M13)
WP21	*MS172*	*MS4.1.3 Open source refined model for NMDA-receptors, including local dendritic NMDA spike model (T4.1.1)*	*Achieved*	*16.05.19 (M14)*
WP21	MS173	MS4.1.4 Public release as software of models realised with MIIND with announcement.(T4.1.3)	Achieved	04.03.19 (M12)
WP21	MS174	MS4.1.5 Separate the time scales in models of networks of spiking neurons (T4.1.3)	Report to M24	
WP21	MS175	MS4.1.6 Thermodynamic limit for networks with correlated Gaussian synaptic weights (T4.1.2)	Achieved	29.01.19 (M10)
WP22	MS184	MS4.2.1 Comparative analysis of model order reduction techniques (T4.2.2)	Achieved	31.03.19 (M12)
WP22	MS457	MS4.2.4 Internal release of first draft of spatially organised connectivity (T4.2.1)	Achieved	25.05.18 (M02)
WP22	MS458	MS4.2.5 Internal release of draft forward model predicting LFP on basis of spatially organised spiking model (T4.2.1)	Achieved	25.05.18 (M02)
WP23	*MS187*	*MS4.3.1 Report on neural networks that perform hierarchical memory retrieval part 1 (T4.3.2)*	*Achieved*	*18.07.19 (M16)*
WP23	MS188	MS4.3.2 Two three-factor rules implemented on Spinnaker and BrainScaleS (T4.3.3)	Report to M24	
WP23	MS196	MS4.3.7 A computational demo of hierarchical navigational planning (T4.3.4)	Achieved	17.09.18 (M06)
WP24	MS193	MS4.4.1 Intermediate report on the network model of retinal processing (T4.4.2)	Achieved	17.10.18 (M07)
WP24	MS194	MS4.4.2 Report on model implementation and testing of a visual task which depends on a top-down contribution (T4.4.2)	Achieved	15.06.18 (M03)
WP24	*MS195*	*MS4.4.3 Simulation of hippocampal and striatal contributions to spatial navigation (T4.4.4)*	*Achieved*	*25.07.19 (M16)*
WP25	MS206	MS4.5.1 Successful characterization of resting state as described by functional connectivity for the mouse before stroke (T4.5.2)	Achieved	25.02.19 (M11)
WP25	MS207	MS4.5.2 Successful reconstruction of structural epilepsy patient data (N > 15) and creation of patient-specific brain network models	Achieved	07.01.19 (M10)

Appendix III: Contributions, Data used and Platform

Task	Key tasks in other SPs to which SP4 current activities will directly contribute.	Datasets (from SPs 1, 2 and 3) used in the development of the theoretical model, and are envision to use in SGA2-Year2.	HBP platforms activities (and related WP or task number) which are needed for the models.
T4.1.1	SP1 Mouse Brain Organisation and Interspecies Comparisons It provide models for SP1 : Models of NMDA synapses and of local dendritic NMDA spikes ; to be used for developing realistic nonlinear detailed models of cortical and hippocampal neurons.	Data from: T1.5.3 Comparative physiology of mouse and human neocortical pyramidal neurons and interneurons in different layers - 3D reconstructed Human L2/3 pyramidal cells (Huib Mansvelder lab., Amsterdam); WP1.4 Molecular, structural and functional integration of data in brain circuits - Detailed reconstruction of dendritic spines (for both mouse and human L2/3 cortical pyramidal cells)	SP6 Brain Simulation Platform
T4.1.2	WP3.2 Sleep/wake transitions and slow-wave activity WP3.4 Neural mechanisms of consciousness: experiments, modelling, quantitative measures	Data from: T1.2.2 Functional in vivo interaction data between synaptic proteins of the neuroligin and the neuroxin families, and their use for the computational modelling of trans-synaptic signalling T2.2.2 Neuronal mechanism transforming a visual stimulus into an eye movement plan T2.2.5 Linking human neocortical microcircuits to human cognition SGA2-Year 2 : Same data are planned to be use and data released in SGA1 by the EPFL-BBP	SP6 Brain Simulation Platform WP6.3 Software tools and model reconstruction workflows WP6.4 Platform services
T4.1.3	WP1.3 Whole Brain CDP1 Mouse whole Brain Model & Related Atlas T3.2.3 Multiscale study of spontaneous activity in physiological and pathological models of the cerebral cortex T3.2.1 Modelling and analysis of heterogeneous cortical spontaneous activity across brain states MIIND on JURON	None	SP6 Brain Simulation Platform
T4.1.4	SP6 Brain Simulation Platform T6.3.6 Subcellular level tools CDP1 Mouse Whle Brain model & Related Atlas SP3 Systems and Cognitive Neuroscience (about spiking NN models)	None SGA2-Year 2: Data from Mavi Sanchez Vives (simultaneaous LFP and intracellular recordings)	No platform is needed because T4.1.4 provides tools, but they could be useful to platforms. e.g. in SP6, to calculate LFPs from detailed models (LFPy), or in neuromorphic simulations to calculate LFPs solely from the spikes produced by the hardware, using a phenomenological LFP model (ph-LFP).

Task	Key tasks in other SPs to which SP4 current activities will directly contribute.	Datasets (from SPs 1, 2 and 3) used in the development of the theoretical model, and are envision to use in SGA2-Year2.	HBP platforms activities (and related WP or task number) which are needed for the models.
T4.2.1	T5.7.1 Elephant, T6.3.3 Simulation engines (NEST), T7.3.5 Optimized network construction on exascale architectures.	None SGA2-Year2: T2.2.1 A common computational architecture for eye and arm movement control - data from visual cortex	NEST: T6.3.3 Simulation engines (NEST) WP7.3 Exascale simulator and visualization technology T7.4.5 NEST user experience and sustainability) HPAC: (WP7.1, WP7.2, WP7.4, WP7.5, WP7.6), ELEPHANT (T5.7.1),
T4.2.2	WP7.3 Exascale simulator and visualization technology T6.2.4 Models of basal ganglia	SGA2-Year 2: T1.2.1 High-resolution reconstruction of striatal and cerebellar neurons: dendritic arbors and axon initial segments	NEST: T6.3.3 Simulation engines (NEST) WP7.3 Exascale simulator and visualization technology MOR (Model Order Reduction)
T4.2.3	T6.3.3 Simulation engines (NEST) WP7.3 Exascale simulator and visualization technology WP9.3 SpiNNaker systems	Data from: T2.5.7 Attentional modulation of sensory processing in monkey and human - Monkey electrophysiology data from parietal cortical areas V6/V6A	NEST: T6.3.3 Simulation engines (NEST) WP7.3 Exascale simulator and visualization technology T7.4.5 NEST user experience and sustainability) HPAC: (WP7.1, WP7.2, WP7.4, WP7.5, WP7.6), Elephant (T5.7.1), SpiNNaker systems (WP9.3), BrainScaleS systems (WP9.2)
T4.3.1	WP9.2 BrainScaleS systems WP9.3 SpiNNaker systems CDP5 The Virtual Brain	None	NEST: T6.3.3 Simulation engines (NEST)
T4.3.2	WP9.2 BrainScaleS systems WP9.3 SpiNNaker systems CDP5 The Virtual Brain	None	NEST: T6.3.3 Simulation engines (NEST)
T4.3.3	WP9.2 BrainScaleS systems WP9.3 SpiNNaker systems CDP5 Biological Deep Learning	None	WP9.2 BrainScaleS systems WP9.3 SpiNNaker systems

Task	Key tasks in other SPs to which SP4 current activities will directly contribute.	Datasets (from SPs 1, 2 and 3) used in the development of the theoretical model, and are envision to use in SGA2-Year2.	HBP platforms activities (and related WP or task number) which are needed for the models.
T4.3.4	T3.3.6 Navigation and planning in hierarchical environments	Data from: T3.3.6 Navigation and planning in hierarchical environments - rodent data	The neurorobotic platform: T10.2.3 Decision making and spatial representation
T4.4.1	CDP1-SGA2-UC2: Mouse network model for the activity before and after stroke WP3.4 Neural mechanisms of consciousness: experiments, modelling, quantitative measures T3.4.2 Exploration of measures and mechanisms of consciousness in multilevel model simulations T3.4.3 From focal stroke to cortical islands: the impact of lesions on brain complexity and consciousness T3.4.4 Brain structure-function dynamical interactions in pathological, pharmacological and physiological modulation of consciousness WP3.2 Sleep/wake transitions and slow-wave activity T3.2.2 Multiscale mapping of cortical activity, reactivity and effective connectivity across states in humans T3.2.3 Multiscale study of spontaneous activity in physiological and pathological models of the cerebral cortex CDP8 The Virtual Brain.	SGA2-Year 1: - ARCHI dataset (resting-state fMRI) (Bertrand Thirion, NeuroSpin, SP2). We employed this dataset in the paper accepted two weeks ago (https://www.sciencedirect.com/science/article/pii/S1053811919305889) - Individual Brain Charting: ARCHI standard (Bertrand Thirion, NeuroSpin, SP2) https://kg.humanbrainproject.eu/instances/Dataset/a0a27e55525511d7c1765bf5c1f4d916 - Fluorescence cortical recording of mouse activity after stroke (Francesco Pavone, LENS, CDP1, SP1) https://kg.humanbrainproject.eu/instances/Dataset/4730b8c4ae603587a04b4c4362869f91 - Cortical recordings from anesthetized Fmr1KO mice (Maria Victoria Sánchez-Vives, IDIBAPS, SP3, T3.4.4 Brain structure-function dynamical interactions in pathological, pharmacological and physiological modulation of consciousness) SGA2 Year-2 also: - EEG data in sleep and anesthesia (Steven Laureys, SP3)	CDP8 – The virtual Brain T5.10.1 (SGA2) Interface between HBP and TVB T5.5.3 (SGA2) Knowledge Graph
T4.4.2	T2.2.1 A common computational architecture for eye and arm movement control T2.2.3 Predicting behavioural symptoms of unilateral spatial hemineglect patients from lesioned visuo-motor integration model T2.2.4 Learning eye movement and grasping control using deep learning networks with brain-constrained architectures T2.5.6 Comparative mapping of visuo-motor cortex in monkey and human T3.1.3 Feedback circuits, and apical amplification	None	SP9 Neuromorphic Computing Platform SP10 Neurobotics Platform

Task	Key tasks in other SPs to which SP4 current activities will directly contribute.	Datasets (from SPs 1, 2 and 3) used in the development of the theoretical model, and are envision to use in SGA2-Year2.	HBP platforms activities (and related WP or task number) which are needed for the models.
	WP3.1 Context-sensitive vision and recognition SP9 Neuromorphic Computing Platform SP10 Neurorobotics		
T4.4.3	T6.2.4 Models of basal ganglia	Data from: T1.2.4 Structure and function of the interneurons of the microcircuits within the basal ganglia	SP10 Neurorobotics Platform
T4.4.4	T3.3.2 Rodent physiology: self motion and visual integration	Data from: SP3 (relating to Chen et al., 2019, and future experiments). This will be deposited in CSCS (https://www.cscs.ch/user-lab/allocation-schemes/) 'Mice-virtual-reality-data-UCL'.	SP6 Brain Simulation Platform NEURON simulator Neuroscience Gateway project
T4.4.5	CDP4 - Visuo-motor integration	None	T5.5.1 Collaboratory T5.5.2 Reproducible Scientific Workflows
T4.4.6	T10.2.3 Decision making and spatial representation	None	The Neurorobotic Platform: T10.2.3 Decision making and spatial representation
T4.5.1	WP3.2 Sleep/wake transitions and slow-wave activity T3.2.1 Modelling and analysis of heterogeneous cortical spontaneous activity across brain states T3.2.5 High-efficiency multi-scale software pipeline for analysis and simulation of experimental slow waves and wakefulness transition.	Data from: various test data generated by the involved partners in SP3, and corresponding simulations of the NEST and DPSNN simulators.	T5.7.1 Elefant T5.7.2 Neural Activity Resource T6.4.1 Simulation engines apps for the platform.

Task	Key tasks in other SPs to which SP4 current activities will directly contribute.	Datasets (from SPs 1, 2 and 3) used in the development of the theoretical model, and are envision to use in SGA2-Year2.	HBP platforms activities (and related WP or task number) which are needed for the models.
T4.5.2	T1.3.1 Whole brain distribution of various cell types SP10 Neurorobotics Platform	Data from: T1.3.1 Whole brain distribution of various cell types SGA2-Year 2: The same data should be used and probably from T1.3.2 Technological development in both imaging and data analysis	SP10 Neurorobotics Platform
T4.5.3	T2.6.1 Multimodal integrationto build the HBP atlas T4.5.1 Comparing activity dynamics of models and living brains T5.4.3 Development of 3D High-Volumetric Interactive Atlas Viewer T8.7.4 Simulating Human Brains WP7.2 Data federation and data-intensive computing technology CDP3 Multi-Level Human Brain Atlas CDP8 The Virtual Brain	Data from: T2.6.1 Multimodal integration to build the HBP atlas SGA2-Year 2: The same data will be used in the SGA2 remaining period.	SP5 Neuroinformtacis Platfom WP7.2 Data federation and data-intensive computing technology WP8.7 The Neurodegenerative Virtual Brain (TVD-NDD) T8.7.4 Simulating human brains
T4.5.4	T2.2.6 Goal-directed navigation in the classic AI four rooms task (fMRI) (CEoI) T2.2.7 Goal-directed navigation in a hierarchical sequential decision task (fMRI)	None SGA2-Year 2: T2.2.6 Goal-directed navigation in the classic AI four rooms task (fMRI) (CEoI) T2.2.7 Goal-directed navigation in a hierarchical sequential decision task (fMRI)	The neurorobotic platform: T10.2.3 Decision making and spatial representation

Appendix IV: List of Publications in SGA2

Note that the publications of SGA2 Year 2 (*in red and italics*) will be reported in the Month 18 report

KR4.1

1) de Kamps M, Lepperød M, Lai YM (2019) Computational geometry for modeling neural populations: From visualization to simulation. PLoS Comput Biol 15(3): e1006729. https://doi.org/10.1371/journal.pcbi.1006729

2) Gorski T, Veltz R, Galtier M, Fragnaud H, Goldman JS, Teleńczuk B and Destexhe A, 2018. Dendritic sodium spikes endow neurons with inverse firing rate response to correlated synaptic activity. Journal of computational neuroscience, 45(3), pp.223-234.

3) di Volo M, Romagnoni A, Capone C, Destexhe A, Biologically realistic mean field models of conductance-based spiking neurons with adaptation, Neural Computation 31: 653-680, 2019.

4) Telenczuk M, Brette R, Destexhe A. and Telenczuk B. Contribution of the axon initial segment to action potentials recorded extracellularly. eNeuro 5: 0068-18, 2018.

5) Fournier N, Tanré E, and Veltz R. "On a Toy Network of Neurons Interacting through Their Dendrites," February 12, 2018. https://arxiv.org/abs/1802.04118. Annales de l'Institut Henri Poincaré, Probabilités et Statistiques, in revision.

6) Goriounova NA, Heyer DB, Wilbers R, Verhoog MB, Giugliano M, Verbist C, Obermayer J, Kerkhofs A, Smeding H, Verberne M, Idema S, Baayen JC, Pieneman AW, de Kock CPJ, Klein M, Mansvelder HD (2018) Large and fast human pyramidal neurons associate with intelligence, eLife 7:e41714, https://doi.org/10.7554/eLife.41714

7) Pampaloni NP, Lottner M, Giugliano M, Matruglio A, D'Amico F, Prato M, Garrido JA, Ballerini L, Scaini D (2017) Single-layer graphene modulates neuronal communication and membrane ion channels expression via its cation–π interactions, Nature Nanotechnology, 13:755–64, https://doi.org/10.1038/s41565-018-0163-6

8) Cormier Q, Tanré E, Veltz R. Long time behavior of a mean-field model of interacting neurons. Stoch Process their Appl. July 2019. doi:10.1016/j.spa.2019.07.010

9) Olivier Faugeras, James MacLaurin, Etienne Tanré The meanfield limit of a network of Hopfield neurons with correlated synaptic weights https://arxiv.org/abs/1901.10248

10) Olivier Faugeras, Émilie Soret, Etienne Tanré Asymptotic behaviour of a network of neurons with random linear interactions https://hal.inria.fr/hal-01986927

KR4.2

1) Willem A.M. Wybo, Benjamin Torben-Nielsen,Thomas Nevian, Marc-Oliver Gewaltig (2019). Electrical Compartmentalization in Neurons. Cell Reports 26, 1759–1773, https://doi.org/10.1016/j.celrep.2019.01.074.

2) M. Llera-Montero, J. Sacramento, R.P. Costa. Computational roles of plastic probabilistic synapses. Current opinion in Neurobiology 54:90-97, 2019 https://doi.org/10.1016/j.conb.2018.09.002

3) Luziwei Leng, R. Martel, O. Breitwieser, I. Bytschok, W. Senn, J. Schemmel, K. Meier & M.A. Petrovici . Spiking neurons with short-term synaptic plasticity form superior generative networks. Nature Scientific Reports 8: 10651, 2018 DOI

4) Work on eligibility traces and 3-factor learning rules has been published as a review paper in Pubin Frontiers: Gerstner et al. (2018) PLUS id 1348, Front. Neural Circuits, 12:53 doi: 10.3389/fncir.2018.00053; C1066 and C2472

5) Deger et al. (2018), Journal of Cerebral Cortex, Volume 28, Pages 1396–1415, https://doi.org/10.1093/cercor/bhx339, PLUS id 1037 (C66)

6) Front. Neural Circuits, 12:53 doi: 10.3389/fncir.2018.00053

7) Suryanarayana SM, Hellgren Kotaleski J, Grillner S, Gurney KN. Roles for *globus pallidus externa* revealed in a computational model of action selection in the basal ganglia. Neural Networks. 2019;109:113-36; model deposited at https://senselab.med.yale.edu/ModelDB/showmodel.cshtml?model=249408#tabs-1

8) M. Katkov, S. Romani & M. Tsodyks. Memory Retrieval from First Principles. Neuron**,** 94:1027-1032 (2017).

9) M. Naim, M. Katkov & M. Tsodyks. Fundamental Law of Memory Recall. bioArxiv, 2018.

KR4.3

1) Schuecker, Goedeke, Helias (2018) Optimal Sequence Memory in Driven Random Networks. *Phys Rev X* 8, 041029

2) Kuehn, Helias (2018) Expansion of the effective action around non-Gaussian theories. *J Phys A Math Theor* 51(17) 375004

3) Owaki, T, Vidal-Naquet, M, Nam, Y, Uchida, G, Sato, T, Câteau, H, Shimon Ullman, S and Manabu Tanifuji, M. Searching for visual features that explain response variance of face neurons in inferior temporal cortex. *PLoS one*, 13, 1-27, 2018

4) Ullman, S. Using neuroscience to develop artificial intelligence. *Science, 363 (6428),* 692-693, 2019

KR4.4

1) https://www.biorxiv.org/content/10.1101/565127v1

2) Nghiem, T. A. E., Tort-Colet, N., Gorski, T., Ferrari, U., Moghimyfiroozabad, S., Goldman, J. S? & Destexhe, A. (2018). Cholinergic switch between two different types of slow waves in cerebral cortex. *bioRxiv*, 430405.

3) Volo, Matteo di, Alberto Romagnoni, Cristiano Capone, and Alain Destexhe. 2018. "Mean-Field Model for the Dynamics of Conductance-Based Networks of Excitatory and Inhibitory Spiking Neurons with Adaptation." bioRxiv. https://doi.org/10.1101/352393.

KR4.5

1) Trensch, G., Gutzen, R., Blundell, I., Denker, M., and Morrison, A. (2018). Rigorous Neural Network Simulations: A Model Substantiation Methodology for Increasing the Correctness of Simulation Results in the Absence of Experimental Validation Data. Frontiers in Neuroinformatics 12, 81.

2) Gutzen, R., von Papen, M., Trensch, G., Quaglio, P., Grün, S., and Denker, M. (2018). Reproducible Neural Network Simulations: Statistical Methods for Model Validation on the Level of Network Activity Data. Frontiers in Neuroinformatics 12, 90.

3) Hagen, Næss, Ness & Einevoll (2018). Multimodal modeling of neural network activity: computing LFP, ECoG, EEG and MEG signals with LFPy2.0. *Front Neuroinform*, 12(92).

4) Skaar, Stasik, Hagen, Ness & Einevoll (2019). Estimation of neural network model parameters from local field potentials (LFPs). *bioRxiv* (submitted to *Journal of Neuroscience*)

5) Pesaran, Vinck, Einevoll, Sirota, Fries, Siegel, Truccolo, Schroeder & Srinivasan (2018). Investigating large-scale brain dynamics using field potential recordings: Analysis and interpretation. *Nature Neuroscience*, 21, 903–919.

6) Ness, Remme & Einevoll (2018). h-Type Membrane Current Shapes the Local Field Potential from Populations of Pyramidal Neurons. *Journal of Neuroscience*, 38(26), 6011–6024.

7) Buccino, Kordovan, Ness, Merkt, Häfliger, Fyhn, … Einevoll (2018). Combining biophysical modeling and deep learning for multi-electrode array neuron localization and classification. *Journal of Neurophysiology*, 120, 1212–1232.

8) Luo, Macias, Ness, Einevoll, Zhang & Moss (2018). Neural timing of stimulus events with microsecond precision. *PLoS Biology*, 16(10), 1–22.

9) Mäki-Marttunen, Krull, Bettella, Hagen, Næss, Ness, … Einevoll (2019). Alterations in Schizophrenia-Associated Genes Can Lead to Increased Power in Delta Oscillations. *Cerebral Cortex* 29(2), 875–891.

10) Buccino, Kuchta, Jæger, Ness, Berthet, Mardal, Cauwenberghs & Tveito (2019). How does the presence of neural probes affect extracellular potentials? *Journal of Neural Engineering*

KR4.6

1) Upscaling of the spiking cortical microcircuit model by Potjans & Diesmann (2014) to the mesocircuit model, parameter investigation and forward-modeling of local field potentials.

2) Senk, J.; Hagen, E.; van Albada, S.; Diesmann, M. (2018a) Reconciliation of weak pair-wise spike-train correlations and highly coherent local field potentials across space. arXiv:1805.10235

3) Interactive visualization with VIOLA: Senk, J; Carde, C.; Hagen, E.; Kuhlen, T.; Diesmann, M; Weyers, B (2018b) VIOLA - A multi-purpose and web-based visualization tool for neuronal-network simulation output. Frontiers in Neuroinformatics 12:75

4) Analytical conditions for spatiotemporal patterns in spiking activity: Senk, J; Korvasová, K.; Schuecker, J.; Hagen, E.; Tetzlaff, T.; Diesmann, M.; Helias, M. (2018c) Conditions for traveling waves in spiking neural networks. arXiv:1801.06046

5) Phase-lags in large scale brain synchronization: Methodological considerations and in-silico analysis. *Plos CB 2018. Petkoski et al.*

6) Petkoski S, Jirsa VK. Transmission time delays organize the brain network synchronization. Philos Trans R Soc A Math Phys Eng Sci. 2019;377(2153):20180132. doi:10.1098/rsta.2018.0132

KR4.7

1) Schmidt M, Bakker R, Hilgetag CC, Diesmann M, van Albada SJ. Multi-scale account of the network structure of macaque visual cortex (2018a) Brain Struct Func 223(3):1409-1435.

2) Schmidt M, Bakker R, Shen K, Bezgin G, Diesmann M, van Albada SJ. A multi-scale layer- resolved spiking network model of resting-state dynamics in macaque visual cortical areas (2018b) PLoS CB 14:e1006359.

3) van Albada SJ, Rowley AG, Senk J, Hopkins M, Schmidt M, Stokes AB, Lester DR, Diesmann M, Furber SB. Performance comparison of the digital neuromorphic hardware SpiNNaker and the neural network simulation software NEST for a full-scale cortical microcircuit model (2018) Front Neurosci 12:291.

KR4.8

1) T. Manninen, R. Havela, M.-L. Linne (2019). Computational models of astrocytes and astrocyte-neuron interactions: Categorization, analysis, and future perspectives. Computational Glioscience, editors M. De Pitta and H. Berry, Springer. (Output: Neuronal-glial network model)

2) Manninen T, Saudargiene A, Linne M-L. A novel excitability-physicochemical model for astrocyte-neuron interactions in long-term plasticity in mouse neocortex. Submitted to PLoS Computational Biology). (Output: Neuronal-glial network model)

3) Lehtimäki M, Paunonen L, Linne M-L. Model reduction of a biophysical network model. Submitted to Proceedings of the IEEE Conference on Decision & Control. (Output: Order reduction for network models)

KR4.9

KR4.10

1) Controlling seizure propagation in large-scale brain networks. Plos CB [in press]. Olmi et al.

2) An S, Bartolomei F, Guye M, Jirsa V. Optimization of surgical intervention outside the epileptogenic zone in the Virtual Epileptic Patient (VEP). PLoS Comput Biol. 2019;15(6):e1007051. doi:10.1371/journal.pcbi.1007051

3) Computational modeling of seizure spread on a cortical surface explains the theta-alpha electrographic pattern. Sip et al [in review]

KR3.3

1) Chen G, Lu Y, King JA, Cacucci F, Burgess N (2019) Differential influences of environment and self-motion on place and grid cell firing. Nature Comms. 10: 630.

2) Bicanski A, Burgess N. A neural-level model of spatial memory and imagery. Elife. 2018 Sep 4;7:e33752.

3) Bicanski A, Burgess N. A Computational Model of Visual Recognition Memory via Grid Cells. Current Biology – in press

CDP7

1) Stoianov IP, Pennartz CM, Lansink CS, Pezzulo G. Model-based spatial navigation in the hippocampus-ventral striatum circuit: A computational analysis. PLoS computational biology. 2018 14(9):e1006316. https://doi.org/10.1371/journal.pcbi.1006316.